JUN 0 6 1995

NAS 1.79/3-2!95-0

NASA Tech Briefs

National Aeronautics and Space Administration

Electronic Components and Circuits

Electronic Systems

Physical Sciences

Materials

Computer Programs

Mechanics

Machinery

Fabrication Technology

Mathematics and Information Sciences

Life Sciences

95-05

May 1995

BEST COPY AVAILABLE

COMPLETED

95-036604

INTRODUCTION

Tech Briefs are short announcements of new technology derived from the research and development activities of the National Aeronautics and Space Administration. These Briefs emphasize information considered likely to be transferable across industrial, regional, or disciplinary lines and are issued to encourage commercial application.

Availability of NASA Tech Briefs and TSP's

Distribution of NASA Tech Briefs, a monthly periodical publication, is limited to engineers in U.S. Industry and to other domestic technology transfer agents. Requests for individual Tech Briefs or for Technical Support Packages (TSP's) announced herein should be addressed to

NASA Center for AeroSpace Information
Technology Utilization Office
P.O. Box 8757
Baltimore, MD 21240.
Telephone No. (301) 859-5300, Ext. 243, 245

Please reference the three-letter, five-digit control number located at the end of each Tech Brief. Information on NASA's Technology Utilization Program, its documents, and services is also available at the same facility.

Technology Utilization Officers and Patent Counsels are located at NASA field installations to provide technology-transfer access to industrial users. Inquiries can be made by writing to NASA field installations listed below.

Technology Utilization Officers and Patent Counsels

Ames Research Center
Technology Utilization Officer
Mail Code 223-3
Moffett Field, CA 94035

Patent Counsel
Mail Code 200-11
Moffett Field, CA 94035

Goddard Space Flight Center
Technology Utilization Officer
Mail Code 702-1
Greenbelt, MD 20771

Patent Counsel
Mail Code 204
Greenbelt, MD 20771

Lyndon B. Johnson Space Center
Technology Utilization Officer
Mail Code IC-4
Houston, TX 77058

Patent Counsel
Mail Code AL3
Houston, TX 77058

John F. Kennedy Space Center
Technology Utilization Officer
Mail Stop PT-PMO-A
Kennedy Space Center, FL 32899

Patent Counsel
Mail Code PT-PAT
Kennedy Space Center, FL 32899

Langley Research Center
Technology Utilization Officer
Mail Stop 143
Hampton, VA 23665

Patent Counsel
Mail Code 279
Hampton, VA 23665

Lewis Research Center
Technology Utilization Officer
Mail Stop 7-3
21000 Brookpark Road
Cleveland, OH 44135

Patent Counsel
Mail Code LE-LAW
21000 Brookpark Road
Cleveland, OH 44135

Jet Propulsion Laboratory
Technology Utilization Officer
Mail Stop 156-211
4800 Oak Grove Drive
Pasadena, CA 91109

NASA Resident Office-JPL
Technology Utilization Officer
Mail Stop 180-801
4800 Oak Grove Drive
Pasadena, CA 91109

Patent Counsel
Mail Code 180-801
4800 Oak Grove Drive
Pasadena, CA 91109

George C. Marshall Space Flight Center
Technology Utilization Officer
Code AT01
Marshall Space Flight Center, AL 35812

Patent Counsel
Mail Code CC01
Marshall Space Flight Center, AL 35812

John C. Stennis Space Center
Technology Utilization Officer
Code HA-30
Stennis Space Center, MS 39529

NASA Headquarters
Technology Utilization Officer
Code CU
Washington, DC 20546

Assistant General Counsel for Patent Matters
Code GP
Washington, DC 20546

Dryden Flight Research Center
Technology Utilization Officer
M/S D21-31
Bldg. 4832 Whse 7
Lilly Dr.
Edwards, CA 93523

NASA TechBriefs

National Aeronautics and Space Administration

May 1995
95-05

5 Electronic Components and Circuits

13 Electronic Systems

23 Physical Sciences

29 Materials

39 Computer Programs

43 Mechanics

51 Machinery

57 Fabrication Technology

67 Mathematics and Information Sciences

71 Life Sciences

This document was prepared under the sponsorship of the National Aeronautics and Space Administration. Neither the United States Government nor any person acting on behalf of the United States Government assumes any liability resulting from the use of the information contained in this document, or warrants that such use will be free from privately owned rights.

BLANK PAGE

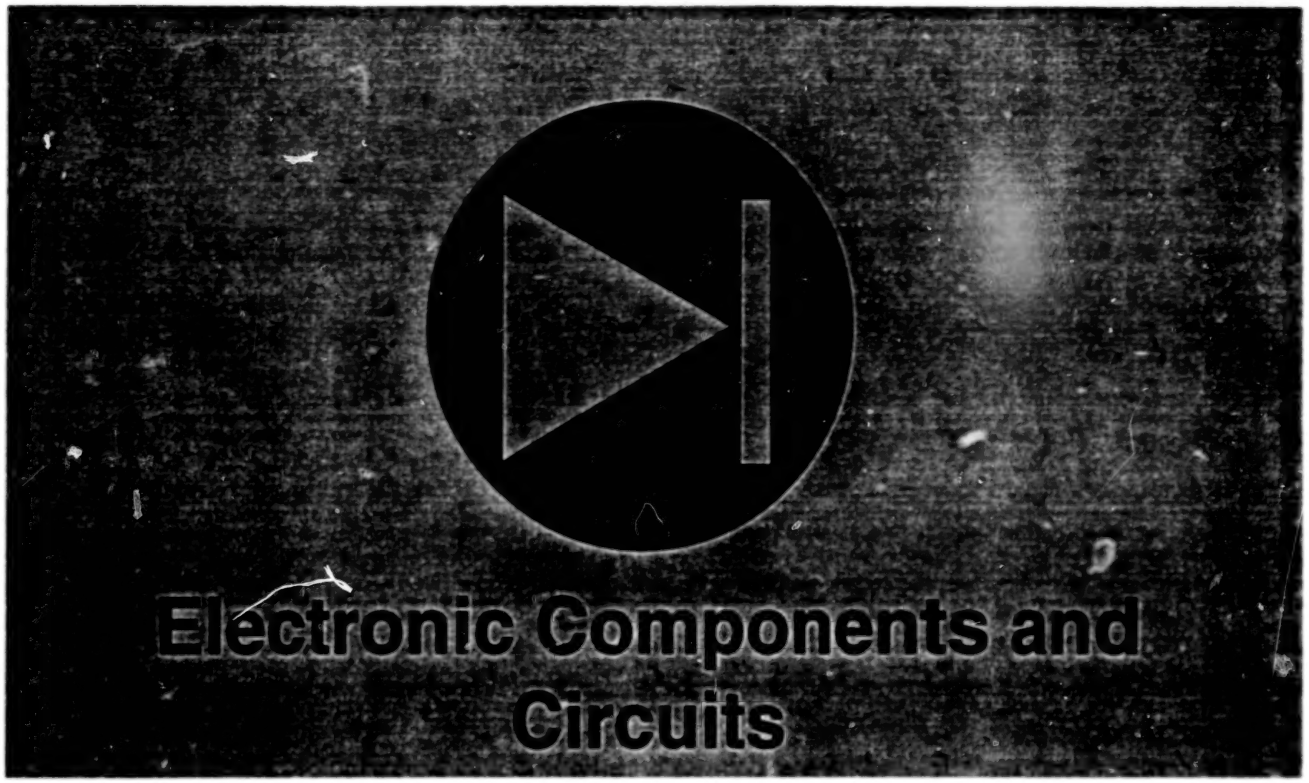

Hardware, Techniques, and Processes

7 Maximum Acceleration Recording Circuit
7 Switch Box for Controlling Flows of Four Gases
8 Circuit for Control of Electromechanical Prosthetic Hand
9 ASIC for Complex Fixed-Point Arithmetic
10 K_u-Band Data-Communication Adapter
10 Transient-Switch-Signal Suppressor
11 Digital Latching Circuit for a Safety-Related Application

Books and Reports

11 Test of a Microwave Amplifier With Superconductive Filter

BLANK PAGE

Maximum Acceleration Recording Circuit

Coarsely digitized maximum levels are recorded in blown fuses.

Lyndon B. Johnson Space Center, Houston, Texas

A circuit feeds power to an accelerometer and makes a nonvolatile record of the maximum level to which the output of the accelerometer rises during a measurement interval. In comparison with inertia-type single-preset-trip-point mechanical maximum-acceleration-recording devices, the circuit weighs much less, occupies less space, and records accelerations within narrower bands of uncertainty. In comparison with prior electronic data-acquisition systems designed for the same purpose, the circuit is simpler, less bulky, consumes less power, costs less, and does not require playback and analysis of data recorded in magnetic or electronic memory devices. The circuit could be used, for example, to record accelerations to which commodities are subjected during transportation on trucks.

The circuit (see figure) includes three 9-V batteries, one of which supplies the 9 V needed by the circuit, and all of which supply the 27 V needed by the accelerometer. Power is supplied to the accelerometer through field-effect diode D_1, which regulates the accelerometer current to keep it in the range of 2 to 4 mA. The accelerometer puts out an ac signal that peaks at a full-scale value of 5 V when the ac component of acceleration reaches 50 g (where g denotes normal Earth gravitation). The acceleration signal is coupled through C_1 and D_2 into C_2, which retains the peak value for a short time.

The signal is fed through potentiometer R_1 to the input terminal (pin 5) of a 10-level display driver, which is basically an analog-to-digital converter. The converter can be an integrated circuit (LM3914) that has equally spaced levels, each representing 5 g; or it can be a similar circuit (LM3915) that has logarithmically spaced levels, each succeeding level representing division of the next higher level by a factor of $\sqrt{2}$ (3 decibels/step).

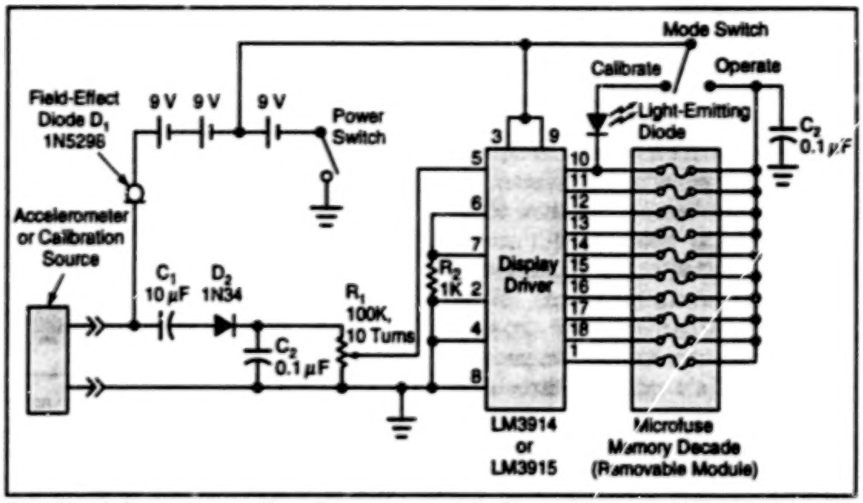

This Circuit Blows One or More Fuses in a module. The position of the blown fuse(s) in the module indicate(s) the maximum level(s) of acceleration reached during a measurement.

Depending on the level of the input signal, the display driver energizes 1 of its 10 output lines, each of which is connected to 1 of 10 2-mA transparent-cap microfuses plugged into a module. If the fuse on a line is still intact, then when that line is energized, the driver delivers a current of 10 mA, blowing the fuse. The fuses can be inspected visually or electrically at any convenient time thereafter to determine which (if any) has blown, thereby determining what level of acceleration was reached.

The circuit is calibrated with the accelerometer disconnected and a 5-V peak-to-peak signal at a frequency of 500 Hz coupled capacitively to the accelerometer terminals. Mode switch S_2 is placed in the "calibrate" position, and power switch S_1 is closed to turn the power on. The potentiometer is first set to minimum, then the setting is increased to the level of the signal reaching the input of the display driver. The circuit is deemed to be calibrated at the setting at which the light-emitting diode on output line 10 (which represents the full-scale signal level) flickers on. The power is then turned off.

The calibration source is disconnected, the accelerometer is connected, and the power is turned on. Next, mode switch S_2 is turned to the "operate" position. (Capacitor C_3 absorbs the resulting turn-on transients and prevents inadvertent triggering of the open-collector drivers in the display-driver circuit.) The circuit can then be left unattended to record the maximum acceleration.

This work was done by Richard J. Bozeman, Jr., of **Johnson Space Center.** *Further information is contained in a TSP [see page 1].*

This invention is owned by NASA, and a patent application has been filed. Inquiries concerning nonexclusive or exclusive license for its commercial development should be addressed to the Patent Counsel, Johnson Space Center [see page 1]. Refer to MSC-21922.

Switch Box for Controlling Flows of Four Gases

Each of four gas controllers can be connected to any one of six mass-flow controllers.

NASA's Jet Propulsion Laboratory, Pasadena, California

A switch box has been designed for use in simultaneously controlling the flows of as many as four out of a total of six available gases into a semiconductor-processing chamber. The switch box contains switches, relays, logic circuitry, display devices, and other circuitry for connecting each of as many as four gas controllers to any one of as many as six available mass-flow controllers. As used here, "gas controller" denotes that part of the programmable process-control circuitry that commands the flow of a specific gas at a specific rate. "Mass-flow controller" denotes that part of the process-control equipment that electromechanically effects the regulation of the flow of one of the six gases at a rate commanded by whichever gas controller is connected to it via the switch box.

To select one of the six gases to be fed to the chamber, the technician flips one of six activation switches on the front panel of the switch box (see figure). The logic cir-

cuitry (which includes logic gates and delay circuits) in the switch box seeks a gas controller for that gas and activates an appropriate relay when it finds an available gas controller. The switch box contains 12 relays on a board. Each relay is assigned to a specific gas controller and mass-flow controller. When a relay is activated by the logic circuit, its assigned gas and mass-flow controller are also activated.

Mounted on the front panel, along with the switches, are six activation lamps, six seven-segment light-emitting-diode alpha-numerical-display devices, and a power-interruption indicator lamp. The activation lamps correspond to the six gases, labeled A through G, while the numbers displayed on the devices correspond to the gas controllers. When the technician turns on a switch for a gas, its activation lamp lights up, and a number from 0 to 4 appears on the adjacent display device. A display of 0 indicates that no gas controller has been assigned to that gas, and so the gas is not flowing. A display of 1 to 4 represents the gas controller to which the gas and its mass-flow controller are assigned.

The power-interruption indicator lamp lights up when power has been interrupted. It tells the technician that all of the mass-flow controllers have been disconnected from all of the gas controllers and thus all flows of gases have been stopped. The technician must reset the system to make the flows resume.

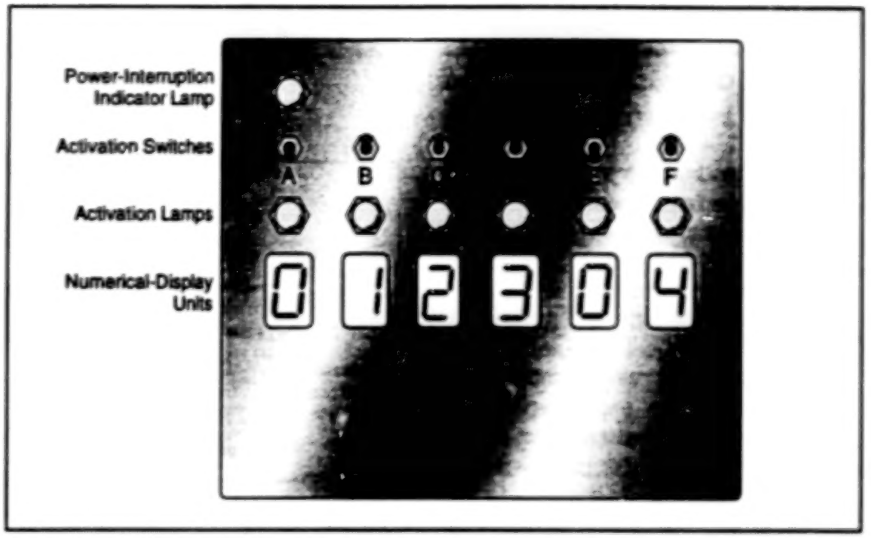

The Front Panel of the Switch Box apprises the technician of the statuses of the flows of the various gases. Gases that have been selected are indicated by illumination of the corresponding activation lamps. The gas controllers assigned to those gases are indicated by the numbers on the numerical-display devices.

This work was done by James R. Wishard and James L. Lamb of Caltech for **NASA's Jet Propulsion Laboratory.** *Further information is contained in a TSP [see page 1].*
NPO-19201

Circuit for Control of Electromechanical Prosthetic Hand

Control signals would be derived from shoulder movements.

Lyndon B. Johnson Space Center, Houston, Texas

A proposed circuit for the control of an electromechanical prosthetic hand would derive electrical control signals from shoulder movements. The circuit can be regarded as an updated, electronic version of a prosthesis, developed in the 19th century, that includes two hooklike fingers actuated via cables from a shoulder harness. Many below-the-elbow amputees still favor prostheses based on that design because of its low cost, reliability, ease of repair, and simplicity of operation. The proposed circuit would be built around the favored shoulder harness, yet would provide more dexterous movement, without incurring the complexity of computer-controlled "bionic" or hydraulically actuated devices.

The harness would contain a linear potentiometer (R_1 in the figure), the resistance of which would be varied by shrugging the shoulder as in the older mechanical system. The variable output voltage of the potentiometer would be fed to an attenuating potentiometer (R_2), which would be set to scale the voltage to the range of shoulder movement. The scaled voltage would be fed to an analog-to-digital converter of the type used to control a bar-graph display. Either a linear or a logarithmic converter could be used, depending on the requirements of the user.

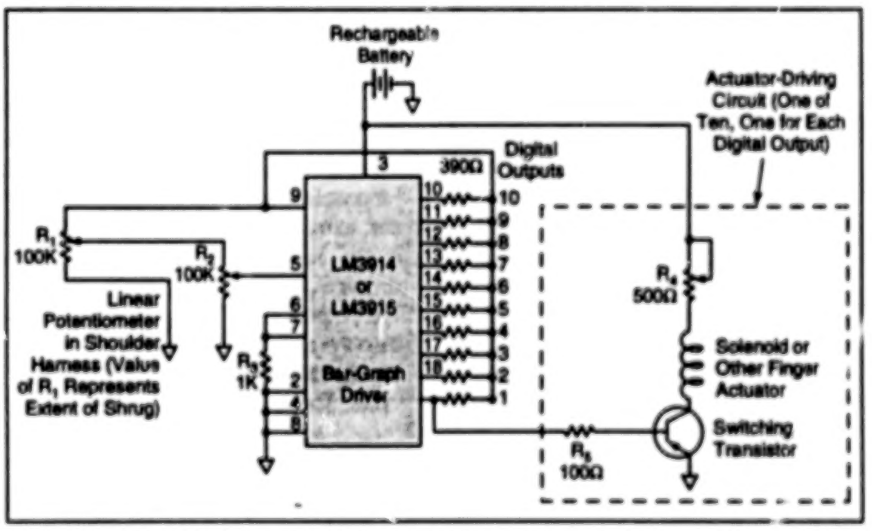

Digital Outputs of the bar-graph driver, representing a sequence of values of R_1, would turn on current to actuators in prosthetic fingers.

Each digital output, in continuous or single-pulse mode, would be fed to a transistor switch, which would supply current to a solenoid or motor to actuate one of the prosthetic fingers. With no shrug, the prosthetic thumb and all of the prosthetic fingers would be extended. As the shrug increased, the digital outputs would turn on in sequence, thereby causing the thumb and fingers to move sequentially to the closed position.

BEST COPY AVAILABLE

8

An additional harness and potentiometer connected to a similar control circuit could be mounted on the other shoulder. This circuit could be used to control a stepping motor that would rotate the hand about the prosthetic wrist to one of a number of angles consistent with the number of digital outputs. The finger-control signals developed by the circuit connected to the first shoulder harness would be transmitted to the prosthetic hand via sliprings at the prosthetic wrist joint.

This work was done by Richard J. Bozeman, Jr., of **Johnson Space Center**. *Further information is contained in a TSP [see page 1].*

This invention is owned by NASA, and a patent application has been filed. Inquiries concerning nonexclusive or exclusive license for its commercial development should be addressed to the Patent Counsel, Johnson Space Center [see page 1]. Refer to MSC-21941.

ASIC for Complex Fixed-Point Arithmetic

A 24-bit design reflects a compromise between precision and speed.

NASA's Jet Propulsion Laboratory, Pasadena, California

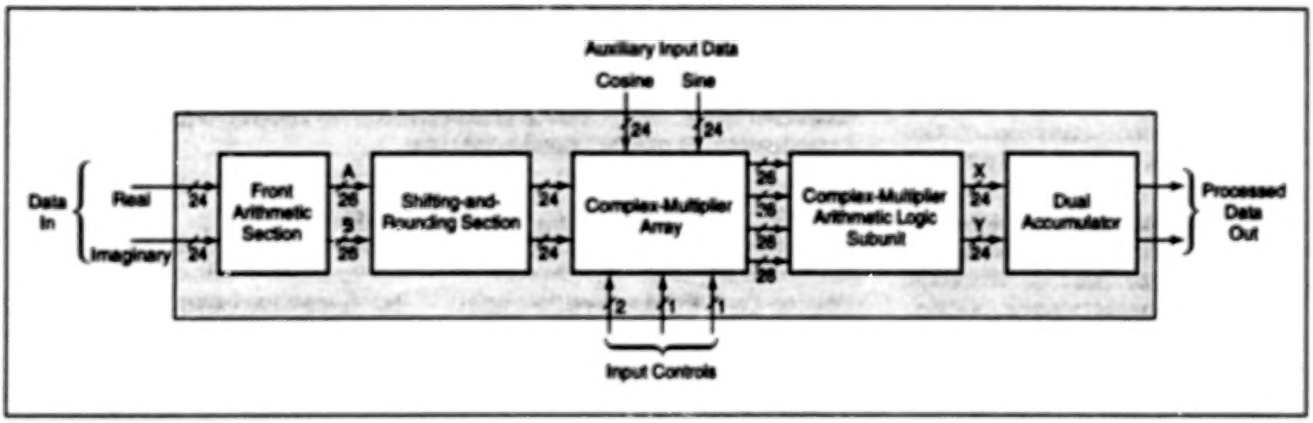

This Digital Signal Processor makes efficient use of an array of more than 110,000 gates in a commercial integrated circuit. It performs a pipeline butterfly FFT operation.

An application-specific integrated circuit (ASIC) performs 24-bit, fixed-point arithmetic operations on arrays of complex-valued input data. It is a high-performance, wide-band arithmetic logic unit (ALU) designed for use in computing fast Fourier transforms (FFTs) and for performing digital filtering functions. Other applications could include general computations involved in analysis of spectra and digital signal processing.

The ASIC was developed to reduce the complexity and cost of a 32-megachannel, 640-MHz digital spectrum analyzer while maintaining the required dynamic range. In comparison with a spectrum analyzer containing a 32-bit ALU, a spectrum analyzer that contains this 24-bit ALU contains fewer processing elements, and the bit width of the required memory is reduced.

At the outset of development of the design of the 24-bit, fixed-point ALU, the only digital-signal-processor parts available were those of 16-bit, fixed-point design and those of 32-bit, floating-point design. The 24-bit, fixed-point design was selected as a compromise between the relative imprecision of the 16-bit design and the relative slowness of processing of the 32-bit design. The 24-bit circuit operates at a rate of 45 MHz in the worst case. The rate of normal operation can be as high as 66 MHz, corresponding to about 800 million operations per second.

The circuit is made from a commercial "sea of gates" integrated-circuit chip, which contains an array of more than 110,000 gates. The chip is fabricated according to 0.8-μm, three-layer complementary metal oxide/semiconductor (CMOS) design rules. The design utilizes more than 95 percent of the available gates: this high fraction of utilization is attributable to the design choice of a pipelined FFT configuration. Inasmuch as data flow in only one direction in a pipeline configuration, the interconnections among gates also flow generally in one direction, thereby making it possible to utilize the array of gates efficiently.

The ASIC (see figure) includes a front arithmetic section that performs the first part of a partitioned FFT butterfly operation. (A butterfly operation is so called because it can be represented by a diagram in which multiple input and multiple output values are shown connected by straight-through and crossover lines that form a pattern that resembles wings of a butterfly.) The front arithmetic unit contains two banks of arithmetic logic subunits, each bank working in parallel. A shifting-and-rounding section that follows the front arithmetic section downshifts the outputs of the front arithmetic section by 0, 1, or 2 bits, according to the user's choice. Ordinarily, the user would choose the downshift parameter to prevent overflow. Downshifted bits are rounded off.

The shifting-and-rounding unit is followed by a complex-multiplier array, which contains four 24-bit multipliers that work in parallel to give 28-bit truncated results. They multiply the shifted and rounded values by cosine and sine inputs. Then a complex-multiplier arithmetic logic subunit combines the products of these multiplications into a complex output, rounded to 24 bits. This completes the pipelined FFT butterfly operation.

The final section of the ASIC is a dual accumulator that makes the ASIC more versatile. The dual accumulator makes it possible to use the ASIC as a multiplier and accumulator, as might be needed, for example, in digital filtering. Each accumulator in the dual accumulator can be operated separately, and 28-bit outputs allow 4 bits of expansion before overflow occurs.

This work was done by Stephen G. Petilli, Michael J. Grimm, and Erland M. Olson of Caltech for **NASA's Jet Propulsion Laboratory**. *Further information is contained in a TSP [see page 1].*
NPO-19102

K_u-Band Data-Communication Adapter

This adapter serves as an interface between a personal computer and a satellite communication system.

Lyndon B. Johnson Space Center, Houston, Texas

A data-communication adapter circuit on a single printed-circuit board serves as a general-purpose interface between a personal computer and a satellite communication system (see figure). The adapter circuit was designed as a direct interface with the K_u-band data-communication system for the payloads on the space shuttle, but can also be used with any radio-frequency transmission systems.

The adapter circuit supports bidirectional communications and can be used at either end of the K_u-band communication link. It can be readily installed in almost any personal computer because it is designed to be connected via the widely used Industry Standard Architecture (ISA) bus; it may also be embedded directly in the space shuttle payload electronics because it provides payload users with a well-documented, well-understood computer interface.

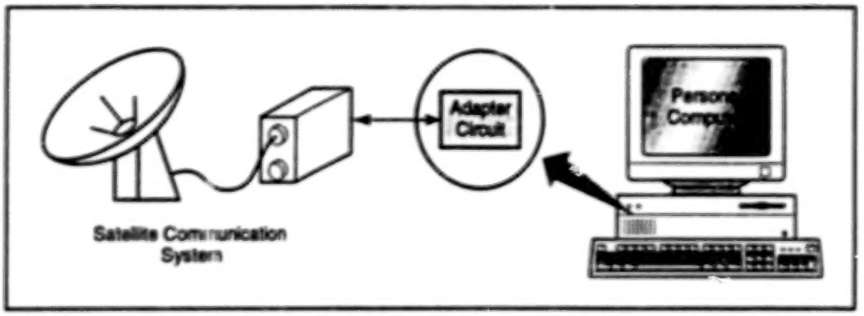

The Adapter Circuit serves as an interface between a computer and a K_u-band data-communication system. It can be readily installed in almost any personal computer via the widely used Industry Standard Architecture (ISA) bus.

The adapter circuit provides extremely reliable data communications by use of a high-performance Reed-Solomon error-correcting code. The integrity of data can be further ensured by implementing computer-to-computer communication protocols, which the circuit supports by virtue of its ISA bus features and its capability for bidirectional communication.

This work was done by Steve Schadelbauer of **Johnson Space Center**. *Further information is contained in a TSP [see page 1].*

MSC-22469

Transient-Switch-Signal Suppressor

The switch-opening or -closing signal is not transmitted until after a preset time.

Lyndon B. Johnson Space Center, Houston, Texas

The figure shows a circuit that delays the transmission of a switch-opening or switch-closing signal until after a preset suppression time. The circuit is used to prevent the transmission of an undesired momentary switch signal. For example, a pressure switch that is meant to be held steadily on or off by a given static pressure in a piping system can also be actuated momentarily by a transient overpressure (sometimes called "water hammer") or underpressure caused by the sudden closure or opening of a valve.

The basic mode of operation is simple. The beginning of the switch signal initiates a timing sequence. If the switch signal persists after the preset suppression time, then this circuit transmits the switch signal to external circuitry. If the switch signal is no longer present after the suppression time, then the switch signal is deemed to be transient, and this circuit does not pass the signal on to external circuitry; from the perspective of the external circuitry, it is as though there were no transient switch signal. The suppression time is preset at a value large enough to allow for the damping of the underlying pressure wave or other mechanical transient.

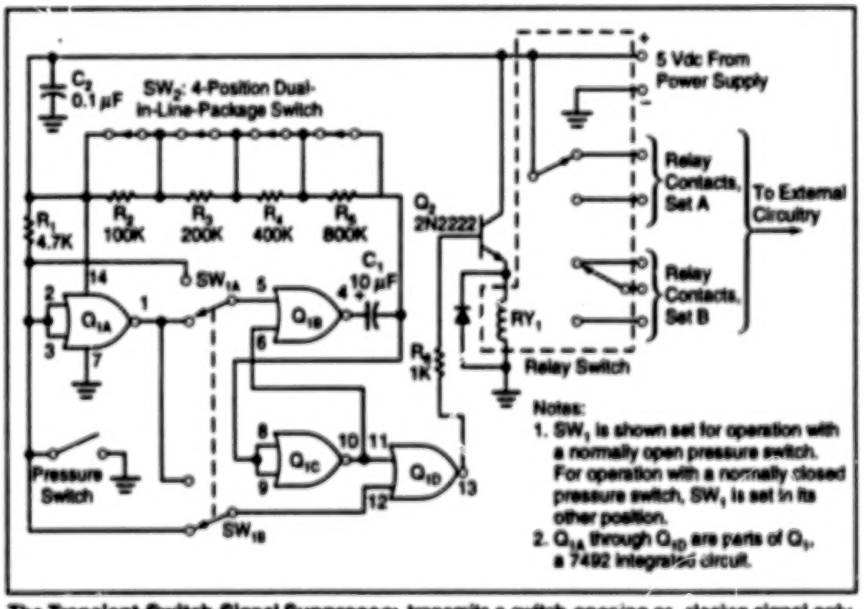

The Transient-Switch-Signal Suppressor transmits a switch-opening or -closing signal only if that signal persists longer than a preset suppression time.

The circuit could be incorporated into a pressure-switch housing. It includes only one transistor/transistor-logic integrated circuit (Q_1) and one discrete transistor (Q_2). It requires a 5-Vdc power supply. By use of double-pole/double-throw switch SW_1, the circuit can be set to operate with either a normally open or normally closed pressure switch. The suppression time is governed by the time constant of the resistor-and-capacitor network of R_1 through R_5 and C_1; the suppression time

can be set between 1 and 15 seconds, in increments of 1 second, by closing or opening the segments of switch S_2 in various binary combinations to remove or insert various combinations of R_2 through R_5 in series.

Suppose, for example, that the circuit is set to operate with a normally open pressure switch. When the pressure switch closes, the output of Q_{1A} goes to logic "high" and remains there during the preset suppression time. This logic "high" pulse gates Q_{1B} and Q_{1C}. The voltage on pin 11 of Q_{1D} is normally at logic "low" except during this pulse. The voltage on pin 12 of Q_{1D} is normally high except when the pressure switch is closed. To generate an output signal through Q_2 and the relay switch, it is necessary to bring the voltages on both pin 11 and pin 12 of Q_{1D} to logic "low"; this does not occur until and unless the pressure switch remains closed after the end of the suppression-time pulse.

This work was done by Richard J. Bozeman of **Johnson Space Center.** *Further information is contained in a TSP [see page 1].*

This invention has been patented by NASA (U.S. Patent No. 5,296,750). Inquiries concerning nonexclusive or exclusive license for its commercial development should be addressed to the Patent Counsel, Johnson Space Center [see page 1]. Refer to MSC-22027.

Digital Latching Circuit for a Safety-Related Application

The "reset" input is effective in resetting the output only when the "set" input is low.

Lyndon B. Johnson Space Center, Houston, Texas

The asynchronous digital latching circuit shown in Figure 1 is designed for use in a safety-related application like turning off power in response to an alarm signal. During normal operation in the absence of an alarm, the "set" (S) and "reset" input voltages are low or off, while the output voltage (Q) is high or on. The "set" input constitutes the alarm signal: whenever "S" goes high (on), Q goes low (off), and thereafter remains low, even when S goes low. Thus, for example, the circuit keeps a power supply turned off even when the alarm has been shut off (see Figure 2).

If a safe condition has been restored, then the circuit can be reset to Q high by applying a high (on) signal to the "reset" (R) input terminal. However, regardless of the R input level, Q cannot be driven high as long as S remains high; that is, the circuit cannot be reset if the alarm signal is still on. Thus, unlike in some other safety-related latching circuits, the "reset" signal cannot override the alarm signal and thereby provide a false indication of safety. Also unlike some safety-related latching circuits, this one does not go into oscillation when the "set" and "reset" inputs change simultaneously.

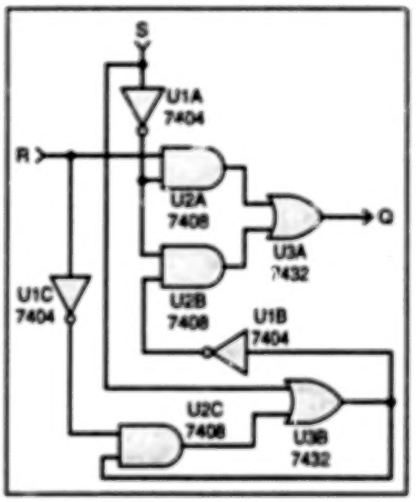

Figure 1.The Asynchronous Digital Latching Circuit is made of standard transistor/transistor logic (TTL) devices. U1 is a hex inverter, U2 is a quad dual-input AND gate, and U3 is a quad dual-input OR gate.

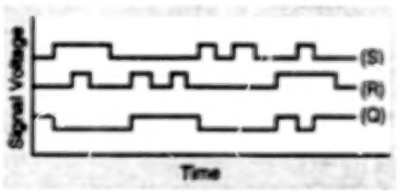

Figure 2. This Timing Diagram illustrates the various modes of operation of the circuit. A high S input causes the output (Q) to go low. Thereafter, a high R input can reset Q to high, but only so long as S remains low.

This work was done by Paul A. Kamp of **Johnson Space Center.** *Further information is contained in a TSP [see page 1].*
MSC-22421

Books and Reports

Test of a Microwave Amplifier With Superconductive Filter

The superconductive filter yielded better performance than did a similar normally conductive filter.

A report describes the design and low-temperature tests of a low-noise GaAs microwave amplifier combined with a microstrip band-pass filter. Two versions of the microstrip filter were used in alternate tests; in one version, the microstrips were formed as films of the high-transition-temperature superconductor Y/Ba/Cu/O on a lanthanum aluminate substrate with a gold film as the ground plane. The other version was identical except that the microstrips as well as the ground plane were made of gold, which is normally conductive. At a test temperature of 77 K, the performance measured with the superconductive filter was superior to that measured with the normally conductive filter: The noise figure with the superconductive filter was 2.1 dB lower, while the gain was 0.5 dB higher.

This work was done by K. B. Bhasin of **Lewis Research Center;** *S. S. Toncich of the National Research Council; C. M. Chorey of Sverdrup Technology, Inc.; and R. R. Bonetti and A. E. Williams of COMSAT Laboratories. To obtain a copy of the report "Performance of a Y-Ba-Cu-O Superconducting Filter/GaAs Low Noise Amplifier Hybrid Circuit," see TSP's [page 1].*
LEW-15908

BLANK PAGE

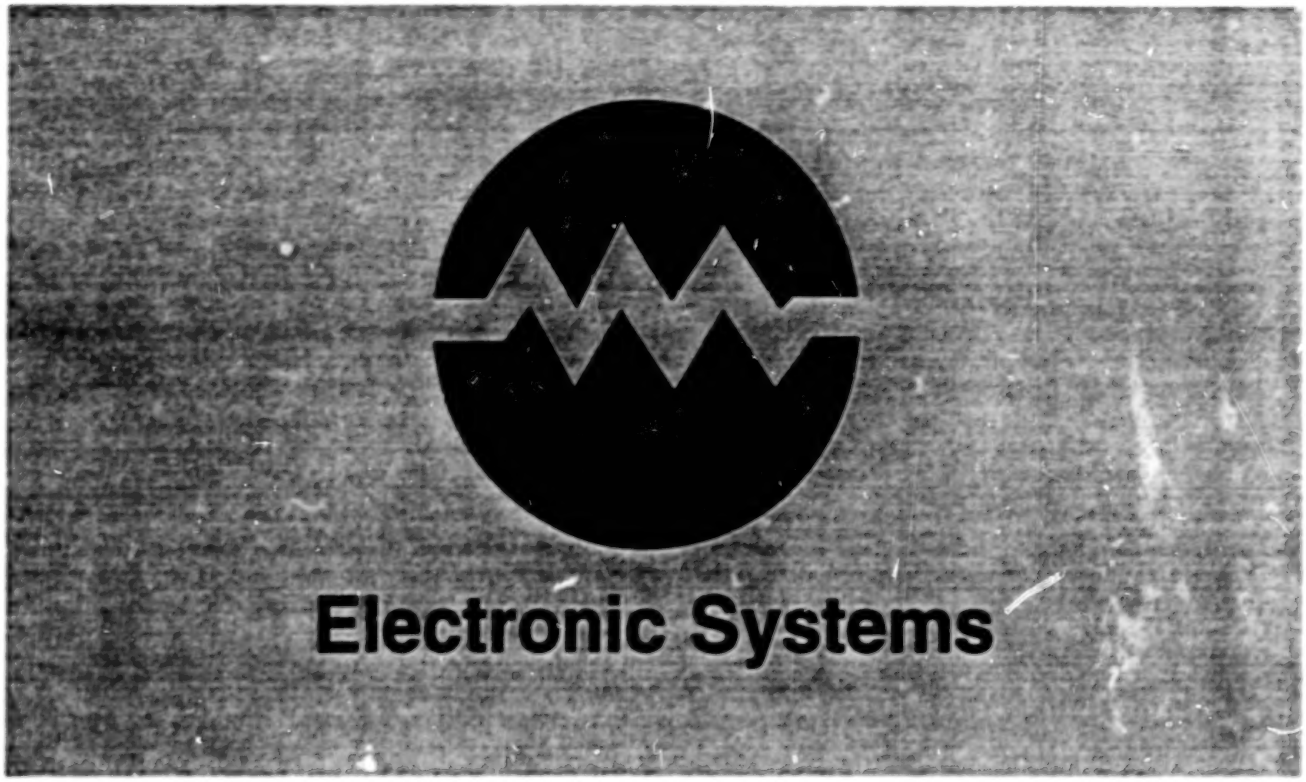

Electronic Systems

Hardware, Techniques, and Processes

15 Optoelectronic Particle-Fallout Sensor
16 Emergency Flight Control Using Computer-Controlled Thrust
17 Optical Interconnection via Computer-Generated Holograms
18 Infrared-Proximity-Sensor Modules for Robot
19 Multiprocessor Adaptive Control of a Dynamic System

Books and Reports

20 Projected-Fringe Profilometer Maps Erosion of Electrode

BLANK PAGE

Optoelectronic Particle-Fallout Sensor

Measured accumulation of particles could be correlated with activities in the vicinity.

John F. Kennedy Space Center, Florida

A portable optoelectronic system monitors fallout of small particles (dust and fibers) onto a surface at a given location during an extended time. Data on the accumulated fallout can be downloaded from this system to a computer for display and analysis. A typical display is a plot of a signal proportional to the amount of accumulated fallout as a function of time and thus can be read to determine when contamination occurs. In many cases, it may be possible to establish correlations between accumulations of particles and activities in the vicinity (see figure). The system is also capable of signaling an alarm in the event that contamination by fallout exceeds a specified level.

The system includes a sensor module and a data-acquisition module. Both modules are battery-powered and contain microcontrollers and other circuitry. The sensor module can operate either independently or under control by the data-acquisition module.

The sensor module includes a black acetal plastic housing with a top opening through which dust can fall onto a mirror. A portion of the mirror is illuminated by an infrared light-emitting diode through a limiting aperture. Particles that have accumulated on the mirror are detected via the infrared light that they scatter. When particles are present on the mirror (and provided that the mirror is not scratched), the infrared light is reflected specularly by the mirror and absorbed by the black sides and top of the housing. When particles are present, the infrared light that they scatter is measured by an optoelectronic detector assembly.

The optics are arranged to minimize the detection of both ambient light and light scattered from surfaces other than that of the mirror. The optoelectronic detector assembly includes two lenses, a long-wavelength-pass filter that helps to suppress ambient visible light, and a large-area silicon photodetector. The output of the photodetector is amplified and digitized, and the digital value is shown on a liquid-crystal display unit.

At the press of a momentary contact button, the sensor module displays a number proportional to the amount of scattered light received by the detector.

To conserve battery energy, the sensor module is designed to operate for only a few seconds — just long enough to take a reading when it is commanded to do so. When separated from the data-acquisition module, the sensor module is turned on to take a reading by pressing a momentary-contact button switch. To increase sensitivity and facilitate discrimination against background signals, the infrared light-emitting diode is turned off and on several thousand times during each sampling interval. The difference between the signals measured in the "on" and "off" states is averaged over the sampling interval to produce a signal that contains relatively low noise.

To operate the two modules together, it is necessary to connect them via a ribbon cable. In this configuration, the data-acquisition module takes control of, and supplies power to, the sensor module. At time intervals selected by the operator, the data-acquisition module commands the sensor module to take readings and records each reading and the time when it was taken. The module can later be connected to a computer to transfer the reading and time data to the computer for display and/or analysis and to program the data-acquisition module for subsequent readings.

The system can be made very inexpensively and can be used to monitor the accumulation of dust and fibers associated with motion of air in a variety of environments. Phenomena that could be monitored indirectly by use of this system might include circulation of air in buildings, and human and animal activity. The system could also serve as an auxiliary intrusion monitor (though probably not a real-time alarm) in a sealed room because motion of an intruder inevitably stirs up some dust.

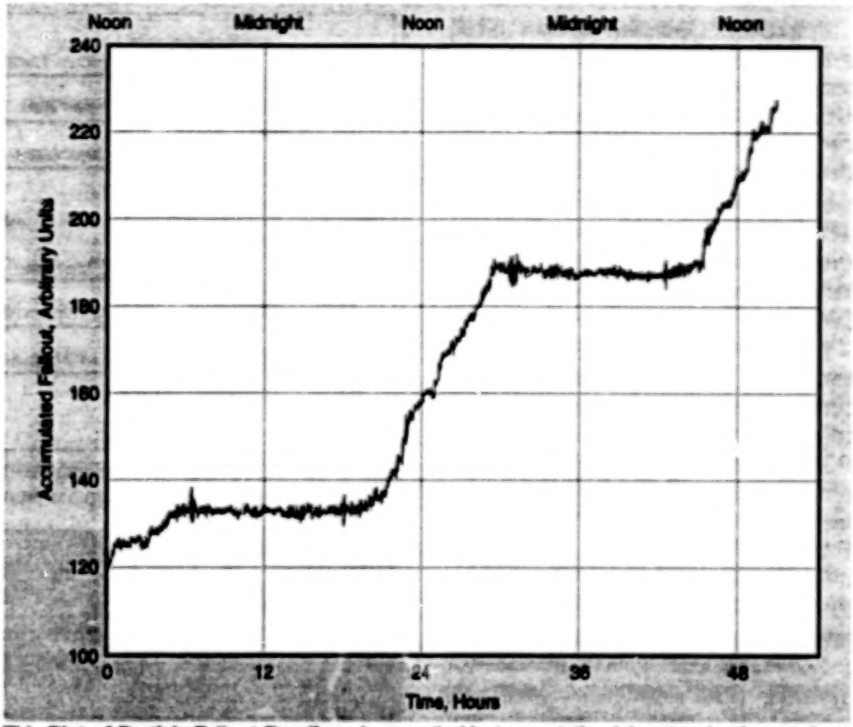

This Plot of Particle-Fallout Readings in an optical-instrumentation laboratory begins at about noon on a work day. During the night, when the air in the laboratory is still, there is little increase in fallout. During the day, there is a significant increase, corresponding to activity in the laboratory.

This work was done by Curtis Ihlefeld and Paul A. Mogan of **Kennedy Space Center** *and Robert C. Youngquist, John S. Moerk, William D. Haskell, Robert B. Cox, and Kenneth A. Rose of I-NET. Further information is contained in a TSP [see page 1].*

Further development of this instrumentation by NASA is anticipated. Potential dual-use development partners are encouraged to call the Kennedy Space Center at (407) 867-3017.

This invention is owned by NASA, and a patent application has been filed. Inquiries concerning nonexclusive or exclusive license for its commercial development should be addressed to the Patent Counsel, Kennedy Space Center [see page 1]. Refer to KSC-11687.

BEST COPY AVAILABLE

Emergency Flight Control Using Computer-Controlled Thrust

Computer-controlled engine thrust provides landing capability when control surfaces are inoperable.

Dryden Flight Research Center, Edwards, California

Propulsion Controlled Aircraft (PCA) systems are digital electronic control systems that are undergoing development to provide limited maneuvering ability through variations of individual engine thrusts in multiple-engine airplanes. PCA systems are meant for emergency use when the flight controls become inoperative. [As used here, "flight controls" includes exterior flight-control surfaces (ailerons, trim tabs, elevators, and/or rudder) and the control systems and subsystems that affect their functions. "Flight controls" as used here does not include engine controls.] The development of PCA systems was prompted by several accidents, in each of which all or part of the flight-control system failed. The NASA F-15 research airplane was equipped with a PCA system and was the first airplane to be intentionally landed using only engine-thrust control for maneuvering.

During the initial efforts to develop PCA systems, flight experiments were performed on a variety of airplanes, from fighters to transports. These studies showed that with the pilot manually controlling the throttles and with all flight controls locked, it was possible to maintain gross control. Altitude could be maintained within a few hundred feet (~100 m) by using both throttles together. To climb, thrust would be increased; to descend, thrust would be reduced. Heading could be controlled to within a few degrees, using differential throttle to generate yaw, which results in roll.

These same flight experiments showed that maneuvering solely through manual throttle control was not precise enough to enable landing on a runway. This was attributed to the small control forces and moments available from engine thrust, difficulty in controlling the phugoid motion of the airplane, and difficulty in compensating for the lag in engine response. Simulation studies at Dryden Flight Research Center and at McDonnell Douglas have been able to duplicate the results of the flight experiments.

Control research and simulation studies at Dryden Flight Research Center also established the feasibility of a thrust control system based on the use of a digital computer with feedbacks of such parameters as flightpath angle, pitch rate, bank angle, and yaw rate (see Figure 1). The flightpath command from the pilot is compared with the measured flightpath, and, using the pitch rate for phugoid damping, collective throttle is commanded to achieve the desired flightpath. The time required to achieve a flightpath command is between 7 and 10 seconds. The bank-angle command from the pilot is compared with the measured bank angle, and, by use of the yaw rate to stabilize the Dutch roll, differential throttle is commanded to satisfy the bank-angle command. A small bank-angle command can be satisfied in about 5 seconds.

Prior to the addition of a PCA system, the NASA F-15 research airplane was already equipped with a digital electronic control system that included a digital engine-control subsystem, a digital flight-control subsystem, and a general-purpose computer and data bus to enable these digital subsystems to communicate with each other, making it an ideal testbed airplane for this research. There was also a cockpit computer panel through which the pilot could provide control-system inputs, select options and vary control-system gains. The only equipment added to the airplane in installing the PCA system was a control panel containing two thumbwheels; one for the pilot's flightpath command, and the other for bank-angle command. All of the needed sensors and actuators were already available from previous research on integrated flight/propulsion control. Control computations were performed in the research computer.

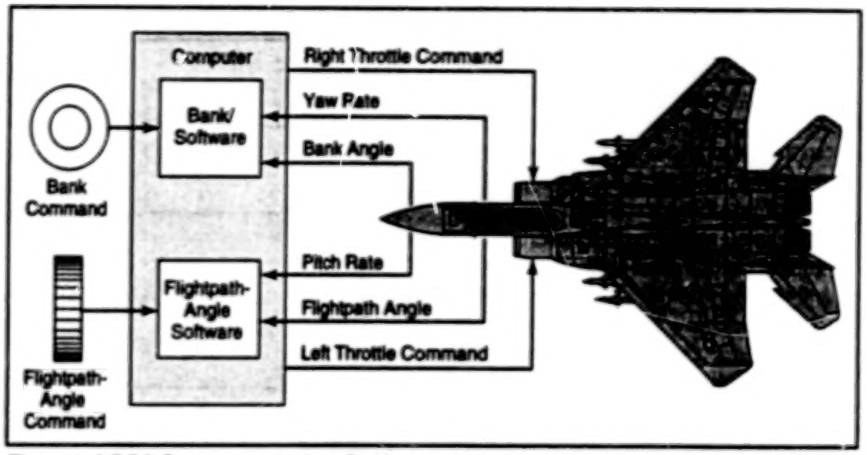

Figure 1. A PCA System can be installed in a multiple-engine airplane to obtain limited emergency maneuvering ability through computer control of engine thrust alone.

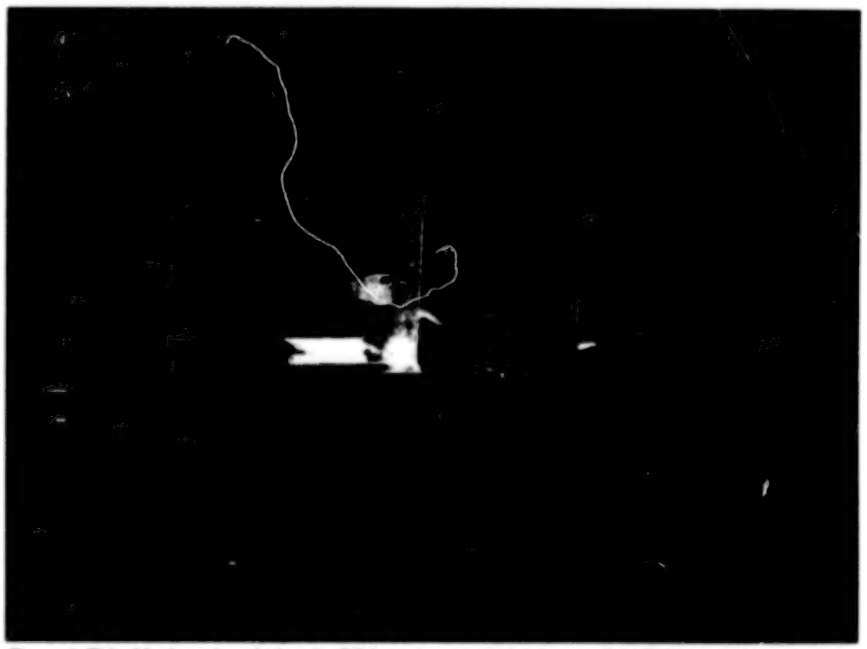

Figure 2. This Airplane Landed under PCA-system control only; no other flight controls were used.

BEST COPY AVAILABLE

16

In flight tests of the PCA system, the NASA F-15 airplane was flown at speeds of 150 knots (77 m/s) with the flaps down and at 170 knots (87 m/s) and 190 knots (98 m/s) with the flaps up. Former astronaut Gordon Fullerton was the project pilot. Initial flights with the PCA system tested response to small-step thumbwheel inputs. Later, low approaches were flown, and finally, PCA control was used for landings (see Figure 2) without using any flight controls.

Several guest pilots, including United States Air Force, United States Navy, NASA, and contractor pilots, also flew the F-15 airplane with the PCA system. All pilots flew with a simulated failure of the flight-control system, engagement of the PCA system, recovery, descent, and landing approach. Pilots' comments were very favorable.

The simulated failure was initiated at a speed of 250 knots (129 m/s) and altitude of 12,000 ft. (3.7 km). To simulate a failure of the hydraulic system, the pilot trimmed the airplane, then rolled into a 90° bank, released the flight controls, and engaged the PCA system as the nose dropped through –20°. The PCA system used full differential thrust to roll the wings level, then varied collective thrust to damp the phugoid motion. The pilot lowered the gear and flaps, and the airplane trimmed at 150 knots (77 m/s). The pilot then turned toward the runway at Edwards Air Force Base, initiated a descent, and made a long straight-in approach to the runway, ending 20 ft (6.1m) high over the end of the runway, in good position to land.

PCA systems can be incorporated on existing and future airplanes that include digital engine controls, digital flight controls, and digital data buses. Depending on the exact configuration, it could be possible to implement the entire PCA system in software, thus adding no weight or additional hardware to an airplane. The PCA system can make the airplane safer by making it possible to handle a total failure of the hydraulic system, depending on how surfaces respond to loss of hydraulic pressure. It may also be possible to handle broken control cables or linkages. The PCA system might also be used to save weight and cost through replacement of mechanical backup flight-control systems. Future airplanes could incorporate PCA systems that would use navigation data from the Global Positioning System for guidance to any suitable emergency runway in the world.

This work was done by Frank W. Burcham, Jr., C. Gordon Fullerton, James F. Stewart, and Glenn B. Gilyard of **Dryden Flight Research Center** *and Joseph A. Conley of Ames Research Center. No further documentation is available.*

This invention has been patented by NASA (U.S. Patent No. 5,330,131). Inquiries concerning nonexclusive or exclusive license for its commercial development should be addressed to the Patent Counsel, Dryden Flight Research Center [see page 1]. Refer to DRC-00004.

Optical Interconnection via Computer-Generated Holograms

Connections between many sources and many detectors can be reconfigured in real time.

NASA's Jet Propulsion Laboratory, Pasadena, California

A method of free-space optical interconnection is being developed for data-processing applications like parallel optical computing, neural-network computing, and switching in optical communication networks. In this method, multiple optical connections between multiple sources of light in one array and multiple photodetectors in another array are made via computer-generated holograms in electrically addressed spatial light modulators (ESLMs).

In comparison with electronic interconnections, free-space optical interconnections in general offer potential advantages of massive parallelism, high space-bandwidth product, high time-bandwidth product, low power consumption, low cross talk, and low time skew. The present method of optical interconnection offers the additional potential advantage of programmability with flexibility of reconfiguration, including variation of the strengths of optical connections in real time.

This method makes possible a large variety of interconnection schemes, including one-to-many, crossover, and many-to-many (see Figure 1). The computer-generated hologram that implements a given interconnection scheme is formed by applying suitable voltages to the terminals of the affected ESLM to obtain the required complex-amplitude (magnitude and phase) transmittance in each pixel of the ESLM. In practice, an ESLM is typically a liquid-crystal television (LCTV) display unit that has some imperfections, including leakage of light and gaps between its pixels.

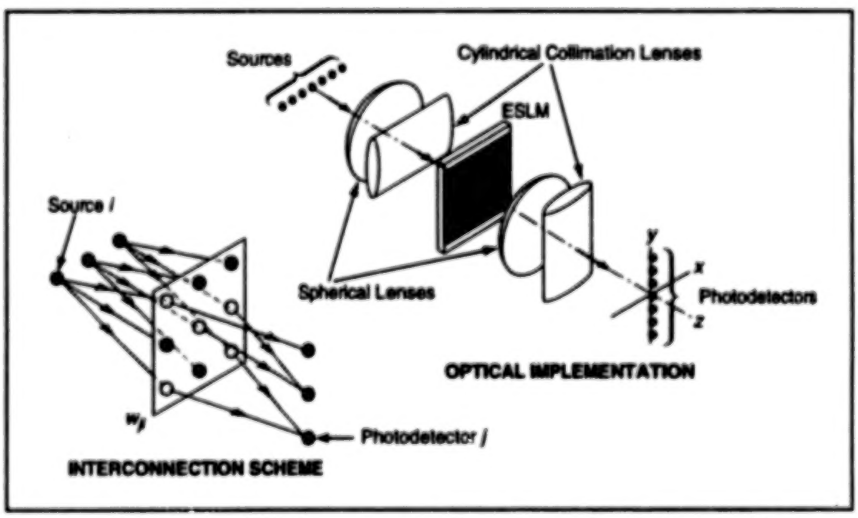

Figure 1. In This Many-to-Many Interconnection Network, a number of different sub-holograms are formed in the ESLM, which is illuminated by a number of sources.

The ESLM holographic pattern needed to produce a given interconnection scheme is computed, taking account of these imperfections, by use of a fast-Fourier-transform algorithm in conjunction with a simulated-annealing iteration algorithm. The hologram can comprise a number of sub-holograms that effect multiple interconnections characterized by a matrix w_{ij} (where w_{ij} denotes the strength of the connection between the ith light source and the jth photodetector).

The error measure used to determine whether a given iteration of the computed ESLM holographic pattern would or

would not achieve a close enough approximation to the desired interconnection scheme is the sum of (1) the root-mean-square error of the intensities of light at the required focal points on the photodetector array and (2) the diffraction efficiency expressed as the sum of powers in the focal spots divided by the total incident power. Once the ESLM holographic pattern has been computed, the voltages needed to produce it are computed with the help of voltage-vs.-complex-amplitude data from calibration measurements on the ESLM.

In a prototype, an LCTV was operated in phase mode, so that only phase-vs.-voltage calibration data were used. The prototype was tested by computer simulation and by experiment on a number of different interconnection schemes. The tests yielded excellent results (for example, see Figure 2), thereby demonstrating the feasibility of the method.

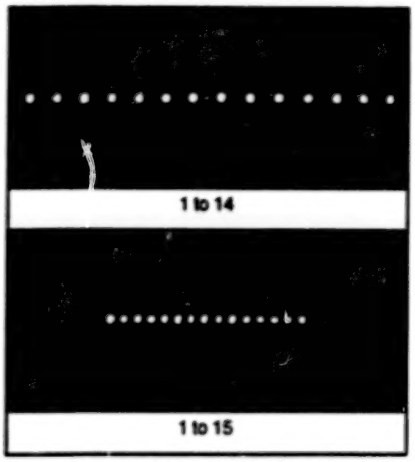

Figure 2. These Output Light-Spot Patterns were obtained in experiments on a 1-to-14 and a 1-to-15 interconnection scheme.

This work was done by Hua-Kuang Liu and Shaomin Zhou of Caltech for **NASA's Jet Propulsion Laboratory.** *Further information is contained in a TSP [see page 1].*

This invention is owned by NASA, and a patent application has been filed. Inquiries concerning nonexclusive or exclusive license for its commercial development should be addressed to the Patent Counsel, NASA Resident Office-JPL [see page 1]. Refer to NPO-19039.

Infrared-Proximity-Sensor Modules for Robot

Proximity alarms are based on data received from multiple sensor modules.

John F. Kennedy Space Center, Florida

A collision-avoidance system for articulated robot manipulators uses infrared proximity sensors grouped together in an array of sensor modules. These sensor modules, called "sensorCells," are distributed processing board-level products for acquiring data from proximity-sensors strategically mounted on robot manipulators. Each sensorCell is self-contained and consists of multiple sensing elements, discrete electronics, a microcontroller and communications components. The modules are connected to a central control computer by a redundant serial digital communication subsystem that includes both a serial and a multi-drop bus. This sensor system is able to detect objects made of various materials at a distance of up to 50 cm (19 in.). For some materials, such as thermal protection system tiles, the detection range is reduced to approximately 20 cm (8 in.).

Each module (see figure) contains light-emitting diodes that illuminate the scene to be monitored with infrared light (wavelength 880 nm), plus up to sixteen positive/intrinsic/negative photodiodes that detect infrared light reflected from objects in the scene. The outputs of the photodiodes are processed into digital signals in a standard format for transmission to the control computer. This arrangement reduces vulnerability to electronic noise, which can degrade the performance of an all-analog sensing system. Since the digital communication is independent of the specific type of sensing media, different types, such as acoustical or capacitive sensors, could be used within the same system.

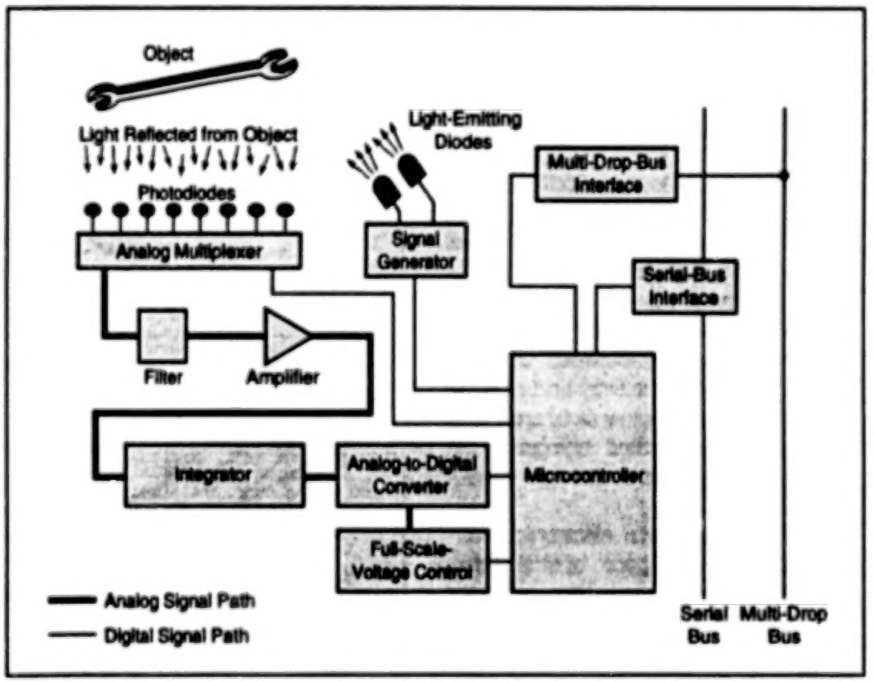

A Proximity-Sensor Module (one of many) contains two infrared-light-emitting diodes, eight photodetectors that detect reflected infrared light, and control and signal-processing circuits. The microcontroller in the module communicates with a central control computer via serial and multidrop buses.

The central component of the sensorCell is the onboard microcontroller. The microcontroller communicates with the control computer via the buses, controls the operation of the sensing elements, and performs low-level processing of sensory data. This distributed processing architecture greatly reduces the computational overhead of a central control computer and, by pre-processing the sensor data with the microcontroller, the communication requirements are also reduced. Operating according to commands from the control computer in conjunction with embedded firmware instructions, the microcontroller causes a signal generator to drive the light-emitting diodes with a signal at a frequency of 31.25-kHz when commanded to perform a scan.

Simultaneously, the microcontroller sends the outputs of the photodiodes in sequence through an analog multiplexer to a high pass filter that removes most ambient noise while preserving the 31.25-kHz signals indicative of infrared reflections detected by the photodiodes.

The filtered signals are fed to a high-gain amplifier, then to an analog integrator that converts the signals to voltages proportional to the energies of the detected infrared reflections. An analog to digital converter then converts the dc voltages to digital form for processing by the microcontroller into proximity data and proximity alarms.

The serial bus is a standard RS-485 serial interface that operates at a data rate of up to 9,600 bits per second. This bus enables the control computer to identify an alarming module by its address, and provides communications by module address for coordination of scanning. The serial-bus scanning time is approximately 10 ms per module when no proximity alarms are encountered.

The multidrop bus enables the control computer to simultaneously command all modules and to receive a proximity alarm from any module immediately, identifying that module by its address, which is part of the alarm signal. The multidrop bus can be used, as a backup to the serial bus, to scan by polling the modules; in this case, the scanning time is approximately 12 ms per module in the absence of proximity alarms. Programs at the control computer initialize hardware ports for communication on the buses, generate sensor cell addresses, and initially set default gain and threshold values for each module.

This work was done by William Parton, Daniel Wegerif, and Douglas Rosinski of Merritt Systems, Inc., for **Kennedy Space Center.** *Further information is contained in a TSP [see page 1].*
KSC-11608

Multiprocessor Adaptive Control of a Dynamic System

A modular, hierarchical architecture combines standardized processing units.

Langley Research Center, Hampton, Virginia

An architecture for a fully autonomous digital electronic control system has been developed for use in identification (defined below) and adaptive control (also defined below) of a dynamic system. The architecture is modular and hierarchical. It combines relatively simple, standardized processing units into complex parallel-processing subsystems. Although the architecture is based on a neural-network concept, the processing units themselves are not neural networks; the processing units are implemented by programming of currently available microprocessors.

As used here, "identification" does not have its usual meaning. In the specialized discipline of mathematical modeling and control of the dynamics of complex systems, "identification" is short for "system identification," which, in turn, is short for identification of the parameters of a mathematical model that represents the dynamics of a system. "Adaptive control" denotes a strategy for adapting a control system, in real time, to changes in the parameters in such a way as to continually strive to optimize the control performance. The relevant modeling and control concepts are not limited to any particular dynamic system; however, in a typical application, the dynamic system comprises a flexible structure equipped with vibration sensors and actuators, and the control objective is to process the sensor outputs into actuator commands to suppress vibrations in the structure.

A control system of the type in question (see Figure 1) implements a model-reference adaptive control (MRAC) scheme. In MRAC, identical training stimuli are applied to both a dynamic system subject to unknown disturbances and to a reference subsystem, which is an idealized mathematical model of the dynamic system implemented in software. The sensor outputs (converted to time series of digitized samples) from the dynamic system are compared with corresponding sensor outputs from the reference subsystem. This comparison yields an error signal, which drives the adaptation of the control system so that the closed-loop input/output relations of the dynamic and control systems (from sensors to actuators) are made to match those of the reference subsystem.

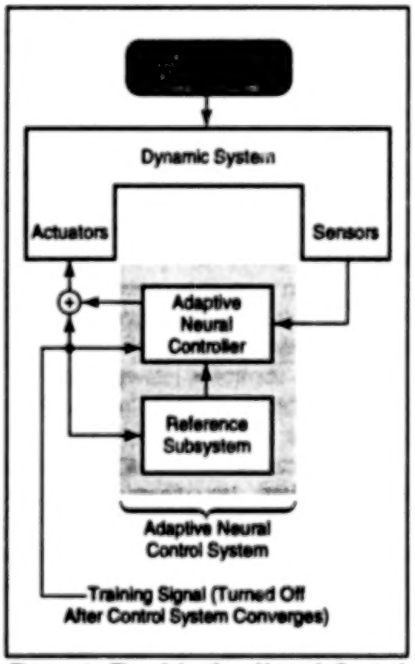

Figure 1. The Adaptive Neural Control System is trained to implement a model-reference adaptive control scheme.

Figure 2 illustrates the hierarchy of modular structures used to implement the control scheme. The processing units at the lowest level of the hierarchy are tapped delay lines and units that implement mathematical models of neurons with both forward and backward signal paths. The adjustment of each of the synaptic weights, W_{ij}, according to a local learning law, is built into each processor. Moreover, the adaptive speeds (or rates of learning) $\mu_{ij}(n)$, are updated so as to guarantee convergence in both system identification and adaptive control.

The key to using the neurons for dynamic-system identification is to organize them into larger building blocks that are reminiscent of biological ganglia and are therefore called "dynamic ganglia." A dynamic ganglion is an array of L neurons allocated as a unit to process a time series signal and its $L - 1$ delayed values. The neurons in a ganglion are connected to each other via a Toeplitz synapse, which is an array of synapses, the matrix of synaptic weights of which is upper triangular: the upper triangular structure is designed to preserve temporal ordering and causality. The synaptic weights in the Toeplitz synapse are adapted iteratively by a gradient-descent algorithm.

The next higher level of the hierarchy comprises replicator units, each of

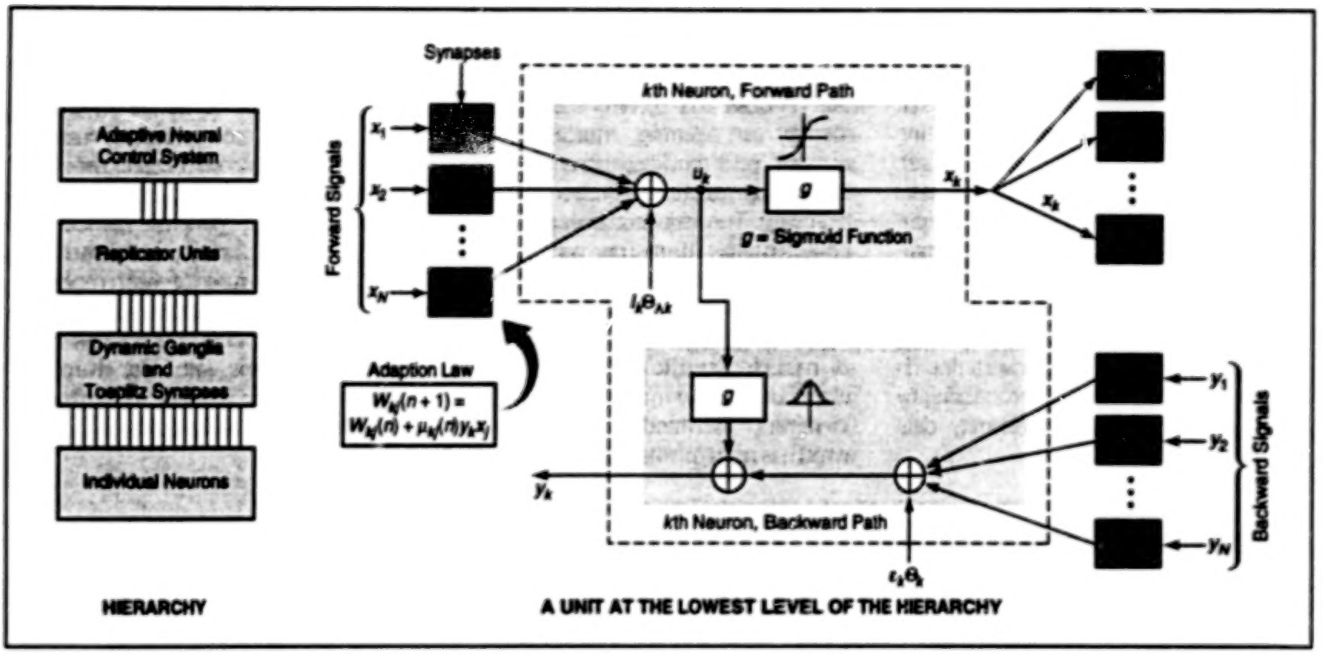

Figure 2. The Hierarchical Structure groups neurons and synapses into modular substructures that, collectively, perform the various adaptive control functions.

which comprises several ganglia connected by a Toeplitz synapse. The fundamental function of a replicator unit is to duplicate the output of a previously unknown sampled-data dynamic system when both the replicator and the system are stimulated by the same training input.

Several replicator units are combined to form an adaptive neural control system. For the present case of MRAC, the most basic adaptive neural control architecture comprises two main parts: a closed-loop modeler and a control adaptor. Each of these parts comprises at least two replicator units. The closed-loop modeler uses the training signal and the sensor outputs from the real dynamic system to adapt matrices of synaptic weights to make the closed-loop behavior of the reference system imitate that of the real dynamic system; in effect, the closed-loop modeler identifies the dynamic system within the closed control loop. The control adaptor, which generates its own internal mathematical model of the dynamic system, uses the training signal, its own output, and the output of the reference system to adjust its matrices of synaptic weights so that the reference system is replicated.

The basic adaptive control scheme involves simultaneous convergence of both the internal dynamical model and the optimal controller. However, subsequent studies have shown that a nonsimultaneous "zigzag" approach to convergence is more efficient and requires half the neural hardware involved in the basic scheme. In the zigzag approach, the control system alternates between refinement of the model and adaptation of control.

Because of the massive parallelism of the architecture, it is possible to configure the modular computing hardware in numerous different ways. As a practical matter, it turns out to be most effective and convenient to group the fundamental processing units into four types of more complex fundamental processing units that constitute the standardized processing units mentioned previously, each of which effects a mixture of neural and synaptic functions. These standard types of units are (1) a modified version of the Toeplitz synapses, (2) a modified version of the dynamic ganglions, (3) branching and summing junctions, and (4) tapped delay lines that also serve as memory units.

This work was done by Jer-Nan Juang of **Langley Research Center** *and David C. Hyland of Harris Corp. No further documentation is available.*

Inquiries concerning rights for the commercial use of this invention should be addressed to the Patent Counsel, Langley Research Center [see page 1]. Refer to LAR-15243.

Books and Reports

Projected-Fringe Profilometer Maps Erosion of Electrode

The capabilities of this instrument are demonstrated.

A report describes the use of a projected-fringe, phase-stepping optical profilometer to measure the three-dimensional shape of the surface of a molybdenum electrode that had been eroded in an ion engine. The instrumentation used in these measurements was very similar to that described in "Projected-Fringe, Phase-Stepping Profilometer" (LEW-14996), *NASA Tech Briefs*, Vol. 16, No. 9 (September, 1992), page 52. To recapitulate: a projected-fringe, phase-stepping profilometer generates phase-controlled beams of light from a split laser beam and manipulates these beams to project interference fringes onto the surface to be mapped. The phases of the interfering beams of light are stepped in such a way that the resulting changes in the fringe pattern yield data equivalent to a topographical map of the surface. Video images of the

fringes are digitized, then processed by a computer to extract the topographical data. In the application described in the report, the capabilities of the projected-fringe profilometer to measure the surface on a variety of resolution scales was demonstrated: Across an area 40 cm wide, the uncertainty in the measured surface height was 2 mm. Across an area about 5 mm wide, uncertainty in the surface height varied between 10 and 25 μm.

This work was done by Gregory S. MacRae and Carolyn R. Mercer of **Lewis Research Center**. *To obtain a copy of the report "Laser Interferometric Measurement of Ion Electrode Shape and Charge Exchange Erosion," see TSP's [page 1].*
LEW-15947

BLANK PAGE

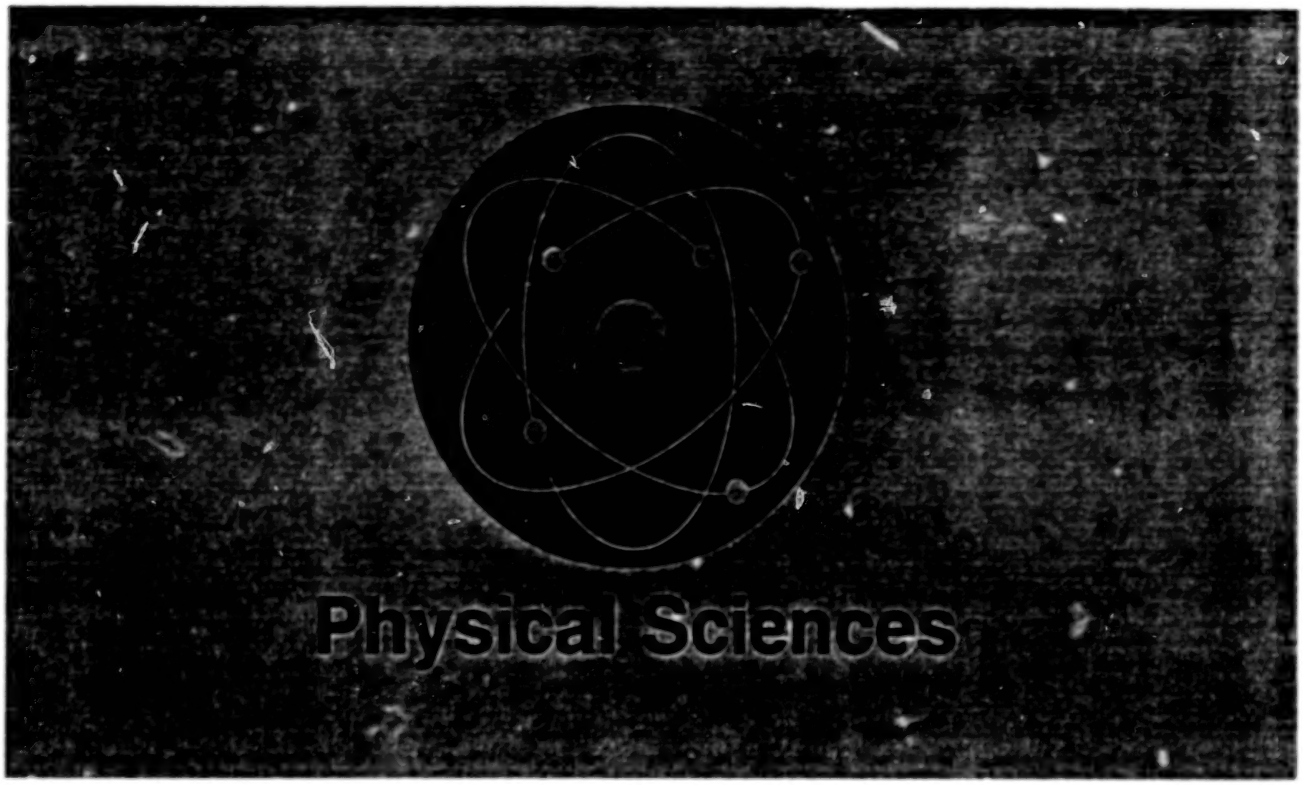

Hardware, Techniques, and Processes

25 Glass-Ampoule Breaker
25 Probes for Measuring Changing Internal Temperatures
26 Bakeout Chamber Within Vacuum Chamber
27 Increasing Precision of Temperature Sensors for Liquid H_2
28 Carbon/Carbon Grids for Ion Sources

BLANK PAGE

Glass-Ampoule Breaker

Ampoules are fractured repeatably, and their contents retained.

Lyndon B. Johnson Space Center, Houston, Texas

A device breaks a glass ampoule in a repeatable manner and retains its gaseous content so that the pressure of the gas can be measured accurately. The apparatus was developed for use in experiments on compatibility of materials. In such an experiment, a combination of materials (typically, a solid and a liquid) is placed in the ampoule, which is then evacuated, sealed, and stored for a suitably long time. The ampoule is then broken, and the pressure of its contents is measured. The magnitude of the pressure indicates the extent to which the materials have reacted and, thus, their compatibility.

The device (see figure) includes a stainless-steel compression ring, a stainless-steel lower housing, a polypropylene sleeve, a stainless-steel sleeve, and an upper stainless-steel housing. A technician inserts an ampoule into the polypropylene sleeve in the lower housing, slips the stainless-steel sleeve over the ampoule and into the lower stainless-steel housing, slips the compression ring over the ampoule, and threads the upper housing part way onto the lower one, leaving a small gap between the lip of the upper housing and the flange of the lower housing. An O-ring between the lower and upper housings makes a pressure seal, which makes it possible to evacuate the interior chamber created by assembly of the housings. The evacuation is performed via one of two ports near the top of the device.

After evacuation, the technician closes a valve on the evacuation port to preserve the vacuum, disconnects the vacuum pump, and further tightens the upper housing on the lower housing until the lip contacts the flange. This final threading forces the compression ring to collapse radially against the neck of the ampoule, thereby breaking the ampoule and releasing its gas. The technician reads the pressure of the gas by use of a pressure gauge connected to the other port.

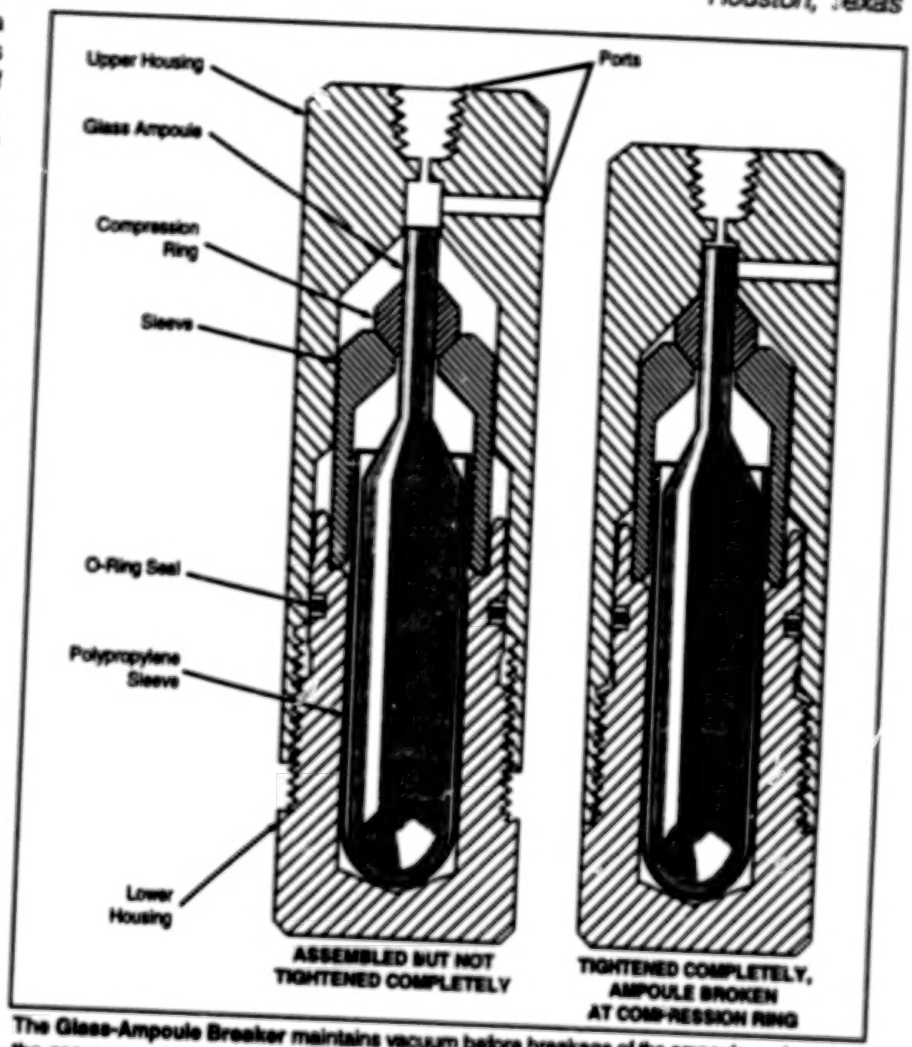

The Glass-Ampoule Breaker maintains vacuum before breakage of the ampoule and retains the gaseous content of the ampoule after breakage.

The device breaks ampoules reliably, always at the same location, forming a repeatable pressure-retaining cavity volume, thereby helping to ensure accurate measurements. In addition, it protects the technician from the gaseous contents, which may be hazardous. Broken glass and sample materials may easily be removed for disposal or analysis.

This work was done by R. C. Christianson, Surender M. Kaushik, and Dennis D. Davis of Lockheed Engineering & Sciences Co. for **Johnson Space Center**. *Further information is contained in a TSP [see page 1].*

MSC-22101

Probes for Measuring Changing Internal Temperatures

The thermal characteristics of a probe are chosen for accuracy and speed of response.

Marshall Space Flight Center, Alabama

Improved thermocouple probes have been devised for measuring rapidly changing temperatures within layers of solid materials. In the original application, the layers in question are carbon-cloth phenolic liners in solid-rocket motor nozzles, and the probes are inserted in the layers to various depths of the order of 0.5 in. (about 13 mm) to measure changing temperatures in the layers during hot-fire tests. The basic probe concept can be adapted to measurements of temperatures inside various other layers, materials, and components, including material test specimens.

The thermocouple probes used previously to measure temperatures within the liners during the hot-fire tests responded too slowly and inaccurately. This is because the probe bodies conducted substantial amounts of heat away from the thermocouple junctions and the junctions were in poor thermal contact with the surrounding materials under test. The bodies of the improved probes are made of the same materials as those of the layers to be tested. In constructing an improved probe to be inserted in a composite material to be tested, the plies in the probe body should also be oriented the same as in the material under test. In preparation for installation of a probe, a flat-bottomed hole is machined to the desired depth in the material layer to be tested. The probe is then inserted along with a suitable adhesive to hold it in place and enhance thermal contact.

The innermost end of the probe is flat, and the thermocouple wires in the vicinity of the thermocouple junction are laid out on the flat end, which is assumed to lie on an isotherm approximately parallel to the surface of the layer to be tested: This minimizes conduction of heat along the thermocouple wires in the immediate neighborhood of the thermocouple junction, thus helping to ensure that the temperature of the junction closely follows that in the material under test. The remainder of the thermocouple wires are laid in a groove along the probe body and brought out to connect them to measuring circuitry.

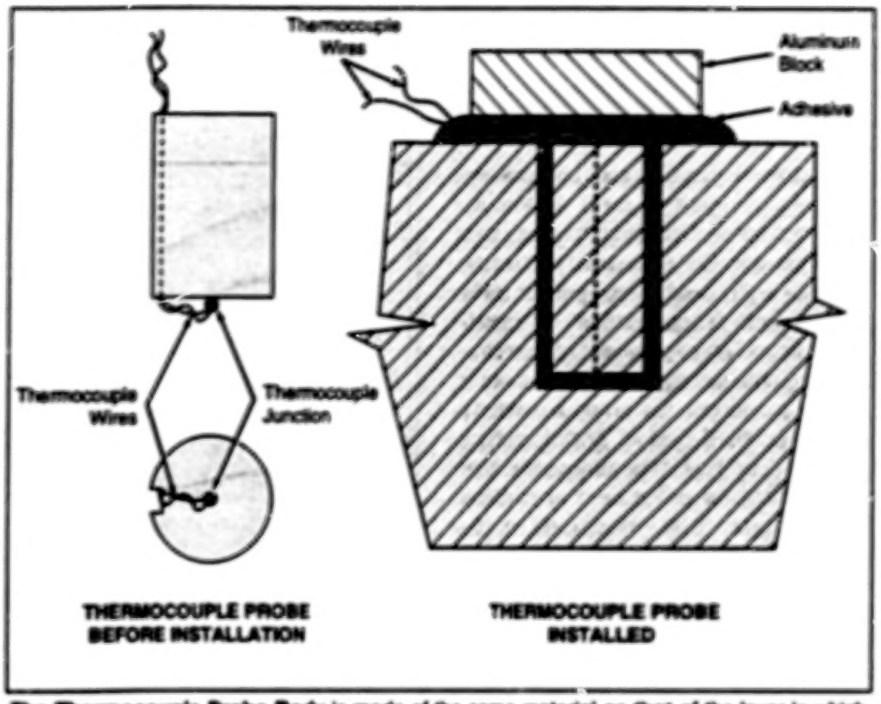

The Thermocouple-Probe Body is made of the same material as that of the layer in which it is to be inserted.

This work was done by S. B. Hunt, J. Durtschi, D. Smith, Joel Maw, M. Sakaguchi, L. Smart, and B. Blake of Thiokol Corp. for **Marshall Space Flight Center.** *Further information is contained in a TSP [see page 1].*

Inquiries concerning rights for the commercial use of this invention should be addressed to the Patent Counsel, Marshall Space Flight Center [see page 1]. Refer to MFS-28840.

Bakeout Chamber Within Vacuum Chamber

Outgassing of components outside the bakeout chamber does not interfere with measurements.

NASA's Jet Propulsion Laboratory, Pasadena, California

A vacuum-bakeout apparatus for decontaminating and measuring outgassing from pieces of equipment has been constructed by mounting a bakeout chamber within a conventional vacuum chamber (see figure). The concept of upgrading an old or new conventional vacuum chamber to provide a vacuum-bakeout capability has been applied before: what is new here is the specific design to satisfy stringent requirements regarding outgassing — specifically, the requirement to prevent contaminants that originate in the vacuum chamber outside the bakeout chamber from entering the bakeout chamber, where they could interfere with measurements of contamination of the piece of equipment to be vacuum-bakeout tested and/or decontaminated. This upgrade is cost effective: fabrication and installation of the bakeout chamber are simple, installation can be performed quickly and without major changes in an older vacuum chamber, and the upgraded apparatus provides quantitative data on outgassing from pieces of equipment placed in the bakeout chamber.

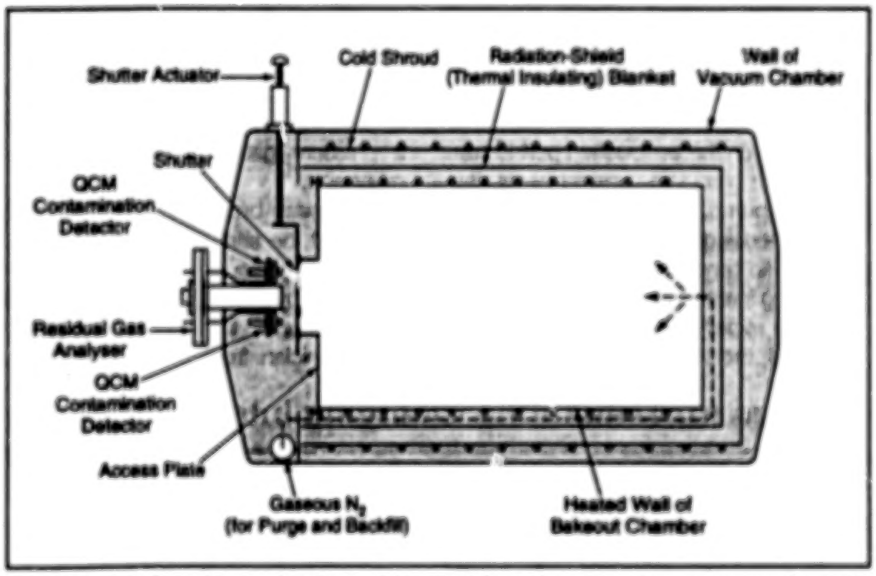

The Bakeout Chamber makes it possible to satisfy stringent requirements regarding outgassing while using an ordinary vacuum chamber.

In preparation for a vacuum bakeout, the piece of equipment to be outgassed is placed in the bakeout chamber, which is thermally insulated from the surrounding vacuum chamber by a radiation-shield blanket. During bakeout, only the bakeout chamber is heated. A cold shroud that lies within the vacuum chamber and surrounds the thermally insulating blanket is used to reduce the background pressure in the vacuum chamber and thereby reduce the deposition of the background contamination on contamination detectors located within the bakeout chamber.

A shutter assembly within the bakeout chamber contains orifices that direct the outgassing flow to the residual gas analyzer and one of the quartz crystal microbalance (QCM) contamination detectors or alternatively to the other QCM only. In this arrangement, the detectors respond specifically to the outgassing flow; the contributions of contaminants from elsewhere in the vacuum chamber are minimized.

To reduce background contamination before a full vacuum bakeout, the bakeout chamber and the cold shroud are warmed, the bakeout chamber is purged with pure N_2, and the vacuum system removes contaminants outgassed from the shroud. The chamber is then backfilled by use of the bakeout-chamber purge.

This work was done by Daniel M. Taylor, David M. Soules, and Jack B. Barangoltz of Caltech for **NASA's Jet Propulsion Laboratory**. *Further information is contained in a TSP [see page 1].*
NPO-18959

Increasing Precision of Temperature Sensors for Liquid H_2

Recalibration involves careful attention to details.

Lewis Research Center, Cleveland, Ohio

Commercial silicon-diode temperature sensors intended for use in boiling or nearly boiling liquid hydrogen at temperatures near 37 °R (about 20 K) have been recalibrated to greater precision by a method that involves careful attention to details of design, operation, and computation. The sensors were specified by the manufacturer to be accurate within ±0.90 °R (±0.5 K); after recalibration by this method, they were accurate within ±0.20 °R (~±0.1 K) in the temperature range of interest. Because the method is based on fundamental electrical and thermodynamic principles and good engineering practice, it should also be applicable to recalibration of other temperature sensors intended for use in other boiling or nearly boiling liquids.

The sensors were prepared for recalibration by mounting them in a rakelike array that was to be subsequently immersed in liquid hydrogen. Great attention was paid to good design and installation practices to minimize spurious transfers of heat that could affect the sensor readings. For example, thermal conduction along the sensor lead wires could exert significant effects. Thus, one good design practice was to minimize the number of lead wires and connectors to minimize the number of conduction paths. Another was to minimize thermal conduction along the leads by using leads made of thin manganin wire. Still another was to run the leads along isotherms to the extent possible to minimize conduction caused by thermal gradients along the leads.

The number of leads was minimized by wiring the diodes in groups of nine in series to supply the measurement current. By supplying the current to each diode through one pair of leads while measuring the voltage between these leads, one eliminates the need to carry current on the voltage-measuring leads, thereby eliminating the voltage drop along the leads that occurs in a simple two-leads-per-diode configuration.

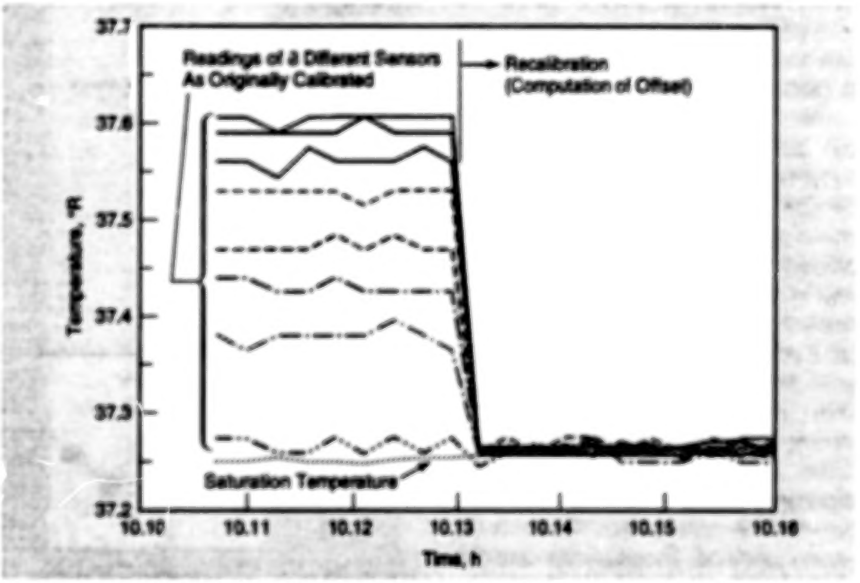

Temperature Readings of each sensor were corrected, after the ninth reading, by use of an offset obtained by subtracting the average of the first nine readings from the saturation temperature.

Another technique used to increase the accuracy of the measurement was to verify that each sensor was in contact with the correct medium, the temperature of which was to be measured. For example, each sensor had to be mounted so that it sensed the temperature of liquid or gas only — not the temperature of the mounting fixture.

The essence of the calibration procedure was the following: First, the sensors were operated while dipped in liquid nitrogen at atmospheric pressure to verify that they were functioning at least approximately as specified. Then the sensors were placed in a tank of liquid hydrogen, which was gradually brought to a boil at controlled pressure to obtain liquid/vapor saturation, as indicated by steady temperature readings and a steady rate of vented gas due to boil-off. The temperature in liquid/vapor saturation depends only on the pressure; in this case, the pressure was set at about 17 psia (about 120 kPa) and the saturation temperature for the actual pressure was computed from a table of properties of hydrogen supplied by the National Institute of Standards and Technology.

During saturation, the temperature reading of each diode (according to its original calibration) was taken 20 times at intervals of 1 second. The first nine readings from each diode were digitized and averaged, and the average was subtracted from the saturation temperature to obtain an offset for recalibration. The validity of the recalibration was verified by applying the offset on the tenth and following readings (see figure) and to readings taken under a different saturation condition (pressure of 29 psia (about 200 kPa), corresponding to a temperature of 41.03 °R (about 22.79 K)).

This work was done by Paula J. Dempsey and Richard H. Fabik of **Lewis Research Center**. *Further information is contained in a TSP [see page 1].*
LEW-15912

Carbon/Carbon Grids for Ion Sources

Advantages would be better alignment and slower erosion.

NASA's Jet Propulsion Laboratory, Pasadena, California

Ion-extraction grids made of carbon/carbon composites would be used in spacecraft ion engines and industrial ion sources in place of the molybdenum grids that are now used, according to a proposal. In principle, the carbon/carbon grids could offer greater extraction efficiency and longer life. A grid would be fabricated by mechanical drilling, laser drilling, or electrical-discharge machining of an array of holes in a sheet of carbon/carbon. Typically, the holes would have a diameter of 0.075 in. (about 1.9 mm) and would be in a hexagonal array with a center-to-center distance of 0.087 in. (about 2.2 mm).

The maximum ion-beam current that can be extracted from an ion source depends on how precisely the gaps between screen, accelerator, and decelerator grids are maintained and on how precisely each hole in the screen grid is kept in alignment with the corresponding holes in the accelerator and decelerator grids. At present, for example, the grids in a 30-cm-diameter ion engine are made from molybdenum sheets chemically etched to contain as many as 15,000 holes. Because of the finite thermal expansion of molybdenum, the gaps between the grids tend to change as the engine heats up. To reduce the distortion of the gaps, the grids are dished to a depth of about 0.8 in. (about 2 cm). The dishing process results in nonuniform gaps and can introduce slight misalignments between the holes, with consequent reduction of ion-beam-extraction efficiency.

Carbon/carbon materials like those to be used in the proposed grids can be made to have nearly zero coefficients of thermal expansion over the operating-temperature range of an ion engine (see figure). Therefore, dishing would be unnecessary, and without dishing, better alignment of holes should be possible. A bonus is that carbon/carbon is eroded at only one-fifth the rate of molybdenum under bombardment by xenon ions. Carbon/carbon grids should therefore last much longer than molybdenum grids do.

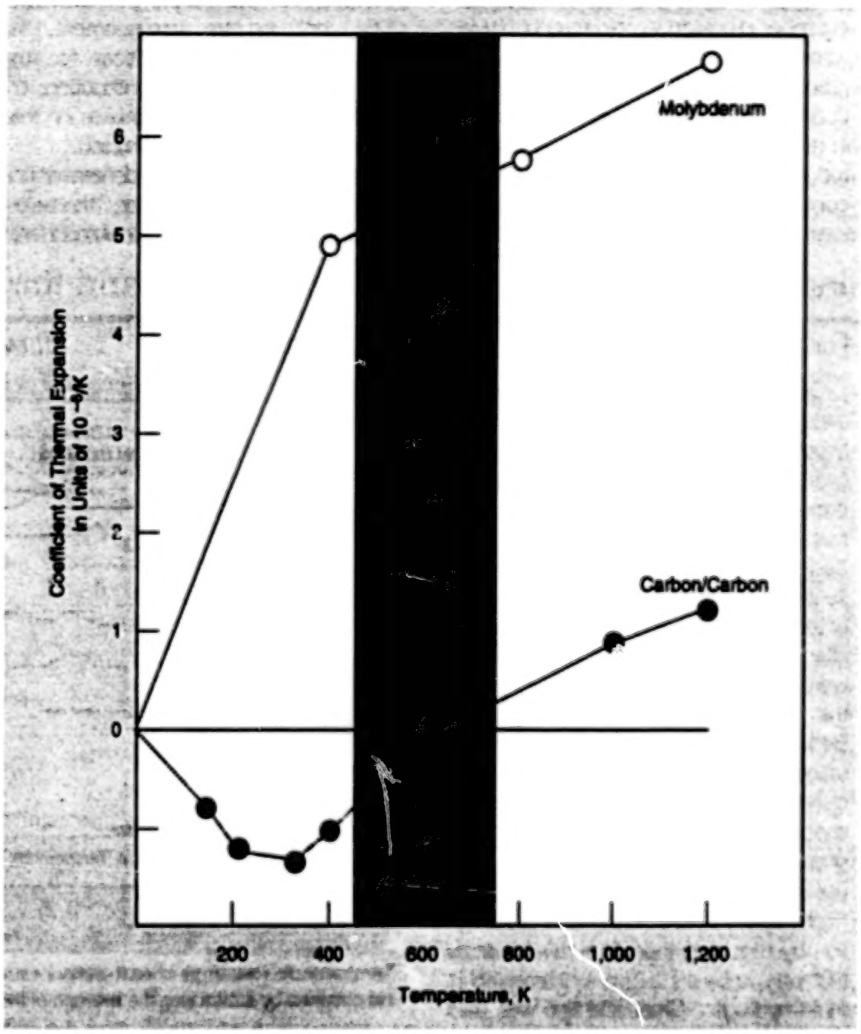

Over the Range of Operating Temperatures of an ion extraction grid, the coefficient of thermal expansion of a commercial carbon/carbon composite material is low and, at some temperatures, even slightly negative. In contrast, the coefficient of thermal expansion of molybdenum is large and positive.

This work was done by Charles E. Garner of Caltech for **NASA's Jet Propulsion Laboratory.** *Further information is contained in a TSP [see page 1].*

This invention is owned by NASA, and a patent application has been filed. Inquiries concerning nonexclusive or exclusive license for its commercial development should be addressed to the Patent Counsel, NASA Resident Office - JPL [see page 1]. Refer to NPO-19174.

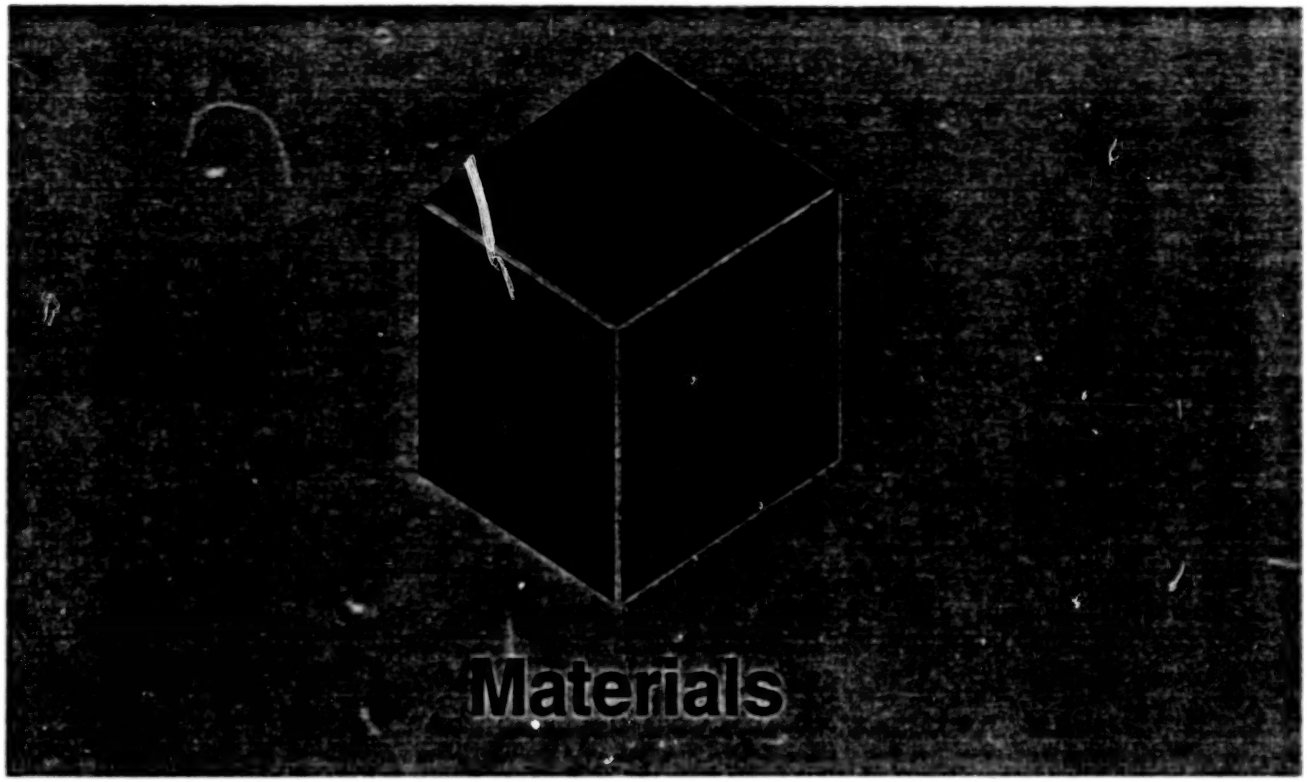

Hardware, Techniques, and Processes

31 Modified Polyimides Are More Compression Moldable
33 Controlled Thin-Film Growth of Silicon Carbide Polytypes
34 Modified Silicone-Rubber Tooling for Molding Composite Parts
34 Polyimides That Contain Cyclobutene-3,4-Dione Moieties
35 Stabilized Alkali Metal Ultraviolet-Band-Pass Filters
36 LaRC™-IA Copolyimides
37 Revealing Slip Bands in a Metal-Matrix/Fiber Composite
37 Combination Thermal Barrier and Wear Coatings for Engines

Books and Reports

38 Tests of Materials for Repair Coating of Carbon Steel

BLANK PAGE

Modified Polyimides Are More Compression Moldable

Offset stoichiometries and end-capping agents impart the desired properties.

Langley Research Center, Hampton, Virginia

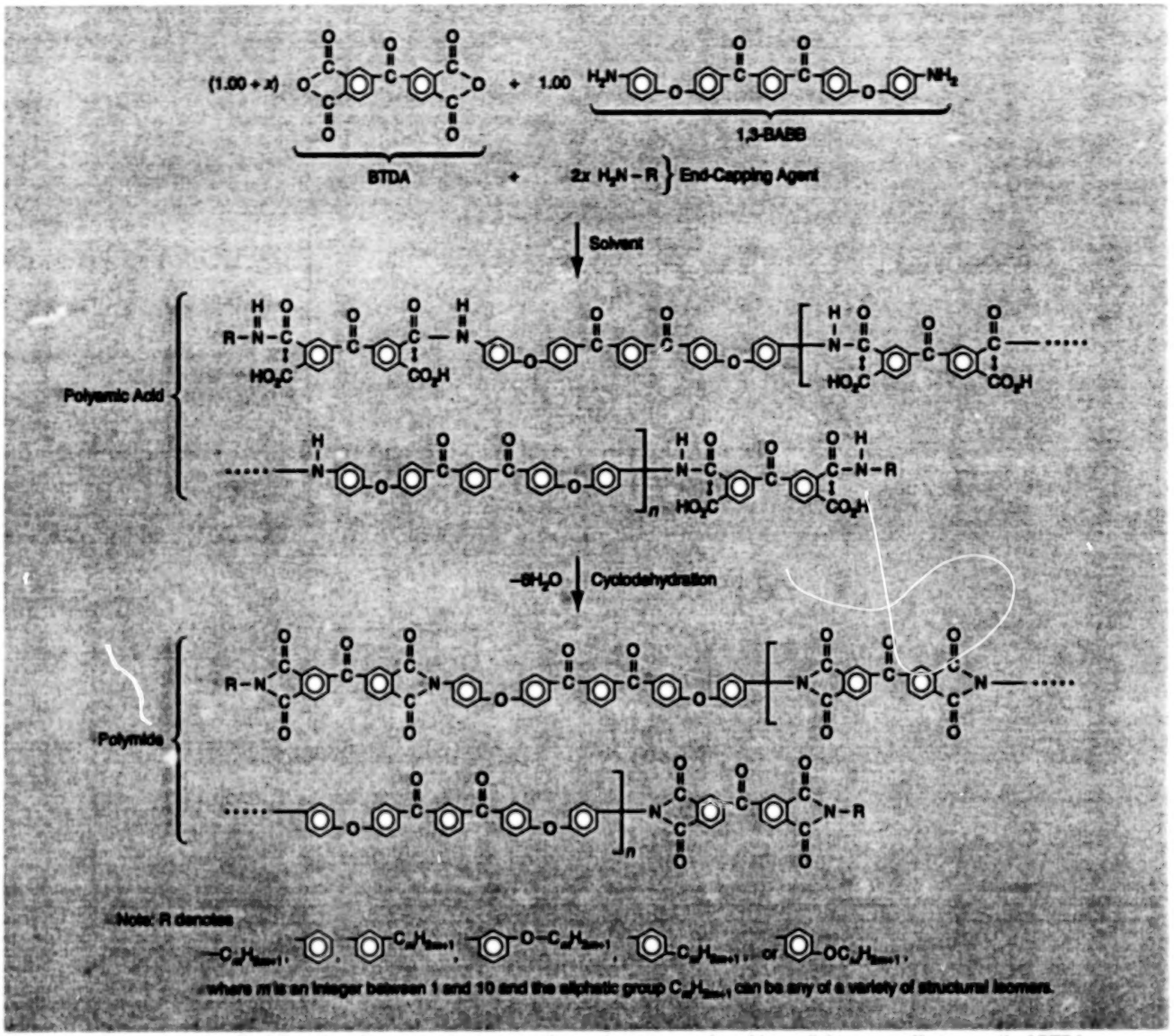

Figure 1. A Primary Amine End-Capping Agent passivates reactive end groups produced by a slight excess ($0 \leq x << 1$) of BTDA.

The semicrystalline polyimides that are synthesized from 3,3′,4,4′ benzophenonetetracarboxylic dianhydride (BTDA) and 1,3-bis(4-aminophenoxy-4′-benzoyl)benzene (1,3-BABB) can be modified to increase melt flow. In comparison with the unmodified versions of these polyimides, the modified versions are more amenable to compression molding, processing to form adhesive bonds, and use as matrices in matrix/fiber composite materials.

The first step in the synthesis of an unmodified, high-molecular-weight polyimide of this type involves the chemical reaction of BTDA with an equimolar amount of 1,3-BABB to form a high-molecular-weight polyamic acid intermediate product. To obtain a modified polyimide of this type, the first step is modified by the use of a small calculated excess of either BTDA or 1,3-BABB to obtain a polyamic acid of calculated lower average molecular weight and narrower statistical distribution of molecular weights around the average.

When excess BTDA is used, reactive anhydride groups are present at the ends of the polyamic acid chains; when excess 1,3-BABB is used, reactive amino end groups are present. In either case, the reactive end groups can cause undesired chemical reactions that result in degradation, extension, or branching of the polymer molecules. Therefore, it would be advantageous to end-cap these reactive end groups to form nonreactive end groups, making the polyamic acid and the polyimide end product more thermally stable. This leads to a second, optional modification; namely, the use of an end-capping agent in the small stoichiometric amount needed to react with all of the reactive end groups. When excess BTDA is used, the end-capping agent can be a primary amine (see Figure 1); when excess 1,3-BABB is used, the end-capping agent can be an aromatic anhydride (see Figure 2).

The resulting modified polyamide acid can be used in the usual ways: for example, while still dissolved in the solution in which it was synthesized, it can be used

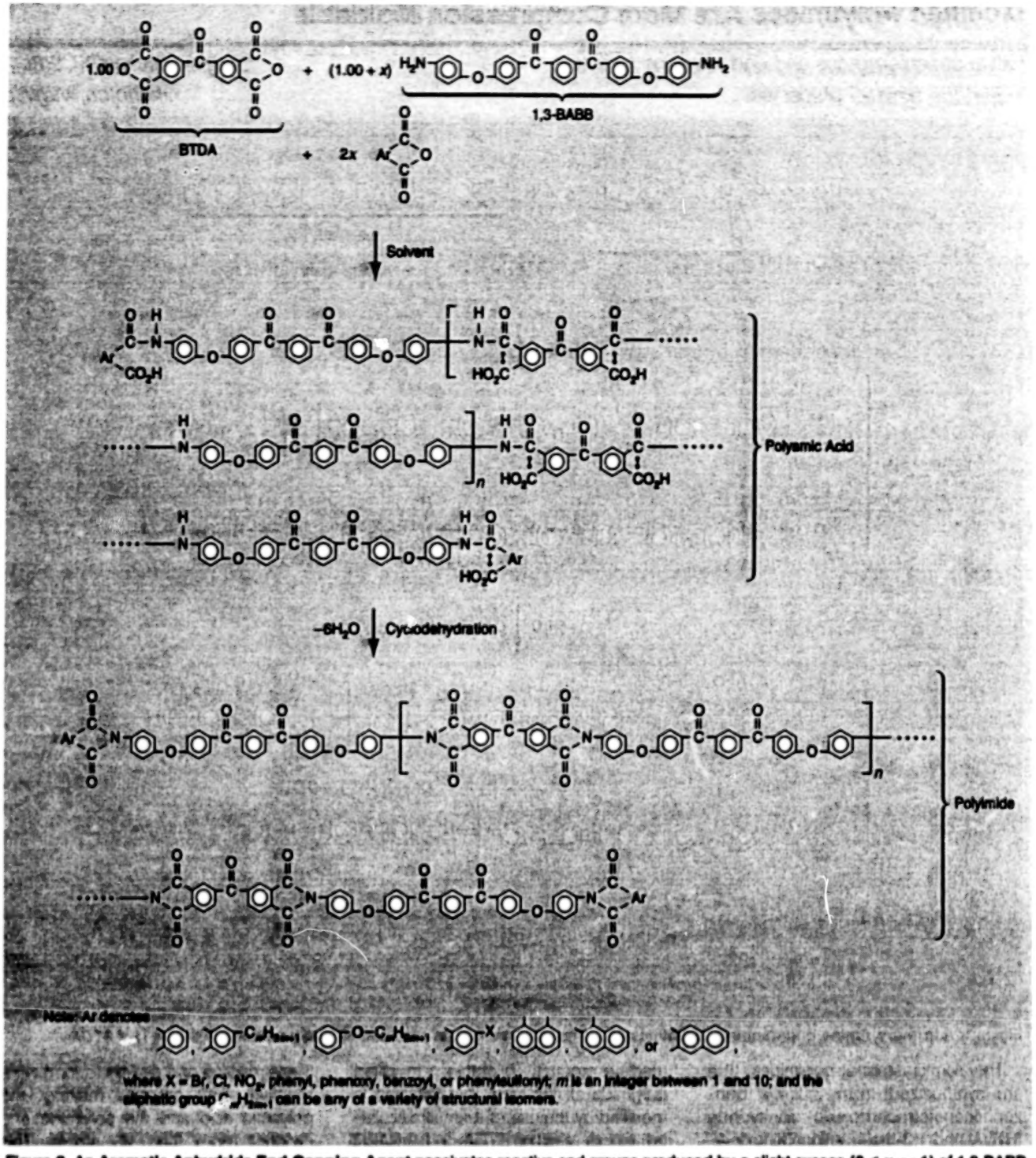
1.00
BTDA
+ (1.00 + x)
1,3-BABB
+ 2x
Solvent
Polyamic Acid
−6H2O
Cycodehydration
Polyimide
Note: Ar denotes
where X = Br, Cl, NO2, phenyl, phenoxy, benzoyl, or phenylsulfonyl; m is an integer between 1 and 10; and the aliphatic group CmH2m+1 can be any of a variety of structural isomers.

Figure 2. An Aromatic Anhydride End-Capping Agent passivates reactive end groups produced by a slight excess ($0 \leq x << 1$) of 1,3-BABB.

to impregnate glass or carbon fiber reinforcement, then dried to remove solvent and to convert the polyamide acid to the polyimide. Alternatively, the polyamide acid can be either thermally or chemically converted to the polyimide. The resulting solid can be used as is to make moldings or as finely divided particles to impregnate glass or carbon fiber reinforcement. Regardless of the imidization method used in a specific case, the stoichiometrically offset, end-capped polyimide is more stable during melt processing and can be melt-processed at temperatures somewhat lower and pressures considerably lower than those needed to process the unmodified, high-molecular-weight polyimide with the same repeat unit.

This work was done by Paul M. Hergenrother of **Langley Research Center**, *Stephen J. Havens of Lockheed Engineering & Sciences Co., and Mark W. Beltz of the University of Akron. Further information is contained in a TSP [see page 1].*

This invention has been patented by NASA (U.S. Patent No. 5,212,276). Inquiries concerning nonexclusive or exclusive license for its commercial development should be addressed to the Patent Counsel, Langley Research Center [see page 1]. Refer to LAR-14457.

BEST COPY AVAILABLE

Controlled Thin-Film Growth of Silicon Carbide Polytypes

Layers can be grown with desired crystalline structures. *Lewis Research Center, Cleveland, Ohio*

An improved deposition process makes it possible to grow thin layers of silicon carbide that have chosen crystalline structures. The process can be incorporated into the sequences of deposition and etching steps used to fabricate silicon-carbide-based semiconductor devices. This is an important advance because silicon carbide is emerging as a superior semiconductor for devices that must operate under conditions of high power, high temperature, and/or high frequency. Furthermore, the various crystalline structures of SiC have different electronic properties, each suited to a specific application.

SiC grows in many different crystalline structures called "polytypes." The most common are the cubic polytype, called "3C," and a hexagonal polytype, called "6H." The difference between the structures of the polytypes is the sequence of stacking of double layers of Si and C atoms. Each double layer can occupy one of three positions and each polytype structure has a unique stacking sequence. The 3C polytype has the sequence ABC . . . (repeating 3-layer sequence) and the 6H polytype has the sequence ABCACB . . . (repeating 6-layer sequence).

The mobility of electrons in the 3C polytype is greater than that in 6H; hence, some electronic devices made from 3C may outperform similar devices made from 6H. On the other hand, the electron-energy band gap of 6H is greater than that of 3C, and this greater band gap is needed for blue-light-emitting diodes. Thus, the different electronic properties of the polytypes make it desirable to grow specific polytypes for particular devices.

A thin film of SiC or other material is generally grown in either a homoepitaxial or a heteroepitaxial mode. In homoepitaxy, the crystalline structure of the deposited material is the same as that of the substrate as, for example, in the deposition of 6H on 6H. In heteroepitaxy, the crystalline structure of the deposited material differs from that of the substrate, as in the deposition of 3C on 6H.

Usually, homoepitaxial growth is desired. Previously, it was found that to achieve homoepitaxial growth of a thin film of 6H SiC, one must use a 6H SiC substrate with a growth surface that has been polished several degrees off-axis from the basal plane. As shown in Figure 1, the resulting growth surface consists of a series of steps and terraces formed by the exposed edges of the double layers. During growth, molecules that arrive on terraces from the gas phase migrate to steps; homoepitaxial growth involves deposition on the narrow faces of the steps, so that each terrace grows along the underlying terrace. If the terraces are large (that is, if the tilt angle is small) or if there are defects on the terraces, then 3C nucleates on the terraces, yielding heteroepitaxial growth of 3C on 6H.

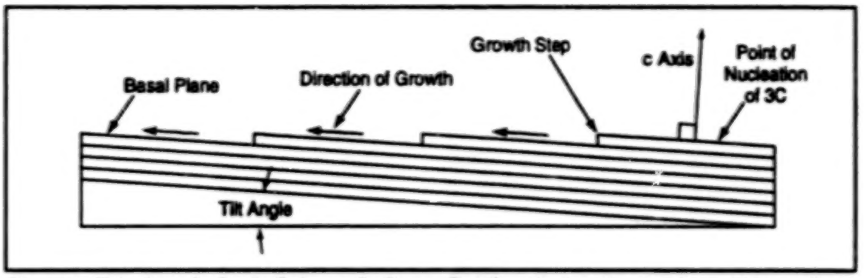

Figure 1. This Atomic-Scale Schematic Cross Section depicts the structure of the surface of a 6H SiC substrate polished slightly off axis (that is, at a small tilt angle).

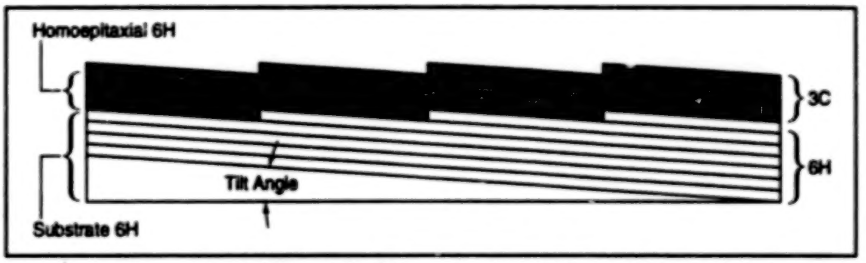

Figure 2. A Heteroepitaxial Film of 3C SiC can be deposited on a 6H SiC substrate, possibly even on top of a homoepitaxial film of 6H SiC.

The improved deposition process includes pregrowth etching of the substrate by gaseous HCl in H_2 at a temperature ≈1,350 °C. This etch significantly reduces defects caused by the cutting and polishing of the wafer, thereby eliminating sites where unwanted nucleation of 3C can occur. The result is that a thin homoepitaxial film of 6H can be grown, at a temperature ≈1,450 °C, on a 6H substrate that has been polished to a tilt angle as small as 0.1°. Previously, tilt angles > 1.5° were necessary for homoepitaxy.

A variation of the improved deposition process can be used to effect heteroepitaxial growth of high-quality 3C on a 6H substrate. First, the 6H substrate is polished with a tilt angle of < 0.5°. The growth surface is then grooved to produce millimeter-sized mesas upon which the 3C film can be grown. The 6H substrate is then subjected to a pregrowth etch to remove unintentional nucleation sites. At the highest atomic plane on each mesa, the surface can be intentionally altered to make sites for the nucleation of 3C. For example, damaging the surface or adding contamination can cause the nucleation of 3C. From these sites of intentional nucleation of 3C, a film of 3C grows laterally until the entire mesa is covered with a 3C film, as shown in Figure 2.

Because the nucleation of 3C is confined to a small region of each mesa, the 3C film is free of a defect known as double positioning boundaries (DPBs). Previously, high densities of DPBs were typically observed in 3C films grown on 6H substrates. DPBs can form because two orientations of 3C are possible on a polished 6H surface and the intersection of 3C regions with different orientations gives rise to a DPB. The improved process eliminates unintentional nucleation of 3C and yields 3C films that are free of DPBs.

The improved process has been used to fabricate 3C SiC diodes that have a reverse breakdown voltage > 200 V; this is four times the greatest breakdown voltage of any diode previously made of 3C SiC.

This work was done by J. Anthony Powell and David J. Larkin of **Lewis Research Center.** *Further information is contained in a TSP [see page 1].*

This invention has been patented by NASA (U.S. Patent No. 5,363,800). Inquiries concerning nonexclusive or exclusive license for its commercial development should be addressed to the Patent Counsel, Lewis Research Center [see page 1]. Refer to LEW-15222.

Modified Silicone-Rubber Tooling for Molding Composite Parts

Silica powder is added selectively to adjust the pressures applied to molded parts.

Langley Research Center, Hampton, Virginia

Reduced-thermal-expansion, reduced-bulk-modulus silicone rubber for use in mold tooling can be made by incorporating silica powder into the silicone rubber. The molds and associated tooling in question are used to make composite-material parts; the molding processes in which they are used involve the application of pressure via thermal expansion of silicone-rubber tooling within confines of rigid, lower-thermal-expansion tooling. For example, a typical process of this type involves thermal expansion of a silicone rubber core to press a layer of composite material outward into intimate contact with the surface of a stainless-steel mold during heating to cure the composite material.

The need to reduce the thermal expansion and bulk modulus of silicone-rubber mold tooling arises because most commercially available silicone rubbers expand at such high rates that it is difficult to control the pressures that they apply. By reducing the coefficient of thermal expansion and the bulk modulus of a silicone-rubber mold-tooling part, one can control the pressure that it applies (as a function of temperature) with greater precision.

Experiments to demonstrate the feasibility of this concept were conducted on a commercial silicone rubber supplied in two liquid parts (liquid rubber plus catalyst). Preparation of specimens began with mixing the two liquid parts. Silica powder in a proportion of 5 weight percent was added to the liquid mixtures for some of the specimens. Some of the mixtures were deaerated in a partial vacuum, while others were not deaerated. The liquid mixtures were cast and heated in molds to form the solid silicone rubber specimens.

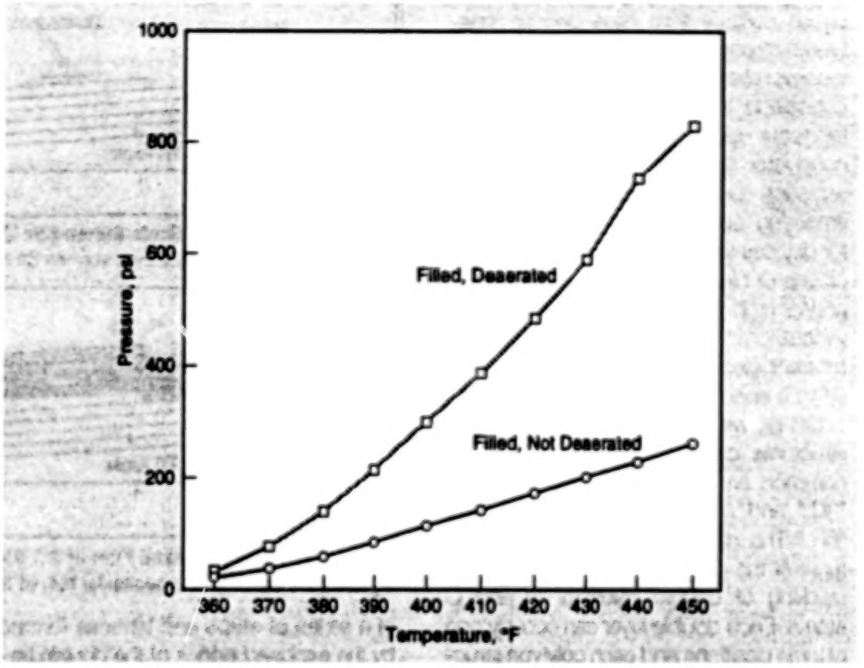

The Pressure Exerted by Thermal Expansion is reduced even further by allowing air bubbles to remain in the silicone rubber instead of deaerating it. The bubbles reduce the bulk modulus of the material.

Measurements and calculations for specimens in a test rig indicated that the pressure exerted by the unfilled, deaerated silicone rubber increased with temperature at a rate of about 20 psi/°F (about 250 kPa/°C), while that of the filled, deaerated silicone rubber increases with temperature at about 10 psi/°F (about 120 kPa/°C). The bubbles that remained in the filled, nondeaerated specimens reduced their bulk modulus, so that the pressure that they exerted increased with temperature at a very manageable rate of about 2 psi/°F (about 25 kPa/°C) (see figure).

This work was done by Robert M. Baucom and John J. Snoha of **Langley Research Center** *and Erik S. Weiser of Georgia Institute of Technology. For further information, contact*

John Hildebrandt
Tecnico Corporation
831 Industrial Avenue
Chesapeake, VA 23324

or Greg Manuel of NASA-Langley Applications Group at (804) 864-3864.

LAR-15217

Polyimides That Contain Cyclobutene-3,4-Dione Moieties

These polymers exhibit high thermo-oxidative stabilities and some potentially useful photoelectric properties.

Langley Research Center, Hampton, Virginia

Linear aromatic polyimides that contain cyclobutene-3,4-dione moieties have been synthesized in experiments. These polymers exhibit high thermal and thermo-oxidative stabilities, which make them useful in structural components exposed to hot and/or oxidative environments, as in jet engines and on the outer surfaces of supersonic aircraft. In addition, electrons in the cyclobutene-3,4-dione moieties are readily excited to states of higher energy upon exposure to ultraviolet light, giving rise to electronic properties with potential utility in photovoltaic, photoconductive, and/or photoemissive devices, for example.

One of the monomeric ingredients of a polyimide of this type is 1,2-bis(4-aminoanilino)cyclobutene-3,4-dione, which is also known as squaric acid derivatized diamine (SQDA). It is prepared by stirring 1,4-diaminobenzene dissolved in methanol with solution of diethylester of squaric acid in methanol at room temperature under a nitrogen atmosphere. The stirring is stopped after 3 days, and the SQDA precipitates as a crystalline material when the reaction mixture is allowed to stand for several hours. The SQDA is collected by filtration, washed with methanol, and dried in a vacuum. The SQDA that was used in this work was obtained from

Kyowa Hakko Kogyo Co., Ltd., in Japan.

The figure illustrates the general scheme for synthesis of a linear aromatic polyimide that contains cyclobutene-3,4-dione moieties. SQDA is mixed with an equimolar amount of an aromatic dianhydride and this mixture is dissolved in N,N-dimethylacetamide (DMAc) at a solids concentration between 7.45 and 15 weight percent, the optimum concentration depending on which dianhydride is used. The solution is stirred at room temperature, typically for 1 to 24 h, the exact time depending on which dianhydride is used. Polymerization manifests itself as an increase in the viscosity of the poly(amic acid) solution.

The polymerization is completed (the polymer is "cured") by heating the poly(amic acid) solution. For example, the solution can be cast on a plate, then placed in a nitrogen-filled dry box to evaporate the DMAc solvent and form a film. The film can then be cured by heating in a forced-air oven, typically up to a temperature between 200 and 400 °C: the exact temperature depends on the dianhydride used and on the effect of the heat treatment on various physical and chemical properties of the final polymeric product.

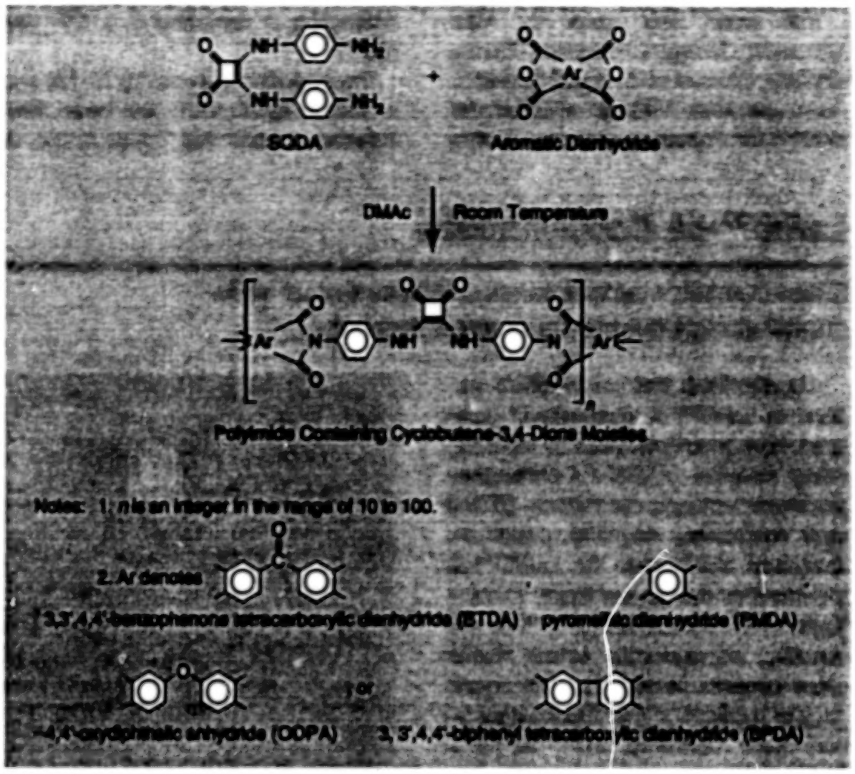

A Polyimide That Contains Cyclobutene-3,4-Dione Moieties is synthesized from SQDA and any of several aromatic dianhydrides. Polyimides of this type are highly thermo-oxidatively stable and have interesting photoelectric properties.

This work was done by Terry L. St. Clair of **Langley Research Center** *and Catherine Fay of Lockheed Engineering and Sciences Co. Further information is contained in a TSP [see page 1].*

This invention has been patented by NASA (U.S. Patent No. 5,212,283). Inquiries concerning nonexclusive or exclusive license for its commercial development should be addressed to the Patent Counsel, Langley Research Center [see page 1]. Refer to LAR-14775.

Stabilized Alkali Metal Ultraviolet-Band-Pass Filters

The stabilizing effect is exerted by layers of bismuth.

NASA's Jet Propulsion Laboratory, Pasadena, California

Layers of bismuth 5 to 10 A thick have been incorporated into alkali-metal ultra violet-band-pass optical filters by use of advanced fabrication techniques. The basic problem in making alkali-metal optical filters is to establish and maintain thin layers of alkali metal (usually sodium) with optically smooth surfaces. Heretofore, the high chemical reactivity and low melting point of alkali metals have given rise to difficulties in fabrication and to instability of the filters after fabrication. In the new filters, the layer of bismuth helps to reduce surface migration of the sodium. Thus, the sodium layer is made more stable and has a decreased tendency to form pinholes by migration.

Typically, a filter of this type consists essentially of a layer of sodium 5,000 to 9,000 A thick, sandwiched between two magnesium fluoride windows, along with an indium gasket (see figure). Prior to deposition of the sodium and bismuth layers, chromium annuli that serve as aperture stops are deposited on the windows. The windows are cleaned and placed in a vacuum deposition chamber in tooling fixtures that make it possible to perform the subsequent deposition steps without breaking vacuum. Water, oxygen, and any other reactive materials are removed from the chamber by use of a sodium getter.

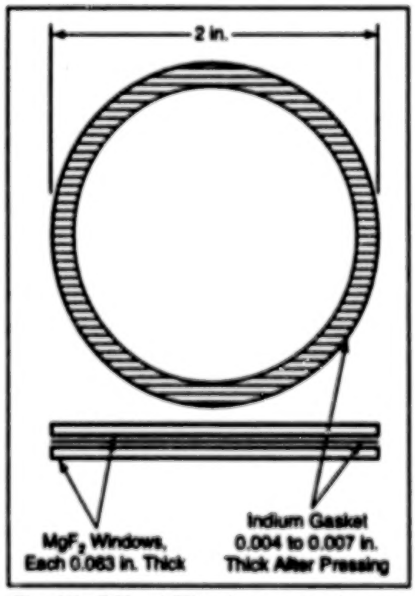

The Alkali Metal Filter is contained by two magnesium fluoride windows and an indium gasket.

The first step is to evaporate sodium onto one of the windows. Then a layer of bismuth is evaporated onto the sodium layer. Next, the same window is moved into position over the window with the indium ring, and the two windows are squeezed together by a hydraulic press mounted in the chamber, at a pressure of 800 psi (5.5 MPa). Air is then admitted to the chamber, and the completed filter is removed from the press.

This work was done by Nick Mardesich, George A. Fraschetti, Timothy McCann, Sherwood D. Mayall, Donald E. Dunn, and John T Trauger of Caltech for NASA's Jet Propulsion laboratory. Further information is contained in a TSP [see page 1].

This invention is owned by NASA, and a patent application has been filed. Inquiries concerning nonexclusive or exclusive license for its commercial development should be addressed to the Patent Counsel, NASA Resident Office-JPL [see page 1]. Refer to NPO-18433.

LaRC™-IA Copolyimides

Glass-transition temperatures and retention of shear moduli at high temperatures are increased.

Langley Research Center, Hampton, Virginia

Copolyimides that are modified versions of LaRC™-IA thermoplastic polyimide have been formulated by incorporating moieties of 3,3′,4,4′-benzophenonetetracarboxylic dianhydride (BTDA) and, alternatively, isophthaloyldiphthalic anhydride (IDPA) into the LaRC™-IA polymer backbones (see figure). In comparison with unmodified LaRC™-IA, the resulting copolyimides exhibit higher glass-transition temperatures and retain greater fractions of their lower-temperature shear moduli at higher temperatures. This enhancement of high-temperature performance is achieved without sacrificing the melt-flow processibility of unmodified LaRC™-IA polyimide: like unmodified LaRC™-IA polyimide, the LaRC™-IA copolyimides can be synthesized as semicrystalline powders that exhibit high melt flow at temperatures in the vicinity of 330°C. These copolyimides can be spun into fibers or used as adhesives, molding powders, or matrix resins in many applications, especially in the fabrication of strong, lightweight structural components of aircraft.

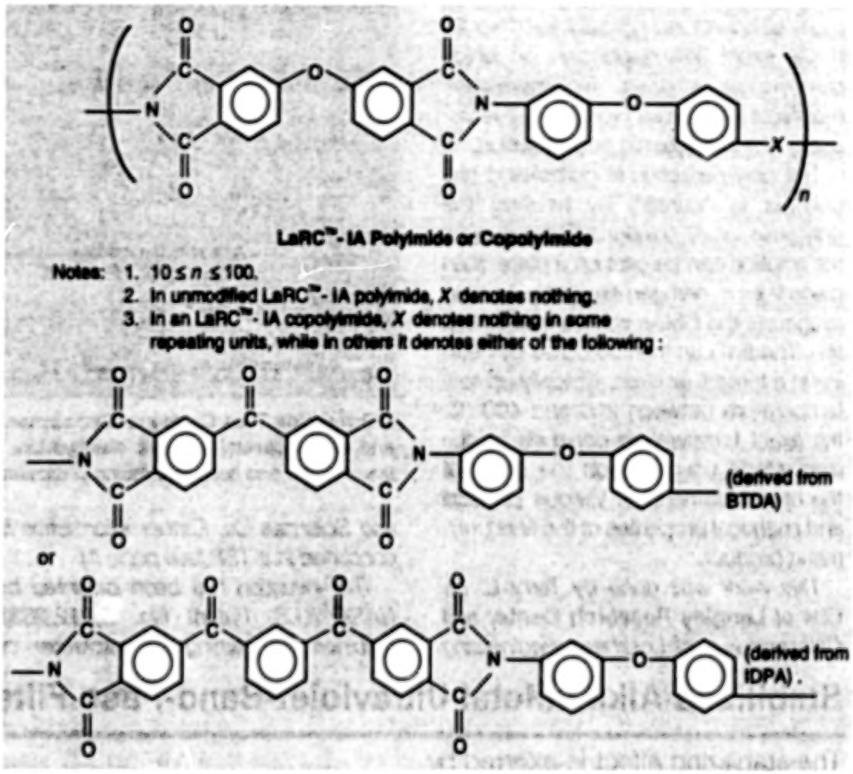
LaRC™-IA Polyimide or Copolyimide
Notes: 1. 10 ≤ n ≤ 100.
2. In unmodified LaRC™-IA polyimide, X denotes nothing.
3. In an LaRC™-IA copolyimide, X denotes nothing in some repeating units, while in others it denotes either of the following:
(derived from BTDA)
or
(derived from IDPA).

In a Molecule of LaRC™-IA Copolyimide, some fraction (usually 20 to 50 percent) of repeating units contain moieties derived from BTDA or IDPA.

The incorporation of BTDA or IDPA follows a cohesive-energy-density approach to obtain the desired enhancements in thermomechanical properties. The BTDA and IDPA bring in additional carbonyl moieties; the cohesive energy density is directly related to the number of carbonyl moieties per polymer repeat unit. Thus as the number of carbonyl units increases, interactions between chainlike polymer molecules also increase.

Unmodified LaRC™-IA has been synthesized from 3,4′-oxydianiline (3,4′-ODA) and 4,4′-oxydiphthalic anhydride (4,4′-ODPA) at 15 percent solids content dissolved in γ-butyrolactone. In synthesizing an LaRC™-IA copolyimide, one substitutes BTDA or IDPA for some portion of the 4,4′-ODPA in the reaction mixture (see figure). The molecular weight of the copolyimide is controlled by using a slight excess of 3,4′-ODA and reacting this excess with monofunctional phthalic anhydride, which thus serves as an end-capping agent. Eventually, glacial acetic acid is added to the reaction mixture, and the mixture is heated until the copolyimide forms and precipitates from the solution.

For example, in one experimental synthesis, 33 mole percent of 4,4′-ODPA was replaced with BTDA, and 3,4′-ODA was present in about 3 mole percent excess. The resulting copolyimide powder exhibited a glass-transition temperature of 238.0°C (vs. 229.6°C for unmodified LaRC™-IA). At a temperature of 150°C, this copolyimide retained 77.0 percent of its lower-temperature shear modulus (vs. 72.6 percent for unmodified LaRC™-IA).

This work was done by Terry L. St. Clair of **Langley Research Center** *and Alice C. Chang of Lockheed Engineering & Sciences Co. No further documentation is available.*

This invention is owned by NASA, and a patent application has been filed. Inquiries concerning nonexclusive or exclusive license for its commercial development should be addressed to the Patent Counsel, Langley Research Center [see page 1]. Refer to LAR-15109.

Revealing Slip Bands in a Metal-Matrix/Fiber Composite

Plastic flow of the stressed matrix can be detected.

Lewis Research Center, Cleveland, Ohio

An experimental procedure that includes heat treatments and metallographic techniques has been developed to facilitate studies of the deformation of a metal-matrix/fiber composite under stress. The procedure reveals slip bands, which are indicative of the plastic flow that can occur in the matrix during mechanical tests of specimens of the composite (usually at low temperatures).

The composite material in question consists of SiC fibers in a matrix alloy of 76Ti/15V/3Cr/3Sn/3Al (numbers indicate weight percentages). Prior to mechanical testing at room temperature, a specimen of the composite is heated at a temperature of 700 °C for 24 h in a vacuum. After mechanical testing, the specimen is heat-treated at 427 °C for 24 h in a vacuum. The second heat treatment precipitates fine particles on slip bands. The particles are believed to be α-phase titanium.

Following the second heat treatment, the specimen is mounted and polished by metallographic techniques, then etched by a 3-percent aqueous solution of ammonium bifluoride. This solution preferentially attacks the α phase of titanium and thus highlights the slip bands (see figure).

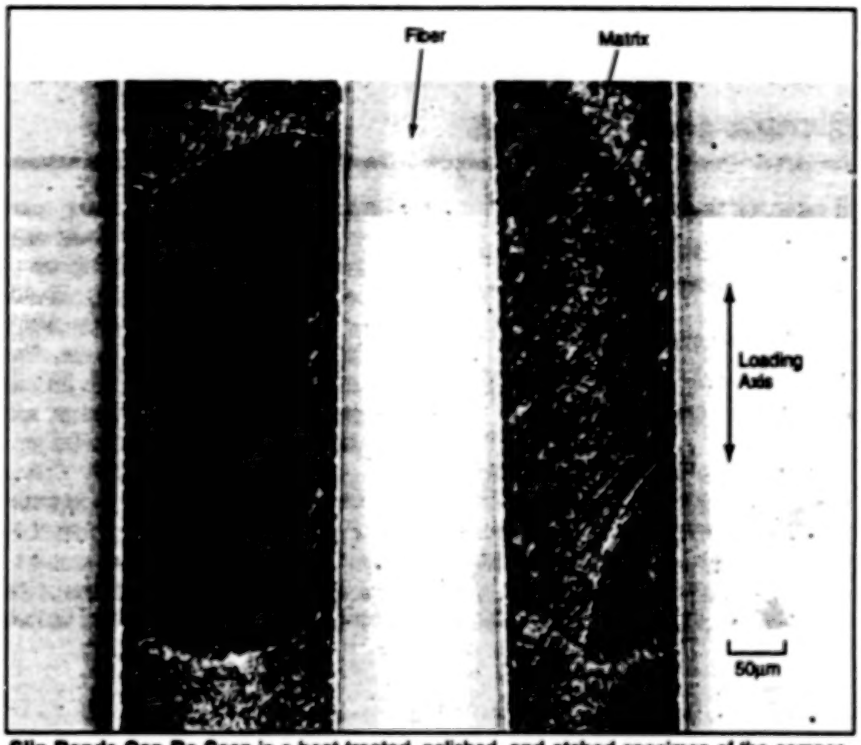

Slip Bands Can Be Seen in a heat-treated, polished, and etched specimen of the composite material described in the text. This view shows a plane in the middle of one ply of an eight-unidirectional-ply, continuous-fiber specimen that had been strained to 0.85 percent.

This work was done by Bradley A. Lerch of **Lewis Research Center.** *Further information is contained in a TSP [see page 1].*

LEW-15729

Combination Thermal Barrier and Wear Coatings for Engines

Thermal-barrier layers are covered with self-lubricating surface layers.

Lewis Research Center, Cleveland, Ohio

Thermal-barrier layers coated with wear-resistant self-lubricating surface layers are being developed for use as liners subject to sliding contact in advanced high-temperature engines (see figure). The thermal-barrier layers are needed to reduce cooling loads and enable operation at the high temperatures that are needed for high efficiency. For example, the power densities of air-cooled rotary engines are limited by the ability to maintain acceptable temperatures in their housings, which are typically made of aluminum. The wear-resistant, self-lubricating surface layers are needed because thermal-barrier materials are not sufficiently resistant to wear in sliding contact, and oil-based lubricants cannot survive the high temperatures.

In the development efforts undertaken thus far, zirconia has been shown to be effective as a thermal-barrier material, but it resists wear very poorly. The resistance to wear can be increased greatly by coating zirconia with PS-200, a self-lubricating material developed by NASA for use in turbine bearings and Stirling engines, where traditional lubrication with oils and greases is impossible. PS-200 consists of 80 percent silicon carbide [430 NS (Metco Powder), or equivalent] 10 percent silver, and 10 percent calcium fluoride/barium fluoride eutectic. The silicon carbide serves as a hard matrix. The silver is soft and compliant and provides low friction. The eutectic mixture provides lubricity at high temperature.

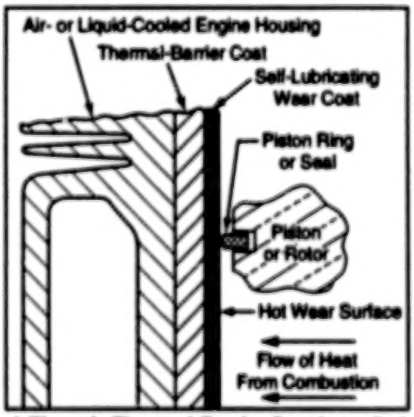

A Zirconia Thermal-Barrier Coat is applied to the surface of a combustion chamber in an engine by plasma-arc spraying. Then the PS-200 self-lubricating coat is plasma-arc sprayed onto the zirconia. The self-lubricating coat prevents sliding contact between the thermal barrier and the piston ring, effectively preventing both wear and the production of additional heat via friction.

Both the zirconia and the PS-200 coatings can be applied by plasma-arc spraying to substrates made of conventional engine materials like aluminum and iron. They adhere well to the substrates and to each other. Other combinations of thermal-barrier and self-lubricating, wear-

BEST COPY AVAILABLE

resistant coating materials could be used as long as the two materials adhere to each other, can be applied by use of similar or compatible processes, have similar coefficients of thermal expansion, are sufficiently strong at high temperatures [generally, > 600 °F (> about 320 °C)], and are affordable.

This work was done by Mike Weingart and Paul Moller of Moller International for **Lewis Research Center**. *Further information is contained in a TSP [see page 1].*
LEW-15356

Books and Reports

Tests of Materials for Repair Coating of Carbon Steel

Materials designated to be applied over tightly adhering rust were evaluated.

A report describes tests of paints (primers and topcoats) for use in recoating rusted carbon steel for protection against further corrosion. The paints selected for evaluation were all designated by their manufacturers as suitable for application over tightly adhering rust. Steel panels that had been severely rusted were prepared for coating using several methods, such as a rotary sander, rotary wire brush, pneumatically driven needle descaler, or rotary grinder. The coated panels were exposed to artificial salt fog for 12 weeks; those that passed the salt-fog test were exposed to the seaside environment at Kennedy Space Center for 18 months. Gloss-retention readings of the topcoats were taken at 6-month intervals. The report presents results of these tests, with analyses of the relative performances obtained by various combinations of surface preparation and coating materials.

This work was done by Louis G. MacDowell III of **Kennedy Space Center**. *To obtain a copy of the report, "Status Report — Protective Coating Systems for Repaired Carbon Steel Surfaces — 18-Month Exposure," see TSP's [page 1].*

Inquiries concerning rights for the commercial use of this invention should be addressed to the Patent Counsel, Kennedy Space Center [see page 1]. Refer to KSC-11635.

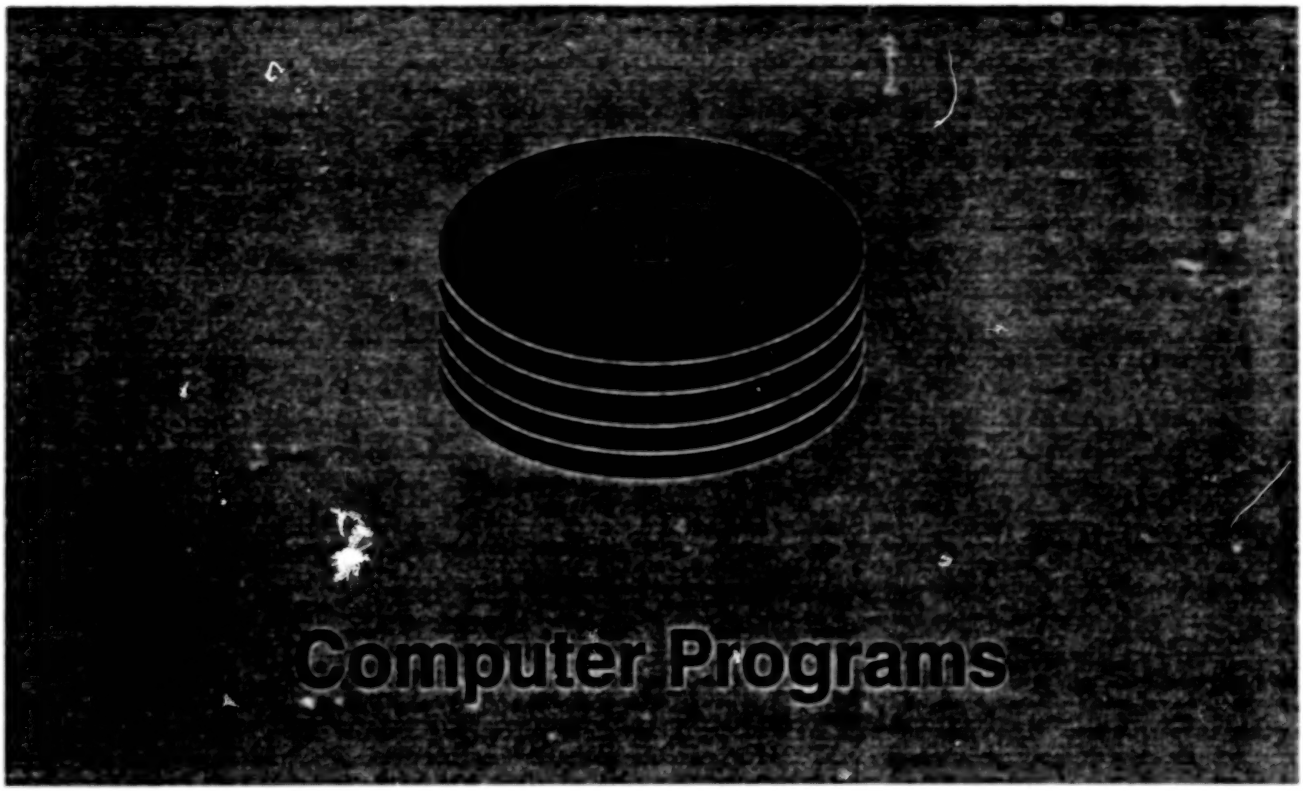

Physical Sciences

41 Program Helps To Determine Chemical-Reaction Mechanisms
41 Program for Tracking the Sun From the Moon

Fabrication Technology

42 Easing the Calculation of Bolt-Circle Coordinates

BLANK PAGE

Computer Programs

These programs may be obtained from COSMIC. Please contact

COSMIC®
Computer Services Annex
University of Georgia
Athens, GA 30602
Telephone No. (404) 542-3265.

Physical Sciences

Program Helps To Determine Chemical-Reaction Mechanisms

This program implements efficient and accurate chemical-kinetics and sensitivity-analysis computations.

The General Chemical Kinetics and Sensitivity Analysis (LSENS) computer code has been developed for use in solving complex, homogeneous, gas-phase, chemical-kinetics problems. The motivation for the development of this program is the continuing interest in developing detailed mechanisms of such complex chemical reactions as those of the combustion of fuels and the formation and destruction of pollutants.

A reaction mechanism is the set of all elementary chemical reactions that are necessary to describe a process of interest. Mathematical descriptions of chemical-kinetics problems constitute sets of coupled, nonlinear, first-order ordinary differential equations (ODEs). The number of ODEs can be very large because of the numerous chemical species involved in the reaction mechanism. Further complicating the situation are the many simultaneous reactions needed to describe the chemical kinetics of practical fuels. For example, the mechanism that describes the oxidation of the simplest hydrocarbon fuel, methane, involves over 25 species participating in nearly 100 elementary reaction steps.

The validation of a chemical-reaction mechanism involves repetitive solutions of the governing ODEs for a variety of reaction conditions. Analytical solutions to the systems of ODEs describing chemistry are not possible, except for the simplest cases, which are of little or no practical value. Consequently, there is a need for fast and reliable numerical solution techniques for chemical-kinetics problems.

In addition to solving the ODEs that describe chemical kinetics, it is often necessary to know the effects exerted on the solution by variations in either (1) the initial conditions or (2) the rate-coefficient parameters. Such a need arises in the development of reaction mechanisms from experimental data. Rate coefficients are often not known with great precision, and in general, the experimental data are not sufficiently detailed to enable the accurate estimation of rate-coefficient parameters. The development of a reaction mechanism is facilitated by a systematic sensitivity analysis, which provides the relationships between the predictions of a kinetics model and the input parameters of the problem.

LSENS provides for efficient and accurate chemical-kinetics computations and provides for sensitivity analysis for a variety of problems, including problems that involve nonisothermal conditions. LSENS replaces the previous NASA general-chemical-kinetics codes GCKP and GCKP84. LSENS is designed for flexibility, convenience and computational efficiency. A variety of chemical-reaction models can be considered. LSENS incorporates mathematical models for a static system, steady one-dimensional inviscid flow, reaction behind an incident shock wave (with boundary-layer correction), and a perfectly stirred reactor. In addition, computations of equilibrium properties can be performed for the following assigned states: enthalpy and pressure, temperature and pressure, internal energy and volume, and temperature and volume. For static problems, LSENS computes sensitivity coefficients with respect to the initial values of the dependent variables and/or the three rate-coefficient parameters of each chemical reaction.

To integrate the ODEs that describe chemical-kinetics problems, LSENS uses the packaged code Livermore Solver for Ordinary Differential Equations (LSODE), because it has been shown to be the most efficient and accurate code for solving such problems. The sensitivity-analysis computations are done according to decoupled direct method, as implemented by Dunker for isothermal problems and extended by Radhakrishnan to nonisothermal kinetics. In comparison with other methods of sensitivity analysis, this method has shown greater efficiency and stability with equal or better accuracy.

LSENS is written in FORTRAN 77 with the exception of NAMELIST extensions used for input. While this makes the code fairly machine-independent, execution times on IBM PC-compatible computers would be unacceptable to most users. LSENS has been successfully implemented on a Sun4 computer running SunOS and on a DEC VAX computer running VMS. With minor modifications described in the user's guide, it could also be easily implemented on other computers and operating systems with FORTRAN compilers that support NAMELIST input. LSENS required 4MB of random-access memory (RAM) under SunOS 4.1.1 and 3.4MB of RAM under VMS 5.5.1. The standard medium for distribution of LSENS is a 0.25-in. (6.35-mm) streaming-magnetic-tape cartridge (QIC-24) in UNIX tar format. It is also available on a 1,600-bit/in. (63-bit/mm), 9-track magnetic tape or a TK50 tape cartridge in DEC VAX BACKUP format. Alternate distribution media and formats are available upon request. LSENS was developed in 1992.

This program was written by D. A. Bittker and K. Radhakrishnan of **Lewis Research Center.** *Further information is contained in a TSP [see page 1].*
LEW-15758

Program for Tracking the Sun From the Moon

The direction to the Sun is computed for a given position on the Moon.

The SUNTRACKER program computes the azimuth and elevation angles of the Sun, as viewed from a given position on the Moon, during a time defined by the user. The program gets the selenographic (moon-centered) position of the Sun at a given Julian date, then converts the selenographic position of the Sun into azimuth and elevation at the given position on the Moon.

The selenographic coordinate system is based on the equatorial plane of the Moon. The origin of this system is referenced to the mean center of the apparent lunar disk; this center is the point of the surface of the Moon intersected by

the lunar radius directed towards the center of the Earth when the Moon is at its mean ascending node. Selenographic longitudes are measured positive in the direction towards Mare Crisium from the lunar meridian that passes through the origin. Selenographic latitudes are measured positive towards the northern hemisphere containing Mare Serenitatis, from the lunar equator. The selenographic colongitude is obtained by subtracting the selenographic longitude from either 90° or 450°.

SUNTRACKER performs two main operations. The first operation comprises the Julian- and calendar-date calculations. The second operation is calculation of the right ascension and declination of the Sun and Moon, on the equatorial coordinate system of the Earth, as functions of the adjusted Julian date. These coordinates are then transferred into the ecliptic coordinate system, from whence the position of the Moon is transformed into the heliocentric ecliptic coordinate system. The selenographic position of the Sun is determined in the heliocentric ecliptic coordinate system. Algorithms then compute both the physical and optical librations of motion of the Moon.

The limitations, restrictions, and assumptions applicable to SUNTRACKER are the following:

- The orbital elements used in this program do not account for nutation, aberration, and precession.
- The selenographic coordinates computed by this program are based on the 1961 Astronomical Ephemeris algorithms. In 1981, a new analytic theory of the librations of the Moon was adopted by The Astronomical Almanac. This theory improved the method of calculating selenographic coordinates. The selenographic coordinates computed by SUNTRACKER are identical to the pre-1981 Astronomical Almanac values. In a comparison of values computed by the program with values from the 1993 Astronomical Almanac, the maximum deviations in longitude and latitude were found to be 0.030° and 0.034°, respectively. The average deviations were 0.013° in selenographic colongitude and 0.017° in selenographic latitude.

SUNTRACKER is written in FORTRAN 77 for IBM PC-compatible computers running MS-DOS. The sample executable code included on the distribution medium requires 64K of random-access memory and the Lahey FORTRAN 77 run-time library for execution. The standard medium for distribution of this program is a 5.25-in. (13.335-cm), 360K MS-DOS-format diskette.

This program was written by Warren K. Woods and Dustin S. Spires of **Marshall Space Flight Center**. *Further information is contained in a TSP [see page 1].*
MFS-28939

Fabrication Technology

Easing the Calculation of Bolt-Circle Coordinates

This program can assist in many practical situations that arise in machine shops.

The Bolt Circle Calculation (BOLTCALC) computer program can be used to reduce the significant time consumed in manually computing the trigonometry of rectangular Cartesian coordinates of holes in a bolt circle as shown on a blueprint or drawing. Bolt circles are shown on many drawings — for example, drawings of flanges for tubes, sealing flanges, and subassemblies. BOLTCALC can eliminate the risk of computational errors, particularly in cases that involve many holes or in cases in which coordinates are expressed to many significant digits.

BOLTCALC can assist in many practical situations. For example, most small machine shops cannot afford numerically controlled machines or accurate rotary indexing tables for automatically positioning holes in bolt circles; therefore, machinists in such shops must rely on hand calculations and machine-table movements along Cartesian axes to position or index workpieces under drills in the spindles of conventional machines. Layout personnel who lack automatic equipment must perform hand calculations in order to scribe bolthole locations onto workpieces as, for example, when laying out locations of holes for a drill-press operation. Inspectors who lack automatic equipment must perform hand calculations in checking the locations of holes. BOLTCALC can eliminate much of the difficulty involved in all of these situations.

This program is written in BASIC for IBM PC-series and compatible computers running MS-DOS. A sample executable code, which was created by use of Microsoft's QuickBasic v4.5, is included. The program has also been successfully compiled and implemented by use of Microsoft's QuickBasic v4.0. It requires 64K of random-access memory for execution. The standard medium for distribution of this program is a 5.25-in. (13.335-cm), 360K, MS-DOS-format diskette. Documentation is included in the price of the program. BOLTCALC was developed in 1993.

This program was written by Richard K. Burley of Rockwell International Corp. for **Marshall Space Flight Center**. *Further information is contained in a TSP [see page 1].*
MFS-30006

Hardware, Techniques, and Processes

45 Improved Automatically Locking/Unlocking Orthotic Knee Joint
46 Fixture for Crush Testing of Composite Plates
47 Tool Measures Diameters of Posts With Limited Lateral Access
47 Stabilization of Combustion of Sprayed Fuel
48 Stress-Simulating Witness Panels
49 Prosthetic Tool for Holding Small Ferromagnetic Parts
49 Compact Microadjusters for Optical Components

BLANK PAGE

Improved Automatically Locking/Unlocking Orthotic Knee Joint

This joint would offer increased safety and convenience.

Marshall Space Flight Center, Alabama

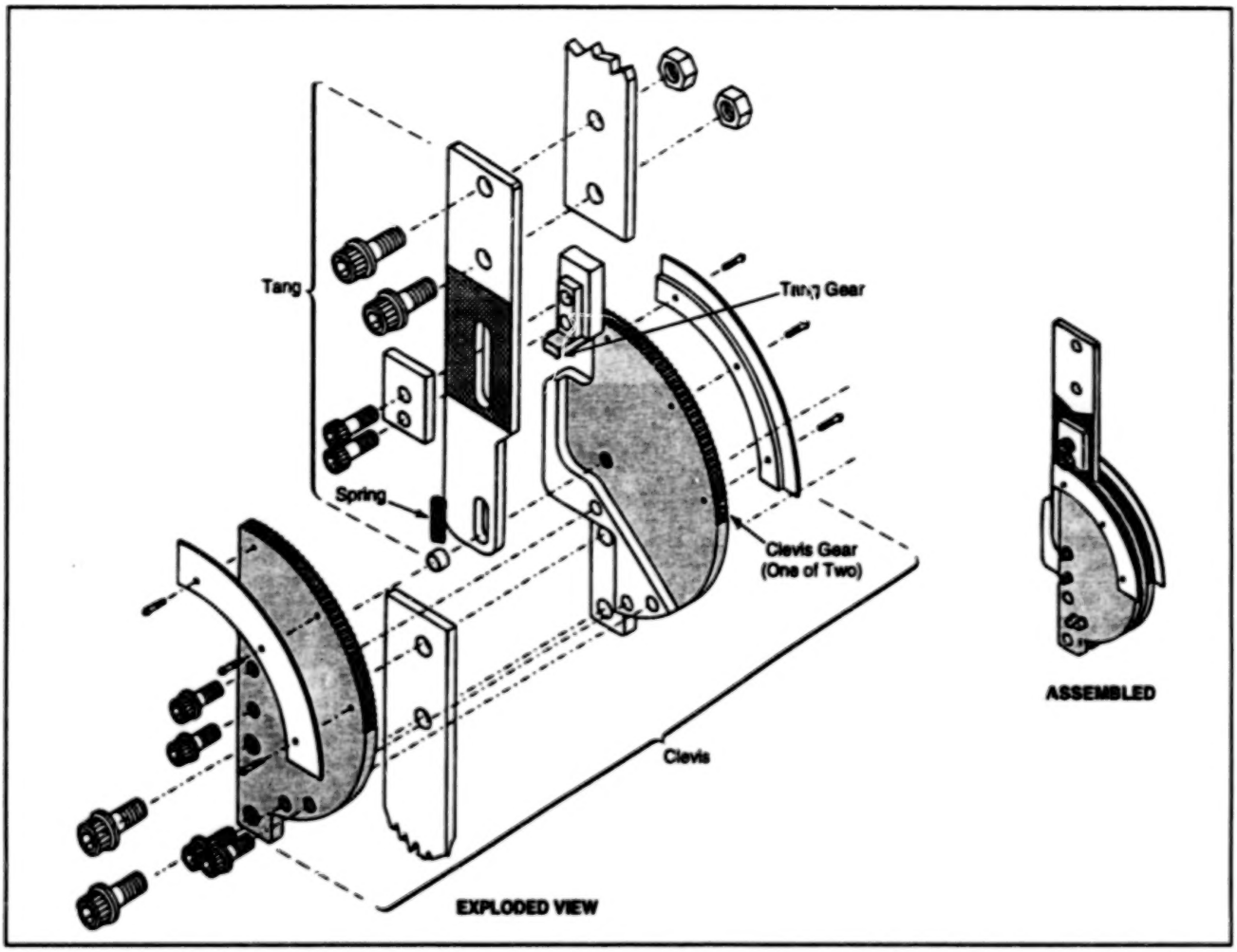

Figure 1. The Improved Orthotic Knee Joint would lock automatically upon initial application of radial force (the wearer's weight) and unlock automatically, but only when all loads (radial force and bending) were relieved.

Figure 1 illustrates a proposed orthotic knee joint that is an improved version of the one described in "Automatically Locking/Unlocking Orthotic Knee Joint" (MFS-28633), *NASA Tech Briefs*, Vol. 18, No. 5 (May, 1994), page 74. Both of these devices would offer increased safety and convenience relative to conventional orthotic knee joints.

Unlike a conventional orthotic knee joint, which locks only at full extension, either of these joints would lock whenever the wearer applied weight to the knee at any joint angle between full extension and a 45° bend. Thus, whereas the wearer of a conventional orthotic knee joint could fall because of lack of support during an inadvertent attempt to apply weight while the knee was bent, the wearer of either of these proposed joints would be supported by locking of the joint at any bending angle up to 45°. Either of these joints would unlock itself automatically when the load was removed, whereas a conventional orthotic knee joint must be unlocked manually. Also, both of these joints would feature hard stops to prevent overextension (that is, back bending).

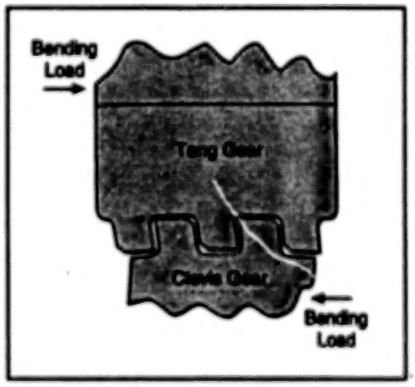

Figure 2. The Back Slope on the Meshing Gears would give rise to a mesh-tightening force when torque was applied to bend the knee.

The improved automatically locking/unlocking orthotic knee joint would offer an additional feature of safety and convenience: Automatic unlocking would not take place until both (1) the torque load (if any) tending to cause rotation of the joint and (2) the radial load that caused the joint to lock in the first place were both relieved. Thus, even if the wearer momentarily pulled weight back from the knee but was still depending on support by resistance of the knee to bending, the joint would provide that resistance.

Like both conventional orthotic knee joints and the joint described in the cited prior article, the improved automatically locking/unlocking orthotic knee joint would be a tang-and-clevis joint incorporating a locking/unlocking mechanism. In the improved joint, locking would be effected by meshing of gear teeth on the clevis with gear teeth on the tang, which would be designed to slide

radially a short distance. The small range of radial sliding would be just enough to enable the gear teeth to be brought into and out of mesh. A small spring would bias the tang radially outward within this range. A compressive radial load (ordinarily, the wearer's weight) would counteract the spring, pushing the gears into mesh.

The additional locking feature of the improved joint would be designed into the gear teeth. Instead of a conventional gear-tooth profile, these teeth would feature a special profile with a 7° back slope (see Figure 2). Once the gears were in mesh, the effect of the back slope would be to drive the gears more tightly into mesh whenever torque was applied in an attempt to bend the joint to a more acute angle. Thus, even when the radial locking load was removed, the gear teeth would remain meshed, locking the joint against loss of support. Only when all loads were relieved would the relatively gentle spring force be sufficient to push the gears out of mesh.

This work was done by Bruce Weddendorf of **Marshall Space Flight Center**. *Further information is contained in a TSP [see page 1].*

Inquiries concerning rights for the commercial use of this invention should be addressed to the Patent Counsel, Marshall Space Flight Center [see page 1]. Refer to MFS-28997.

Fixture for Crush Testing of Composite Plates

Plate specimens are used instead of tube specimens. *Langley Research Center, Hampton, Virginia*

A test fixture holds composite-material (matrix/fiber) plate specimens for crush testing in a universal compression-testing machine to determine energy absorption characteristics of the composite material system and laminate. Crush tests contribute to the development of more crashworthy composite-material structural components of aircraft. Previously, crush tests of composites were performed on cylindrical specimens instead of flat plates. The cylinders were not only expensive and difficult to fabricate, but also yielded data that could not easily be related to aircraft structural components, which are typically platelike.

The fixture accommodates specimens of two different sizes: 6 by 4 by 0.16 in. (≈ 15 by 10 by 0.41 cm)] and 3 by 2 by 0.08 in. (≈ 7.6 by 5.1 by 0.20 cm), designated as full scale and half scale, respectively. The fixture includes a platen equipped with four linear bearings that enable it to slide freely on four vertical guide rods (see figure). The loading rod of the testing machine applies the load to the platen via a large steel ball bearing, which is kept centered by a dimple in the center of the platen and a corresponding dimple in the center of the lower end of the loading rod. The platen, in turn, bears down upon the specimen.

The specimen is aligned by four knife edges attached to four vertical support rods. To eliminate a source of frictional force that could distort the results of tests, clearance holes in the platen prevent contact between the platen and the support rods. Collars are placed over the two pairs of opposing support rods to prevent the support rods from bending apart, thereby ensuring that the knife edges continue to keep the specimen aligned along its entire length while it is being crushed. In so doing, the collars also prevent the support rods from coming into contact with the platen.

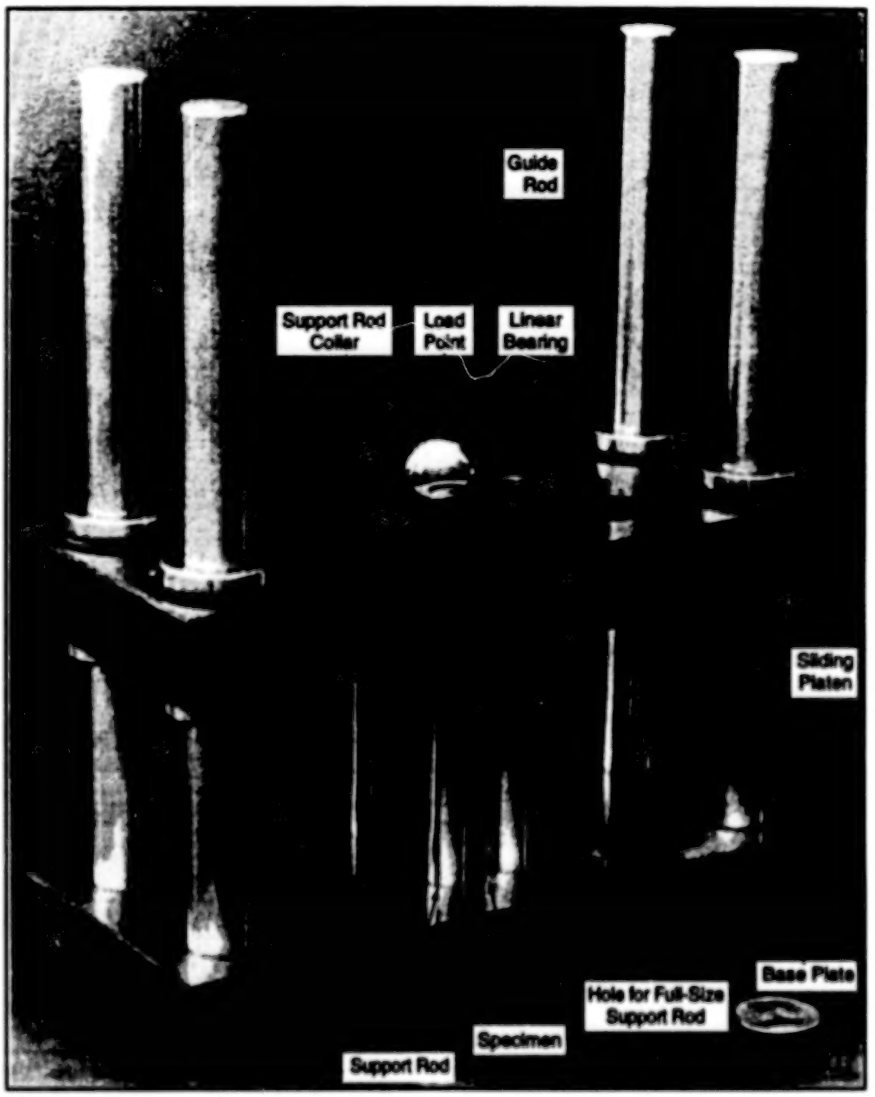

The Test Fixture as shown here is holding a half-scale specimen. To accommodate a full-scale specimen, the support rods would be moved to the more-widely-spaced holes in the base plate.

This work was done by Karen E. Jackson of **Langley Research Center** *and J. Andre Lavoie and John Morton of Virginia Polytechnic Institute and State University. Further information is contained in a TSP [see page 1].*

Inquiries concerning rights for the commercial use of this invention should be addressed to the Patent Counsel, Langley Research Center [see page 1]. Refer to LAR-15212.

BEST COPY AVAILABLE

Tool Measures Diameters of Posts With Limited Lateral Access

Notwithstanding limited accessibility, diameter can be measured with acceptable accuracy.

Marshall Space Flight Center, Alabama

A simple tool is used in conjunction with a conventional vernier caliper to measure the outside diameter of a round post or tube to which lateral access is limited. In the original application, the posts are liquid-oxygen-injector posts surrounded by a forest of many such posts on a rocket engine. The tool can also be used in other applications in which it is desired to measure diameters despite limited lateral access, provided that there is longitudinal access.

The tool (see figure) is made long and thin to fit within the narrow longitudinal access corridor. It includes chuck-like jaws, which are closed or opened by turning a knurled knob: the jaws can be closed snugly but gently onto the end of the post to be measured, providing a micrometer-like "slip feel" sensitivity. Once thus adjusted, the tool is withdrawn from the post and the distance between the insides of the jaws is measured by use of the caliper to obtain the outside diameter of the post. An accuracy of ±0.0005 in. (≈0.013 mm) is achieved.

The original version of the tool is designed to measure diameters within ±0.001 in.(≈ ±0.026 mm) of a nominal diameter of 0.500 in. (≈12.7 mm). Modified versions can be easily made for different diameters.

This work was done by Gene E. Morgan and Gary L. Snyder of Rockwell International Corp. for **Marshall Space Flight Center**. *Further information is contained in a TSP [see page 1].*
MFS-29963

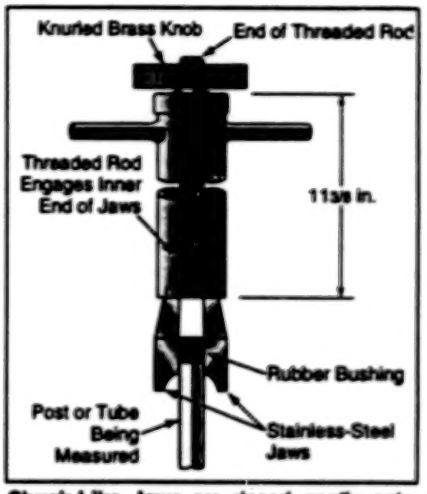

Chuck-Like Jaws are closed gently onto the end of the post or tube. The tool is then slipped off without changing the jaw setting, and the distance between the jaws is measured with a vernier caliper.

Stabilization of Combustion of Sprayed Fuel

Pressure oscillations would be suppressed by reshaping nozzle surfaces.

NASA's Jet Propulsion Laboratory, Pasadena, California

Several modifications of a nozzle that sprays a liquid propellant into a combustion chamber have been proposed to stabilize combustion. In the original application, the combination of the nozzle and the combustion chamber is called a "liquid propellant regenerative gun," and it is used to accelerate a projectile. The combustion process in the liquid-propellant regenerative gun exhibits instability in the form of pressure oscillations, which can make the projectile perform erratically or unsafely and can result in damage to the gun. The proposed changes in the design of the nozzle would alter the flow field in the combustion chamber, according to fluid-mechanical principles, in such a way as to suppress the oscillations. Similar modifications might help to suppress oscillations in industrial combustion chambers and in commercial and domestic oil-burning furnaces.

An important element of the proposed modifications is the introduction of a bluff simple or toroidal body into the flow of fuel (see figure). The bluff body could have any of a variety of alternative shapes, the exact shape being chosen to stabilize the combustion process by performing two important functions: creating turbulence

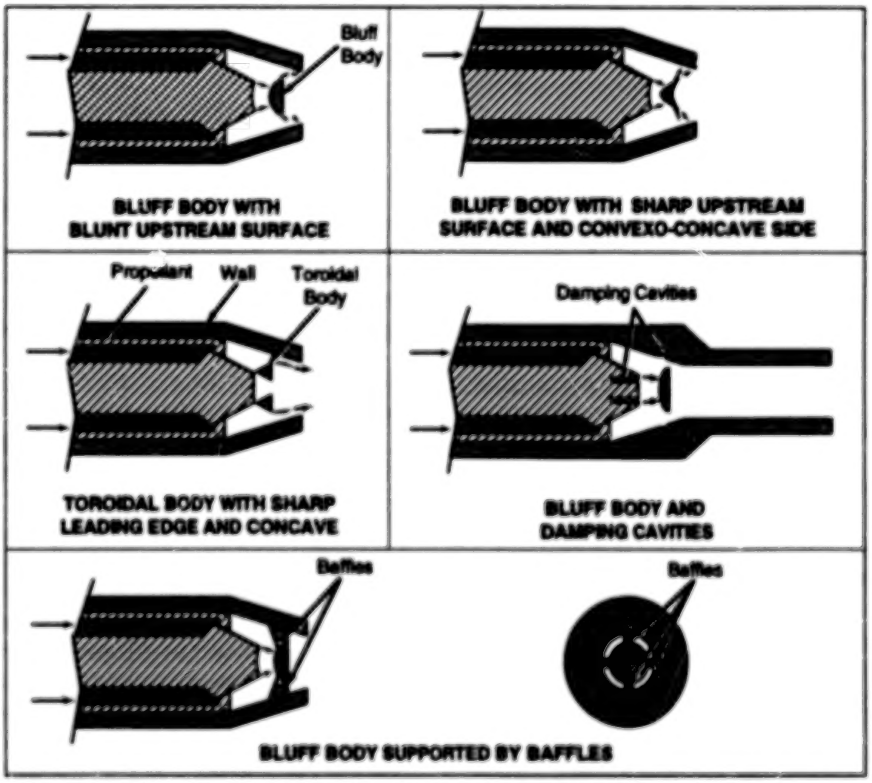

The Various Alternative Nozzle Configurations would all include a bluff or toroidal body to generate turbulence. Other features that could help to suppress oscillations include downstream recirculation zones, baffles, and damping cavities.

to break up the flowing fuel into small drops and creating a stable downstream combustion flow.

With regard to designing a particular nozzle according to the dynamics of flow, the requirement to generate turbulence and to establish a combustion flow field that will be stable downstream could dictate that the upstream surface of the bluff body or toroidal body be sharp or blunt, and that various upstream and side portions of the surfaces near and/or in contact with the flow be cylindrical, conical, convex, concave, smooth, or rough. The downstream surfaces could also be shaped and textured as continuations of the upstream surfaces or shaped to create downstream recirculation zones to suppress oscillations. In addition, any of the surfaces could be made catalytic to assist in decomposition of the fuel.

Of course, a bluff or toroidal body could not remain suspended as shown in the simplistic views in the upper part of the figure; some structural members would have to be added. The structural members could be shaped as baffles, which could be oriented to block radial and/or circumferential flow(s). Additional baffles that do not support bluff or toroidal bodies could also be used. Small openings in the baffles would allow small radial and/or axial flow(s), under the strong influence of viscosity, thereby providing viscous damping of pressure oscillations. For a similar purpose, cavities could be added on downstream surface(s): Oscillating flows of gas into and out of the cavities would encounter viscous damping, which would help to suppress the oscillations.

This work was done by Gerald E. Voecks and Darrell L. Jan of Caltech for **NASA's Jet Propulsion Laboratory**. *Further information is contained in a TSP [see page 1].*
NPO-18977

Stress-Simulating Witness Panels

Stresses should be similar to those in full-scale manufactured parts.

Marshall Space Flight Center, Alabama

Special panel fixtures are being developed for verifying the integrity of bonds between the propellants and insulators in solid-fuel rocket motors by applying, to specimens of propellant and insulator material, stresses similar to those caused by shrinkage during fabrication of the motors. Thus, the assemblies of fixtures and specimens are called "stress-simulating witness panels." The concept may also be applicable to stress testing of bonds in other manufactured products subject to shrinkage or to swelling.

Each fixture includes two parallel steel plates: an upper and a lower plate (see figure). In preparation for use of the fixture, the insulator is bonded to the top plate. The top and bottom plates, together with side plates, constitute a boxlike mold. A specimen of propellant material is cast in the mold. Then the mold is heated to cure the propellant material under the same conditions as in casting and curing the propellant in a rocket-motor case. Stresses accumulate while the propellant is being cured. Additional stresses accumulate as the propellant shrinks more than the mold does during the postcure cooldown to ambient temperature.

Three tensile-test buttons are built into the top plate to provide for direct measurement of the strength of the bond at three places without having to disturb the rest of the bond prior to a test. Similar panels in different sizes and shapes (e.g., different thicknesses, widths, and diameters of the holes for the tensile-testing buttons) could be fabricated to tailor stress levels to match those of a specific rocket motor or other product.

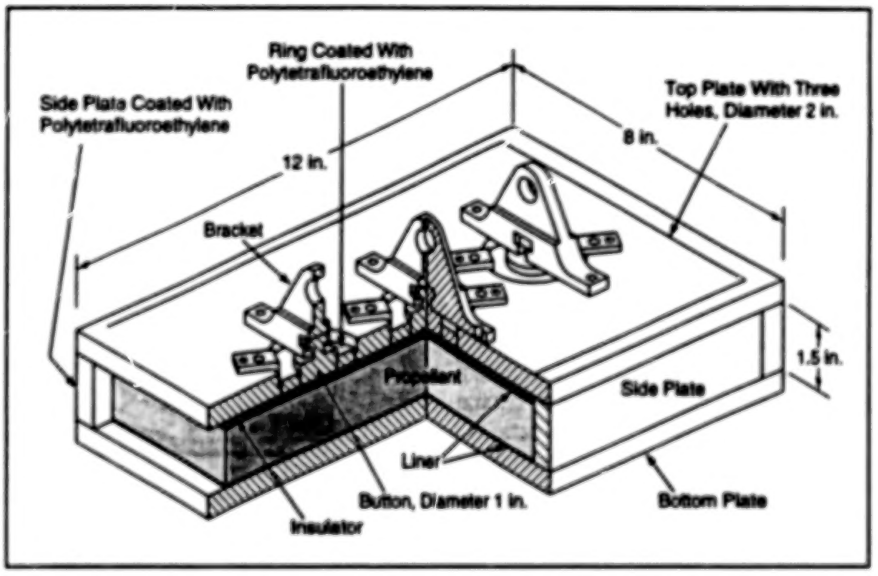

The Stress-Simulating Witness Panel is basically a combination of a specimen of material plus part of a mold in which the specimen was cast and cured.

At the time of submission of information for this article, tests had been performed on seven stress-simulating witness panels. For comparison, tests were also performed on standard carton panels. The results of the tests on the stress-simulating witness panels were found to be more sensitive to changes in the casting and curing processes. Tests of the built-in tensile buttons showed that they could be used to obtain satisfactory measurements of bond strengths. A finite-element structural analysis showed that stresses caused by shrinkage of the propellant in a stress-simulating witness panel should approximate adequately the shrinkage stresses that occur in typical rocket motors.

This work was done by Robert P. Graham and Lydia L. Biegert of Thiokol Corp. for **Marshall Space Flight Center**. *Further information is contained in a TSP [see page 1].*
MFS-28865

Prosthetic Tool for Holding Small Ferromagnetic Parts

This tool can be adjusted to hold nails, screws, nuts, and the like at desired angles.

Marshall Space Flight Center, Alabama

The figure illustrates a tool that can be attached to a prosthetic hand or arm to enable the user to hold nails, screws, nuts, rivets, and other small ferromagnetic objects on a small magnetic tip. The device can be adjusted — for example, to hold a nail or screw at the proper angle for hammering or for use of a screwdriver, respectively.

The tool includes a base connector with a threaded outer surface and a lower male member that can be inserted in a standard spring-action, quick-connect/quick-disconnect wrist adapter on the prosthetic hand or arm. The magnet that holds the part to be positioned is mounted on one end of a rod in a V-notched adapter. The other end of the rod is formed into a ball, which fits into a socket in the base connector to form a ball-and-socket joint that can be used to adjust the angle of the rod. A compression spring (not visible in the figure) is placed in the socket along with the ball. A knurled cap with a hole for the rod is screwed down over the ball; the cap can be tightened or loosened to increase or decrease the spring load and friction in the ball joint as needed.

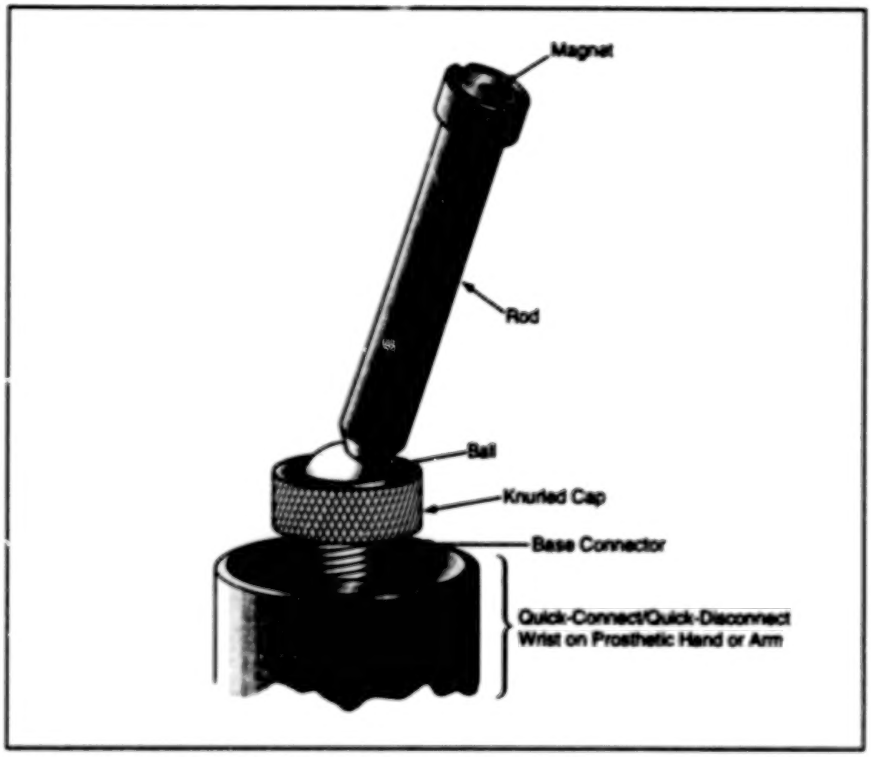

This Simple Adjustable Tool is attached to a prosthetic hand or arm and used to hold small ferromagnetic objects like nails.

This work was done by William E. Norton, James R. Carden, and Jewell G. Belcher, Jr., of **Marshall Space Flight Center** *and Thomas W. Vest of Management Services, Inc. Further information is contained in a TSP [see page 1].*

MFS-28896

Compact Microadjusters for Optical Components

These devices fit into spaces too small to accommodate ordinary adjusters.

Lewis Research Center, Cleveland, Ohio

Compact microadjusters for fine positioning of optical components have been designed to fit into small, confined spaces. Typically, these microadjusters would be used to move corner mirrors of optical interferometers by precise amounts with resolutions of about 1 μm. These microadjusters can be used in place of micrometer-style adjusters, most of which are at least an inch (2.54 cm) long and are often too big for compact optical setups. These microadjusters can also be used in place of other screw adjusters, the resolutions of which are often not fine enough.

A microadjuster of this type (see figure) consists largely of cantilever and non-simply-supported beams joined in a single unit. It can be fabricated relatively inexpensively by machining the beams out of a single piece of metal. Each beam constitutes a stage that attenuates a deflection transmitted to it from the preceding stage. A relatively coarse displacement applied via a screw to the input stage is thus converted to a fine movement at the output stage.

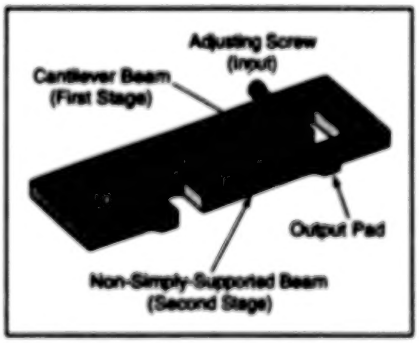

Integral Beam Stages in a stiff structure attenuate the displacement applied via the screw. For greater attenuation, a device of this type could be designed with more stages than the two shown here.

In principle, any number of cantilever stages can be connected together to obtain the desired reduction ratio. The pitch of the screw is selected according to the required reduction ratio and output resolution. The prototype microadjuster shown in the figure is actuated by a common 40-pitch (pitch = 0.635 mm) screw. A quarter turn of the screw results in a displacement of 3 μm at the output.

This work was done by Nathan R. Pfeifer and John B. Hammond of Westinghouse Electric Corp. for **Lewis Research Center.** *Further information is contained in a TSP [see page 1].*

LEW-15422

BLANK PAGE

Hardware, Techniques, and Processes

53 Automated Facility for Cleaning Large Flex Hoses
54 Tailored Precone Rotor
54 Linear Proof-Mass Actuator

Books and Reports

55 Aerodynamic Control-Augmentation Devices for Saturn-Class Launch Vehicles With Aft Centers of Gravity

BLANK PAGE

Automated Facility for Cleaning Large Flex Hoses

Technicians would no longer be exposed to hazardous cleaning materials.

Marshall Space Flight Center, Alabama

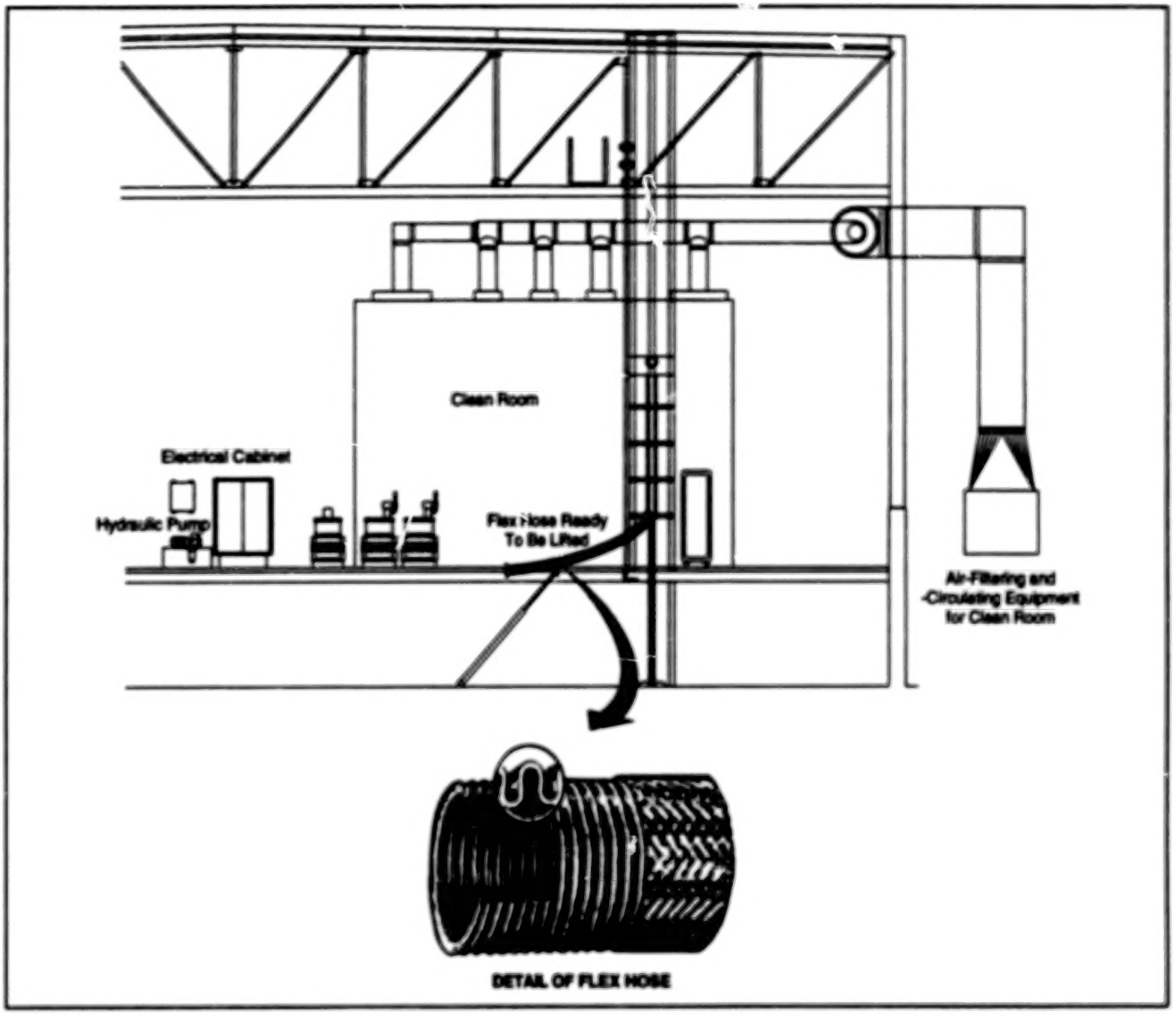

The Automated Cleaning Facility could handle hoses with lengths from 3 to 25 ft (0.9 to 7.6 m) and diameters from 3 to 12 in. (76 to 305 mm).

A proposed computer-controlled facility would clean bellows-type expansion joints and large flex hoses (that is, hoses with bellowslike convolutions). Heretofore, these objects have been cleaned manually in time-consuming operations that expose technicians to hazardous acids and other cleaning materials.

Major portions of the automated cleaning facility would be contained in a clean room. One of the pieces of equipment in the clean room would be a tower in which a hose or expansion joint to be cleaned would be hoisted by hydraulic machinery and hung vertically (see figure). Once the hose or expansion joint was hung in the required position, a technician would initiate a programmed cleaning procedure from a console on a computer monitoring system. The procedure could include degreasing, cleaning with detergents, rinsing, pickling, and passivating operations. (Passivation is a chemical means of increasing the corrosion resistances of metals, and of halting reactions to cleaning solutions.)

The technician would not be exposed to chemicals because all cleaning operations would be performed in the tower. During cleaning operations, a spray nozzle with radially outward jets that cover a full circle would move inside the hose or expansion joint. The jets would traverse the full length of the object to be cleaned. The programmed procedure would select the solutions to be used and the number of passes to be made with each solution.

Each sprayed cleaning material (even rinse water) would be collected from the bottom end of the hose and returned to a storage tank for reuse. A chlorofluorocarbon-solvent system could be used to inspect for nonvolatile residues. After cleaning had been completed, the technician would remove the hose or expansion joint from the tower and wrap the open ends to prevent recontamination of the interior.

This work was done by Louis E. Landry of Sverdrup Technology, Inc., for **Marshall Space Flight Center.** *Further information is contained in a TSP [see page 1].*

MFS-28929

Tailored Precone Rotor

Hub precone values would be passively tailored to increase stability and reduce blade loads.

Langley Research Center, Hampton, Virginia

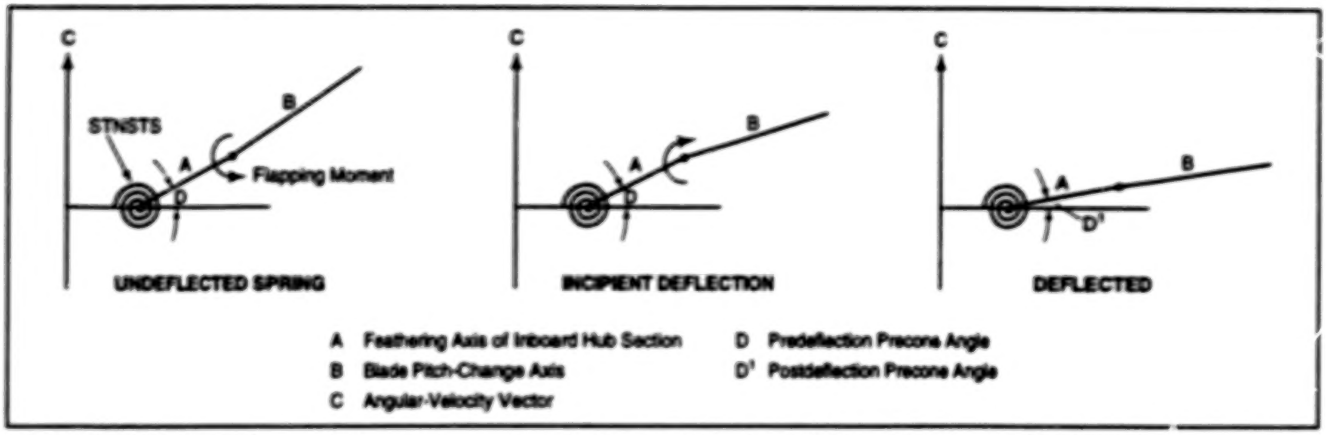

The Stability Boundary of the range of operating parameters of a hingeless helicopter rotor blade would be expanded by changing the precone angle.

The concept of the tailored precone rotor (TPR) provides for changes in precone deflection in a helicopter rotor blade when such changes are needed for enhancement of stability and loads. Heretofore, hingeless rotor designs that incorporate precone deflection have called for fixed values — usually at the inboard location of the flapping flexure. Such a design can result in flap-lag instability through positive pitch-lag coupling. Inasmuch as the precone angle in such a design is fixed, limitations in range of operating parameters of the rotor in flight may occur.

The TPR concept involves the use of the device described in "Structurally-Tailorable, Nonlinear Snap-Through Spring," *NASA Tech Briefs*, Vol. 13, No. 6 (June, 1989), page 77. The structurally-tailorable, nonlinear snap-through spring (STNSTS) would be used to effect a change in precone deflection when such a change is advantageous to the stability of the rotor system. As shown in the figure, when the blade pitch axis is displaced with respect to the inboard rotor hub section, this hub section is subjected to a flap moment. When this flap moment exceeded a prescribed level, the precone angle of the feathering axis would change abruptly because of the action of the STNSTS. When the blade axis once again went above the feathering axis of the inboard hub by a prescribed amount, the precone angle of the feathering axis would return to its original value.

The ability to tailor hub precone values to critical environments during many rotor operations is of great advantage to a designer. The ability to preselect a built-in hub coning angle in a passive manner is compatible with TPR design in that the inboard station of a rotor system would become aligned with the blade, depending on the position of the blade. A typical older precone design was fixed and addressed relief of either a high- or a low-blade phenomenon relief, i.e., loads or stability. The TPR concept would satisfy requirements in both rotor states in a tailored, passive manner. The TPR concept may also be potentially applicable to complex blades of high-speed fans or turbines.

This work was done by Wayne R. Mantay and Gary L. Farley of the U. S. Army Directorates at **Langley Research Center.** *No further documentation is available.*

LAR-13878

Linear Proof-Mass Actuator

This unit is designed for active damping of vibrations in a structure.

Langley Research Center, Hampton, Virginia

The linear proof-mass actuator (LPMA) is a friction-driven linear mass actuator capable of applying a controlled force to a structure in outer space to damp out oscillations. The LPMA is capable of high accelerations and provides smooth, bidirectional travel of the mass. The design of the LPMA eliminates gears and belts, which are parts of prior actuators and which contribute to loose fits.

The LPMA consists of close-tolerance machined parts, four dc torque motors, an encoder, an accelerometer, and controlling hardware and software. Mechanically, the LPMA consists of four major parts: the upper and lower housing assemblies, the mass, and the center support (see figure). The upper housing assembly contains two dc torque motors, shafts, and associated hardware. The lower housing assembly is similar, except that it also contains two sets of guide bearings that laterally position the mass.

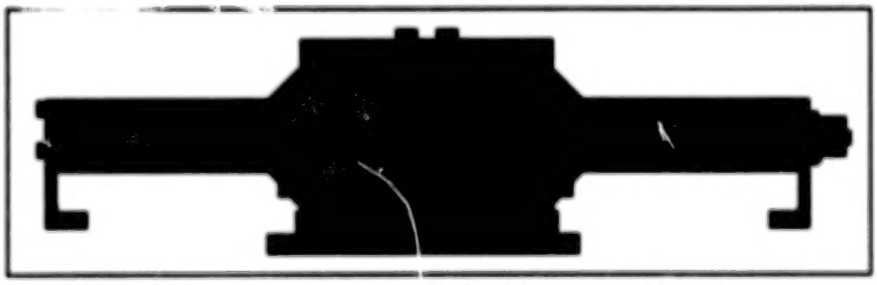

Direct-Current Torque Motors Rotate the Shafts of the upper and lower housing assemblies to accelerate the mass.

The center support is bolted to the lower housing assembly. The mass is positioned on the shafts of the lower housing assembly. The upper housing assembly is positioned on the center support, with the upper housing shafts resting on top of the mass. The upper and lower housing assemblies are then bolted together, providing the clamping force necessary to produce the required amount of frictional force between the shafts and the mass. The shafts and mass are made of dissimilar metals to prevent galling.

The dc torque motors, which fit on the ends of the shafts, rotate the shafts, which in turn translate the mass linearly. For this assembly to function, the parts are designed to very close tolerances. The shafts and mass must remain in contact at all times. The encoder gives the software, which controls the motors, data on the position of the mass, and the accelerometer provides acceleration feedback to the software controls.

The LPMA can be applied to future structures in outer space to provide oscillating forces to damp out vibrations. It is also strong enough to be used terrestrially where linear actuators are needed to excite or damp out oscillations. High flexibility can be designed into the LPMA by varying the size of the motors, the mass, and the length of the stroke, and by modifying the control software.

This work was done by Sidney E. Holloway, III, Edward A. Crossley, James B. Miller, Irby W. Jones, and C. Calvin Davis of **Langley Research Center** *and Vaughn D. Behun and Lewis R. Goodrich, Sr., of Planning Research Corp. Further information is contained in a TSP [see page 1].*

This invention has been patented by NASA (U.S. Patent No. 5,150,875). Inquiries concerning nonexclusive or exclusive license for its commercial development should be addressed to the Patent Counsel, Langley Research Center [see page 1]. Refer to LAR-14352.

Books and Reports

Aerodynamic Control-Augmentation Devices for Saturn-Class Launch Vehicles With Aft Centers of Gravity

A report describes a study of aerodynamic flight-control-augmentation devices proposed for use in increasing payload capabilities of future launch vehicles by allowing more aft centers of gravity. It has been shown, in conducted studies, that payload capability can be increased on certain Saturn-class launch vehicles by an internal rearrangement of propellant tanks. This, however, would give the vehicle an aft center of gravity and insufficient or marginal control torque. The proposed all-movable devices would not only provide increased control authority during the ascent trajectory, but would also reduce engine gimballing requirements and enhance crew safety. The report proposes various aerodynamic control surfaces that can be mounted fore and aft on a Saturn-class launch vehicle. Models have been fabricated and tested in the MSFC wind tunnel.

This work was done by Chris Barrett of **Marshall Space Flight Center.** *To obtain a copy of the report, "Launch Vehicle Aerodynamic Flight Control Augmentation Devices for Launch Vehicles With Aft Center-of-Gravity Locations," see TSP's [page 1]. MFS-31032*

BLANK PAGE

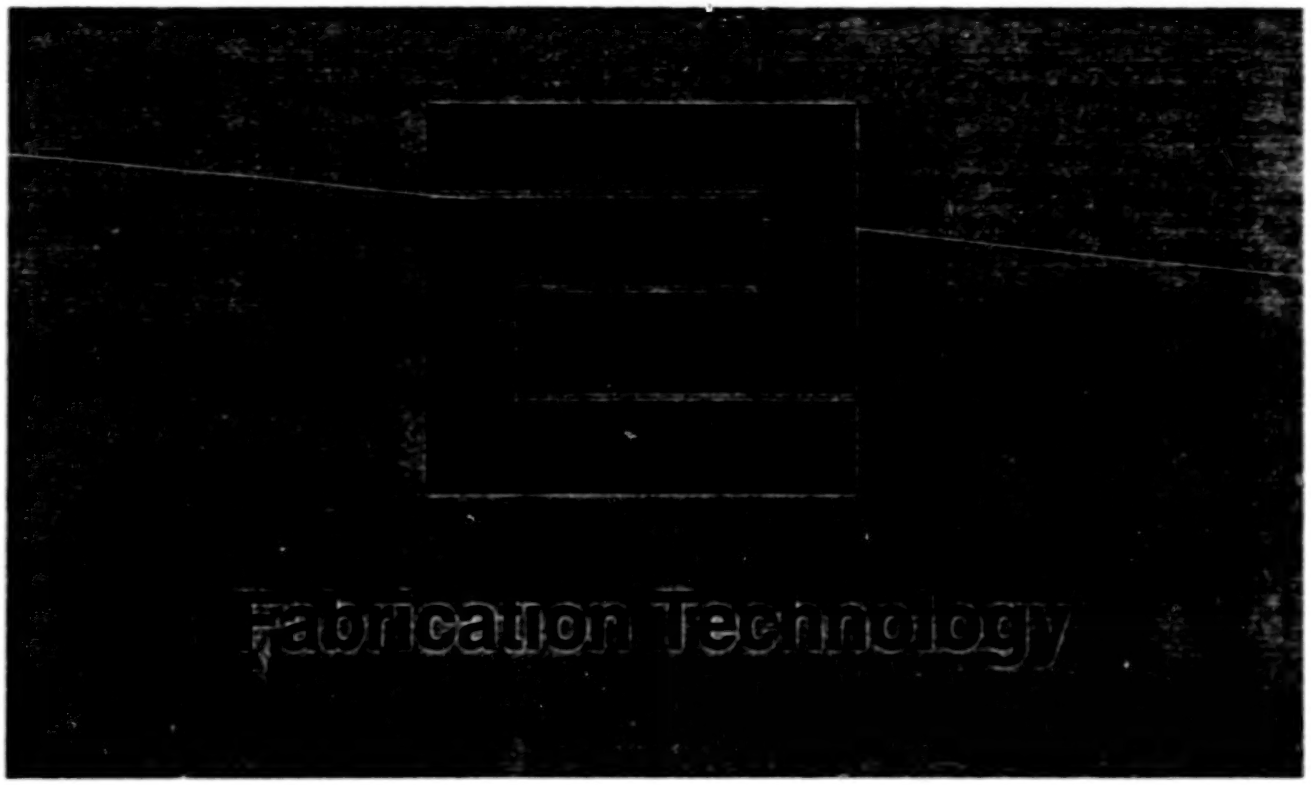

Hardware, Techniques, and Processes

59 Improved Net-Level Filling and Finishing of Large Castings
60 Metal-Matrix Composite Parts With Metal Inserts
61 Removable Mandrels for Vacuum-Plasma-Spray Forming
61 Improved Back-Side Purge-Gas Chambers for Plasma Arc Welding
62 Noncharnber, Root-Side, Inert-Gas Purging During Welding
63 Wire-Arc Spraying of Metal Onto Insulating Foam
63 Computed Tomography for Internal Inspection of Cas' 3
64 Manifold for Flushing Tubes With Cleaning Solution
64 Anodizing and Sealing Aluminum in Nonchromated Solutions
65 Tools for Installing Keys on a Stud

Books and Reports

65 Applying Taguchi Methods to Brazing of Rocket-Nozzle Tubes

BLANK PAGE

Improved Net-Level Filling and Finishing of Large Castings

Exposure of workers to casting material is reduced.

Marshall Space Flight Center, Alabama

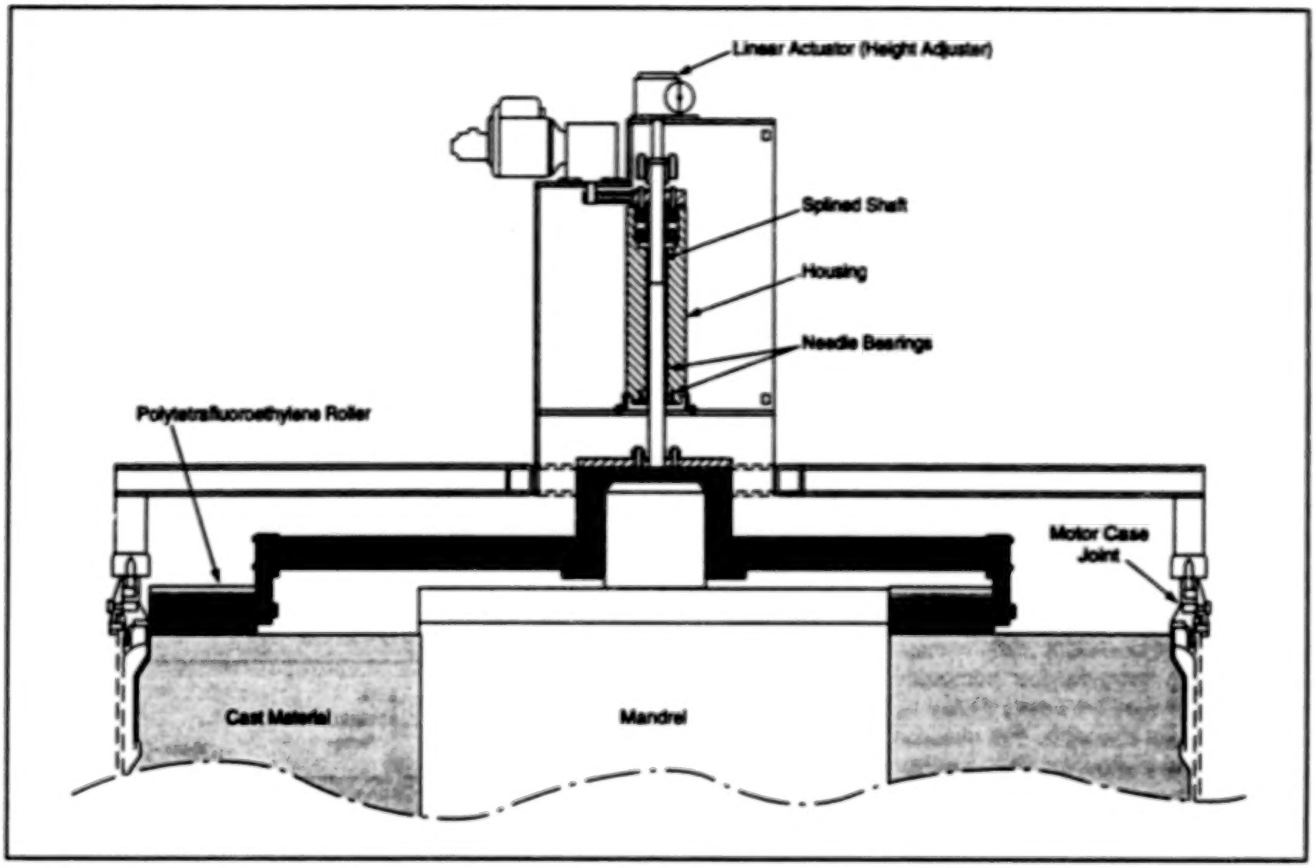

Motor-Driven Ganged Rollers similar to kitchen rolling pins smooth the top surface of the casting.

An improved method of vacuum casting of large, generally cylindrical objects to net sizes and shapes reduces the amount of direct manual labor by workers in proximity to the cast material. The original application for which the method was devised is the fabrication of solid rocket-motor segments containing solid propellant, wherein there is a need to minimize exposure of workers to the propellant material being cast. The improved method may be adaptable to other applications that involve large castings of toxic, flammable, or otherwise hazardous materials.

In the improved method, the propellant, which has a slurrylike consistency, is gravity-fed through a deaeration assembly into a rocket-motor case cylinder mounted inside a vacuum chamber. The slurry fills an annulus around a mandrel that forms a hollow core in the casting after the propellant is cured and the mandrel removed. A laser level detector monitors the rising top surface of the slurry through a window in the top of the vacuum chamber, so that the flow of material can be stopped when the top surface reaches a predetermined level.

To ensure the accuracy of the final level of the cast material, the tendency of the cast material to slump upon release of vacuum after casting is taken into account. When the slurry reaches the predetermined level, filling is momentarily stopped and the vacuum is partially released, in that air is admitted up to a preset subatmospheric pressure. The laser monitor measures the slump, and the measured value of slump under this partial restoration of atmospheric pressure is used to estimate what the slump would be if full atmospheric pressure were restored. The chamber is then reevacuated and material is added in the amount needed to correct for the estimated full-atmospheric-pressure slump.

Thus, when full atmospheric pressure is restored, the final surface of the cast material should be the specified level. In the original rocket-propellant application, this approach keeps the final level within 1/8 in. (3 mm) of the specified level. After casting is completed, mold plates are presently installed on the top surface of the propellant to produce a smooth and uniform finish during the curing process. A process change under consideration, to smooth the cast material surface, is to use a remotely operated set of ganged rollers at various stages of the propellant cure (see figure).

This work was done by Erik P. Johnson and Richard F. Brown of Thiokol Corp. for **Marshall Space Flight Center**. *Further information is contained in a TSP [see page 1].*
MFS-31001

Metal-Matrix Composite Parts With Metal Inserts

Appendages for connection to other parts are cast in place.

Marshall Space Flight Center, Alabama

A developmental fabrication process produces metal-matrix composite (MMC) parts with integral metal inserts. With the inserts, the MMC parts can readily be joined to similar parts by use of brazing, welding, or mechanical fasteners. Until now, the difficulty of joining MMC parts has inhibited the exploitation of the light weight, strength, and dimensional stability of MMCs.

The process was conceived to make strong, lightweight components of structures to be erected in outer space. MMCs may also be useful on Earth, in such automotive parts as rocker arms, cylinder liners, and pistons. Potential industrial applications include parts that are subjected to high stresses at high temperatures, as in power-generation, mining, and oil-drilling equipment.

The feasibility of the process has been demonstrated by making parts of magnesium-matrix/graphite-fiber composite material with titanium inserts (Figure 1). The parts were formed to final shape in a single casting step; no finish machining was necessary. In general, the process involves pressure casting in partly reusable molds made of inexpensive materials.

In the demonstration, the parts were made in a pressure-casting machine that is capable of operating at temperatures up to 1,400 °C and pressures up to 800 lb/in.^{2} (5.5 MPa) and can accommodate parts up to about 4 in. (≈ 10 cm) in diameter and about 6 in. (≈ 15 cm) long.

The machine features a balanced-pressure mold, in which the internal pressure exerted by the molten metal is balanced by an equal pressure on its outer wall from a compressed inert gas (Figure 2). (The internal pressure is needed to make the metal-matrix material infiltrate the graphite-fiber reinforcement.) Because these pressures are balanced and are low relative to compression yield stresses of cheap, machinable, nonstructural-grade materials, it is feasible to make the mold out of such materials. In addition to the graphite and salt used in the demonstration, such materials could include ceramics, quartz, and sheet metal.

In the demonstration, a graphite-fiber preform destined to become the fiber reinforcement of the composite part was placed in the mold along with the titanium insert. The mold and its contents were purged with argon, then evacuated. The magnesium was heated in a crucible to a temperature of 660 °C, while the preform in the mold was preheated to 530 °C. A pneumatic system raised the crucible so that a snorkel on the mold dipped into the crucible. The chamber that contained the crucible was then pressurized with argon at 800 psi (5.5 MPa) to force the molten magnesium into the mold cavity, where it infiltrated the preform. After about 3 minutes, the crucible was lowered and the mold allowed to cool. A boron nitride coating on the graphite mold ensured that the mold released the part easily.

The process temperatures, times, and pressure were chosen to produce com-

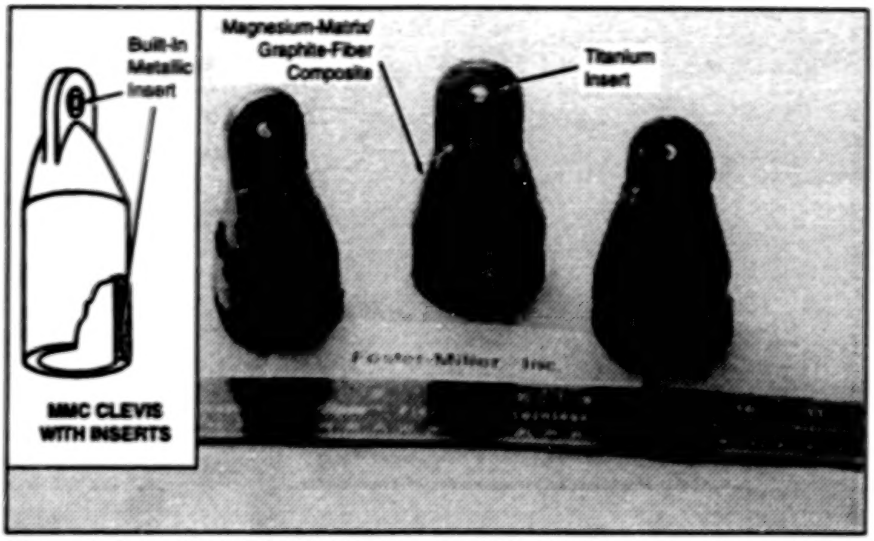

Figure 1. These Clevis Tube-End Fittings are made of magnesium-matrix/graphite-fiber composite with titanium inserts. The composite parts were molded to their final dimensions in a single step.

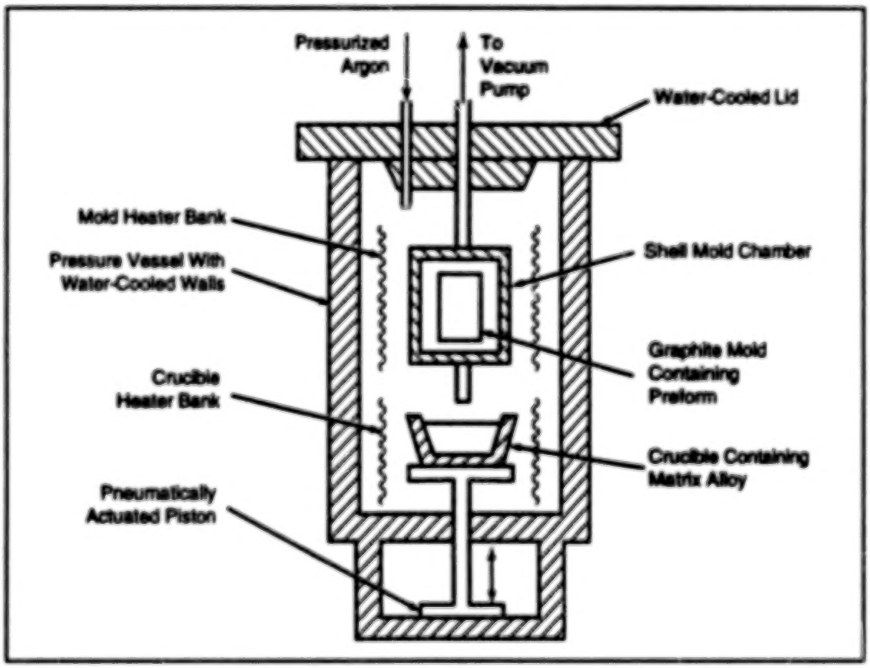

Figure 2. The Pressure-Casting Machine molds under conditions that promote complete infiltration of molten metal into a fiber preform, followed by rapid solidification to ensure good bonding.

BEST COPY AVAILABLE

plete infiltration of the densely packed preform while ensuring quick solidification of the melt (thus inhibiting chemical reactions that could degrade the interface between the matrix and the fibers). These conflicting requirements are satisfied by maintaining the magnesium alloy 60 °C above its liquidus temperature while maintaining the preform at a temperature 60 °C below the liquidus temperature of the magnesium at the chosen pressure.

When tested to failure, a part made by this process fractured at a tensile load of 2,803.1 lb (12,468 N). The fracture occurred in the body of the composite material, well away from the insert, indicating that the interface between the insert and the composite material transferred the tensile load efficiently.

This work was done by T. Majkowski and U. Kashalikar of Foster-Miller, Inc. for **Marshall Space Flight Center.** *Further information is contained in a TSP [see page 1].*

Inquiries concerning rights for the commercial use of this invention should be addressed to the Patent Counsel, Marshall Space Flight Center [see page 1]. Refer to MFS-27306.

Removable Mandrels for Vacuum-Plasma-Spray Forming

The mandrels shrink away from the tubes formed on them.

Marshall Space Flight Center, Alabama

Improved mandrels have been developed for use in vacuum-plasma-spray (VPS) forming of refractory metal and ceramic furnace cartridge tubes. The mandrels are designed so that after the tubes have been formed on them by VPS, the mandrels shrink away from the tubes upon cooling back to room temperature.

To maximize shrinkage, a mandrel of this type is made of a material that has a coefficient of thermal expansion (CTE) significantly greater than the CTE of the material to be deposited on it. On cooling, the mandrel shrinks more than does the deposited tube, so that the mandrel can simply be slipped out of the tube.

Typically, a mandrel of this type is made of stainless steel or high-CTE graphite. In addition to shrinking more than the deposited materials do, these mandrel materials can withstand the harsh, high-temperature vacuum plasma environment. The outer surface of a mandrel is machined to the desired shape of the inner surface of the tube to be formed on it, and preferably with a slight taper to facilitate removal after deposition. The tube to be formed could have a closed end with a shape (e.g., a hemispherical or flat end) that is easily machined onto the narrower end of the mandrel (see figure). Such features as a flange can also be machined onto the mandrel at its wider end.

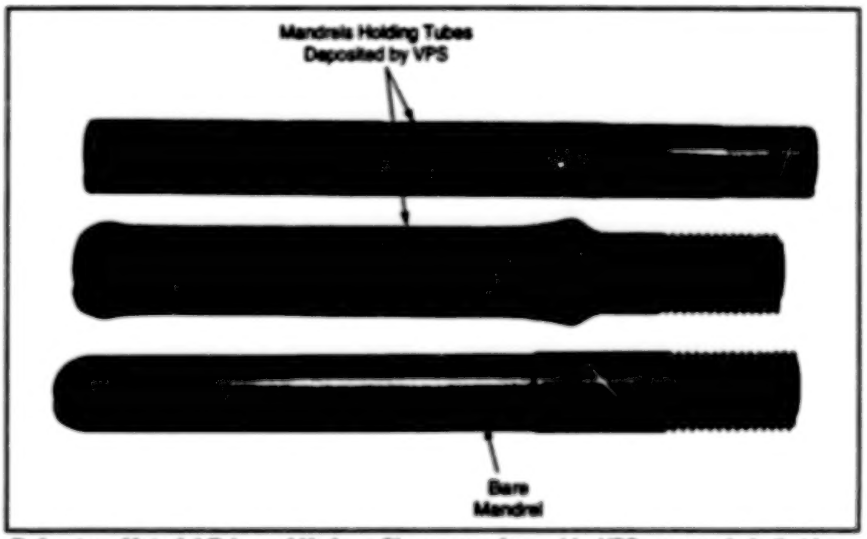

Refractory-Material Tubes of Various Shapes are formed by VPS on mandrels that have the desired shapes. The mandrels are designed for ease of separation from the tubes upon cooldown after the VPS process.

This work was done by Phillip D. Krotz, William M. Davis, Christopher A. Power, William H. Woodford, Douglas M. Todd, Ybon K. Liaw, Richard R. Holmes, Frank R. Zimmerman, and Timothy N. McKechnie of Rockwell International Corp. for **Marshall Space Flight Center.** *Further information is contained in a TSP [see page 1].*

MFS-30005

Improved Back-Side Purge-Gas Chambers for Plasma Arc Welding

Flows are more directed and concentrated.

Marshall Space Flight Center, Alabama

Improved chambers for inert-gas purging of the back sides of workpieces during plasma arc welding in the keyhole (full-penetration) mode are based on a concept of directing flows of inert gases toward, and concentrating them on, the hot weld zones. The designs are developed and verified with the help of experiments on transparent plastic models of purge-gas chambers, in which flows of inert gases are made visible by adding smoke generated by heat-decomposing of ammonium chloride.

A typical purge-gas chamber of older design spreads the inert gas over a larger workpiece area and in a less controlled flow pattern. Depending on the rate of flow, the inert gas can become concentrated in one spot, which is not necessarily the desired spot centered on the weld keyhole. Elsewhere in the chamber, the inert gas can become mixed with air that leaks in through the opening; this is undesirable because it can bring reactive atmospheric gases (oxygen, water, hydrogen, and nitrogen) into contact with hot metal, resulting in weld defects that inert-gas purging is intended to prevent. It is especially important to prevent contamination by atmospheric gases during welding of reactive metals like aluminum/lithium alloys and titanium.

The figure illustrates a representative purge-gas chamber of the improved type. It has a tapered shape with a rectangular

cross section. The inert gas enters the chamber through a distributor at the wide end, and the flow is smoothed there by use of a gas-diffusion mesh. The gas then flows toward an opening at the narrow end of the taper, where it impinges in a stream concentrated on the desired spot on the workpiece. The chamber is moved along the back side of the weld (the opposite side from the welding torch, called the "root side" in the industry) in synchronism with the weld torch on the front side, so that the opening in the chamber always faces the penetrating weld-torch plume and the adjacent hot metal.

The inert gas can be helium, argon, or a mixture of both. The choice of gas for a given application involves consideration of many factors, including the heat-dissipation requirements; the thermal properties, electrical-breakdown properties, and mass density of the gas; and which way the inert gas is required to flow with respect to gravity (depending on the orientation of the torch, it may have to flow up, down, or horizontal). For example, if the inert gas has to flow upward toward the workpiece, then helium would ordinarily be preferable because its density is less than that of the surrounding air and thus it flows upward in air. In any event, the flow of whichever inert gas is chosen can be verified in a smoke flow experiment.

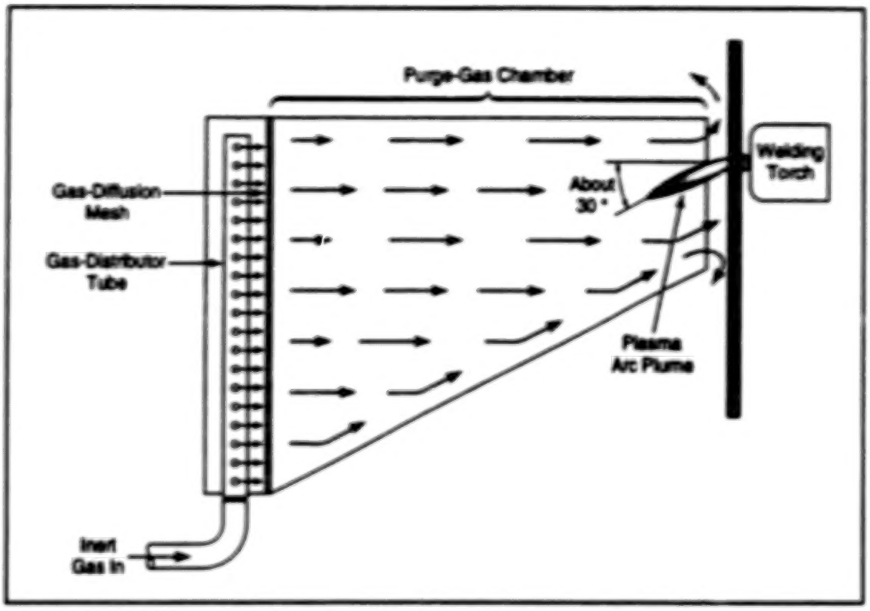

The Tapered Chamber Concentrates the Flow of inert gas on the plasma arc plume and surrounding metal.

This work was done by Kenneth G. Ezell, William F. McGee, and Daniel J. Rybicki of Martin Marietta Manned Space Systems for **Marshall Space Flight Center**. *Further information is contained in a TSP [see page 1].*

Inquiries concerning rights for the commercial use of this invention should be addressed to the Patent Counsel, Marshall Space Flight Center [see page 1]. Refer to MFS-31012.

Nonchamber, Root-Side, Inert-Gas Purging During Welding

A simple, lightweight gas distributor replaces a more-cumbersome purging chamber.

Marshall Space Flight Center, Alabama

The figure illustrates an improved apparatus that distributes inert gas to protect against oxidation on the root side of a weld (the side opposite the welding torch) during welding and after welding while the joint remains hot. Unlike the more-cumbersome purging chambers that have been used heretofore, this apparatus does not obscure the view of the root side of the weld. The apparatus can be used for full-penetration plasma-arc welding of such reactive metals as aluminum/lithium alloys and titanium.

In the apparatus, the inert gas is fed into the region around the weld zone through porous sintered metallic rods, which disperse the gas evenly over their surfaces. Cylindrical shrouds partially enclose the rods and direct the flow of gas through slots toward the weld region. The jetlike thrust of the welding arc as it penetrates the metal draws the inert gas to the hot weld zone (see figure). The metal is thus protected while the weld zone remains open to view.

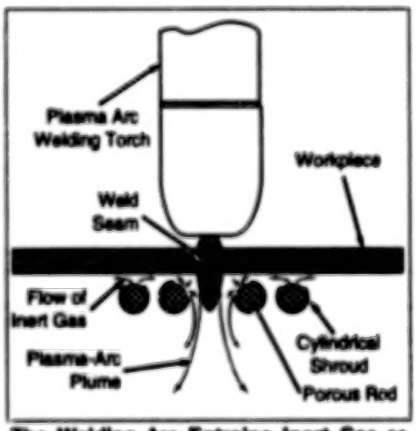

The Welding Arc Entrains Inert Gas as the gas flows from distribution rods. The inert gas envelopes the newly formed weld seam, protecting it against oxidation.

The apparatus is simple and lightweight; it can readily be moved along the weld path in synchronism with the torch. Because it concentrates inert gas where it is needed, it consumes gas at a relatively low rate, and, unlike in a purging chamber, it is not necessary to monitor the oxygen content of the protective atmosphere.

This work was done by William F. McGee and Daniel J. Rybicki of Martin Marietta Corp. for **Marshall Space Flight Center**. *Further information is contained in a TSP [see page 1].*

This invention is owned by NASA, and a patent application has been filed. Inquiries concerning nonexclusive or exclusive license for its commercial development should be addressed to the Patent Counsel, Marshall Space Flight Center [see page 1]. Refer to MFS-28832.

Wire-Arc Spraying of Metal Onto Insulating Foam

This process is relatively fast and cheap, and does not damage the foam.

Marshall Space Flight Center, Alabama

Wire-arc spraying can now be used to deposit protective metallic coats on thermally insulating foams. Heretofore, it has been common practice to deposit such coats by electroplating. Wire-arc spraying costs less than electroplating does. Wire-arc spraying is also faster, and, unlike electroplating, does not involve toxic and polluting chemicals. Moreover, unlike other thermal-spray metal-deposition processes, wire-arc spraying does not degrade or burn the foam.

Metal coats on insulating foams provide several benefits: they protect the foams against damage during handling and provide reflectivity that may be needed for optical and/or thermal-radiation purposes. On foams used to insulate cryogenic hardware, metallic coats help to prevent undesired cryopumping by sealing the foams against leakage of air from the environment to the cold surface of the hardware.

Traditionally, wire-arc spraying has been used to deposit corrosion-inhibiting zinc coats on metal structures and aluminum coats on computer components to suppress electromagnetic interference. Recent advancements in wire-arc spraying have made it possible to use this process to deposit metal on foam without harming the foam. The figure illustrates the basic concept of wire-arc spraying.

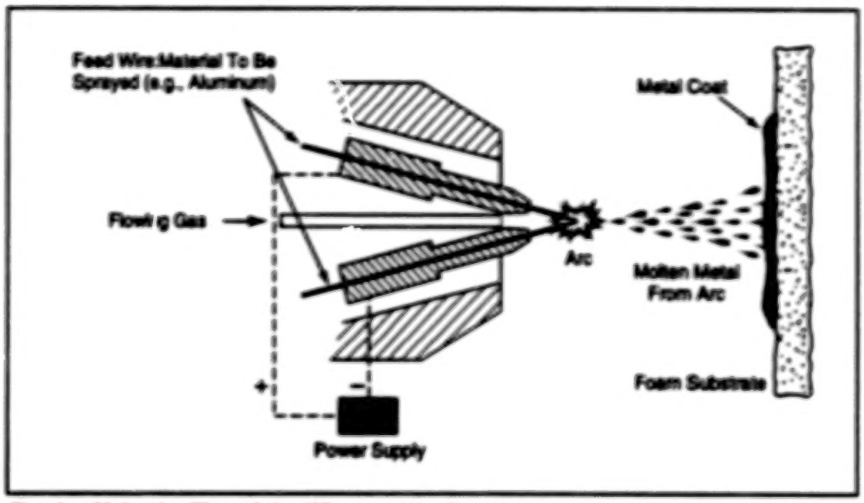

The Arc Melts the Tips of the Wires and the flow of gas sweeps the molten metal toward the substrate.

An electric arc is drawn between the tips of two wires of the metal to be deposited, melting the wires. A high-pressure flow of gas (for example, argon, a mixture of argon and hydrogen, or air) accelerates the molten metal toward the foam or other substrate to be coated.

During wire-arc spraying, the sprayed surface of the foam or other substrate is exposed to temperatures in the range of about 100 to 300 °F (about 38 to 149 °C). Other thermal-spray processes produce greater temperatures, which would degrade insulating foam. In one case in which the density of the foam was so low that wire-arc-sprayed metal particles impinging at high speeds penetrated the surface of the foam, a hard epoxy surface coat was used to stop the penetration.

This work was done by James W. Bonds, Jr., Ronald L. Daniel, Jr., Phillip D. Krotz, Timothy N. McKechnie, and Heather L. Sanders of Rockwell International Corp. for **Marshall Space Flight Center**. *Further information is contained in a TSP [see page 1].*
MFS-30013

Computed Tomography for Internal Inspection of Castings

Internal defects that would eventually cause rejection are detected before further processing.

Marshall Space Flight Center, Alabama

Computed tomography is being used to detect internal flaws in metal castings before machining and otherwise processing them into finished parts. For example, computed tomography can reveal internal porosity and casting shrink, which cannot normally be detected by conventional radiographic inspection.

In one application, computed tomography is being used to reveal and provide information to assess shrink in a high-pressure volute casting used on a space shuttle engine turbopump. The acceptance or rejection of this casting is usually determined after final machining — during the volute leak test. The pre-machining computed tomography of this casting is being used to remove questionable castings from the system, saving machining cost and schedule delays.

In a related application, computed tomography was used to inspect a new casting when the first article inspection data became questionable. The resulting computed tomography data was assessed by the casting foundry with corrections made in the processing to eliminate the problem, which was found to be a ceramic core shift within the investment mold when the molten metal was poured.

In these and other applications, computed tomography saves the time and money that would otherwise be wasted on machining and other processing of castings that must eventually be rejected because of their internal defects. The knowledge of internal defects gained by use of computed tomography can also provide guidance for changes in foundry techniques, procedures, and equipment to minimize defects and reduce costs.

This work was done by Timothy L. Hanna of Rockwell International Corp. for **Marshall Space Flight Center**. *No further documentation is available.*
MFS-30018

Manifold for Flushing Tubes With Cleaning Solution

Many tubes can be cleaned simultaneously.

Marshall Space Flight Center, Alabama

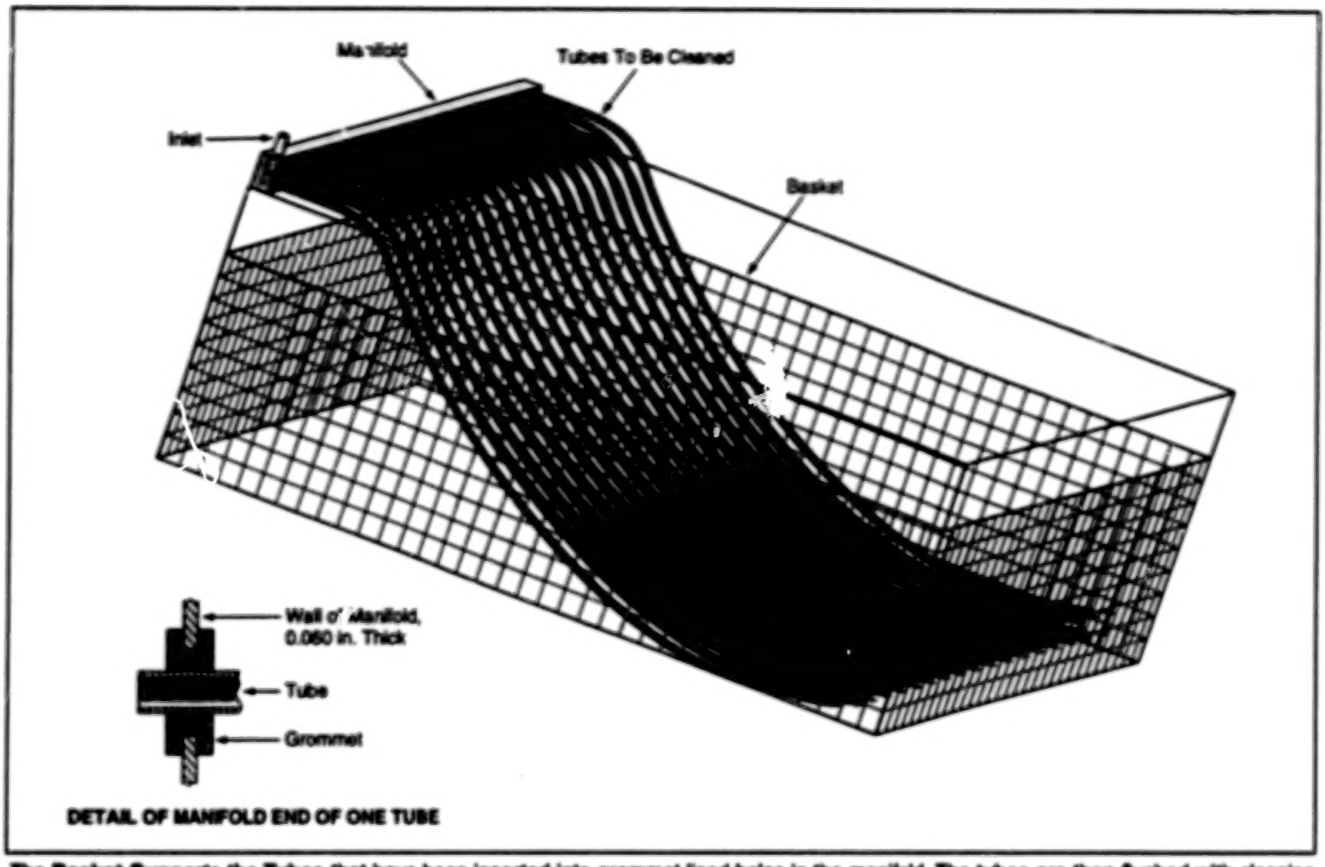

The Basket Supports the Tubes that have been inserted into grommet-lined holes in the manifold. The tubes are then flushed with cleaning solution supplied via the manifold.

A custom-built manifold mounted on a cleaning basket enables the simultaneous flushing of 80 tubes with a cleaning solution (see figure). In the original application, the tubes are components of a rocket-engine nozzle that is under construction. However, the basic manifold configuration could be adapted to other applications (e.g., fabrication of heat exchangers) in which there is need for the simultaneous cleaning of many tubes of identical size and shape.

A pump supplies pressurized cleaning solution to the manifold, which distributes the solution to the tubes. The manifold is made of stainless steel. The holes in the manifold that receive the ends of the tubes are lined with rubber grommets. Thus, it is not necessary to equip the tubes with end fittings: the tubes are simply inserted into the grommets, which act as seals.

This work was done by Gene E. Morgan and Irving Fogel of Rockwell International Corp. for **Marshall Space Flight Center**. *Further information is contained in a TSP [see page 1].*

MFS-29964

Anodizing and Sealing Aluminum in Nonchromated Solutions

Sulfuric acid (anodizing) and nickel acetate (sealing) solutions are used instead.

Marshall Space Flight Center, Alabama

An improved process for anodizing and sealing aluminum involves the use of 5 volume percent sulfuric acid in water as the anodizing solution, and 1.5 to 2.0 volume percent nickel acetate in water as the sealing solution. This process replaces an older process that raises concerns about toxicity and damage to the environment: In the older process, the anodizing and sealing solutions are chromic acid and sodium dichromate, respectively; both of these compounds contain hexavalent chromium, which is carcinogenic.

The improved process also replaces an older process in which sulfuric acid is used at concentrations of 10 to 20 percent. This older process yields anodized coats 1 to 2 mils (about 0.03 to 0.05 mm) thick: this thickness is undesirable in some applications because it is accompanied by degradation of resistance to fatigue. The improved process yields thinner coats [0.09 to 0.2 mils (about 2 to 5 μm) thick] that offer resistance to corrosion, fatigue life, and alloy-to-alloy consistency equal to or superior to those of anodized coats produced with chromated solutions.

The success of the improved process depends critically on precise maintenance of specific process parameters. In one application, for example, the process parameters were anodizing potential of 19 to 21 V, anodizing temperature of 68

to 72 °F (20 to 22 °C), anodizing time of 18 to 22 min, sealing temperature of 160 to 190 °F (71 to 88 °C), sealing-solution pH of 5.5 to 6.0, and sealing time of 10 to 15 min.

This work was done by John R. Emmons and Kelli J. Kollenborn of Rockwell International Corp. for **Marshall Space Flight Center**. *Further information is contained in a TSP [see page 1].*

Inquiries concerning rights for the commercial use of this invention should be addressed to the Patent Counsel, Marshall Space Flight Center [see page 1]. Refer to MFS-30021.

Tools for Installing Keys on a Stud

The tools stabilize the keys during installation, preventing bending and breaking.

Marshall Space Flight Center, Alabama

Two tools are designed to be used together to drive long locking keys axially to install them on a stud. The tools help to prevent bending and breaking of the keys during installation, and make it possible to install all the keys simultaneously, in one motion.

In one older technique for installing multiple keys simultaneously onto a stud, the tooling presses the keys down without support. Long keys tend to bend outward and frequently break. In an alternative older technique, the keys are driven down individually but are still susceptible to motion other than the desired downward translation. The two tools of the present technique are (1) a supporter that holds the keys in the correct relative alignment and (2) a driver that has multiple prongs, each of which fits into one of the holes in the supporter (see figure). The keys are placed in the holes in the supporter and positioned, on the stud, at the tops of the grooves along and into which they are to be pushed. The prongs of the driver are inserted in the holes, and the driver is pushed down within the supporter to drive the keys down.

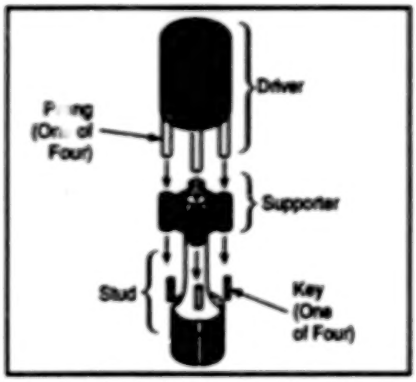

The Tubular Holes in the Supporter are placed over keys positioned for installation in the stud. The prongs of the driver are inserted into the holes in the supporter, and the driver is pushed down to drive the keys down.

This work was done by Robert D. Goodoak of United Technologies Corp. for **Marshall Space Flight Center**. *No further documentation is available.*
MFS-28901

Books and Reports

Applying Taguchi Methods to Brazing of Rocket-Nozzle Tubes

Experiments yielded data on how processing time can be decreased.

A report describes an experimental study in which Taguchi Methods were applied with a view toward improving the brazing of coolant tubes in the nozzle of the main engine of the space shuttle. Taguchi Methods are an integrated system of techniques for achieving high quality (robustness) in products by appropriate design of the products and of the processes used to manufacture them. In this study, Dr. Taguchi's parameter design technique was used to define proposed modifications of the brazing process that would reduce manufacturing time and cost by reducing the number of furnace brazing cycles and the number of tube-gap inspections needed to achieve desired small gaps between tubes. The study involved an experiment, in which subscale panels that were simplified versions of the nozzle jacket and tubes were fabricated under various combinations of brazing time, surface preparation, and other process parameters; in each combination, each parameter was assigned one of two alternative values. Data analysis was performed on the subscale panels thus fabricated to determine the influence of each parameter and which value of each parameter resulted in the smallest gaps. Confirmation tests on panels fabricated under the process parameters derived by this analysis showed that tube-to-tube gaps were nearly eliminated after one furnace brazing cycle. Upon implementation of Taguchi Methods on nozzle hardware, the tube-to-tube gap was shown to be greatly reduced after the first brazing cycle. This gap reduction should lead to the achievement of two braze cycles consistently, in lieu of three or more cycles historically performed.

This work was done by Jeffrey L. Gilbert, William J. Bellows, David C. Daily, Alex Brennan, and John G. Somerville of Rockwell International Corp. for **Marshall Space Flight Center**. *To obtain a copy of the report, "SSME Nozzle Brazing Improvement Using Taguchi Methods," see TSP's [page 1].*
MFS-30046

BLANK PAGE

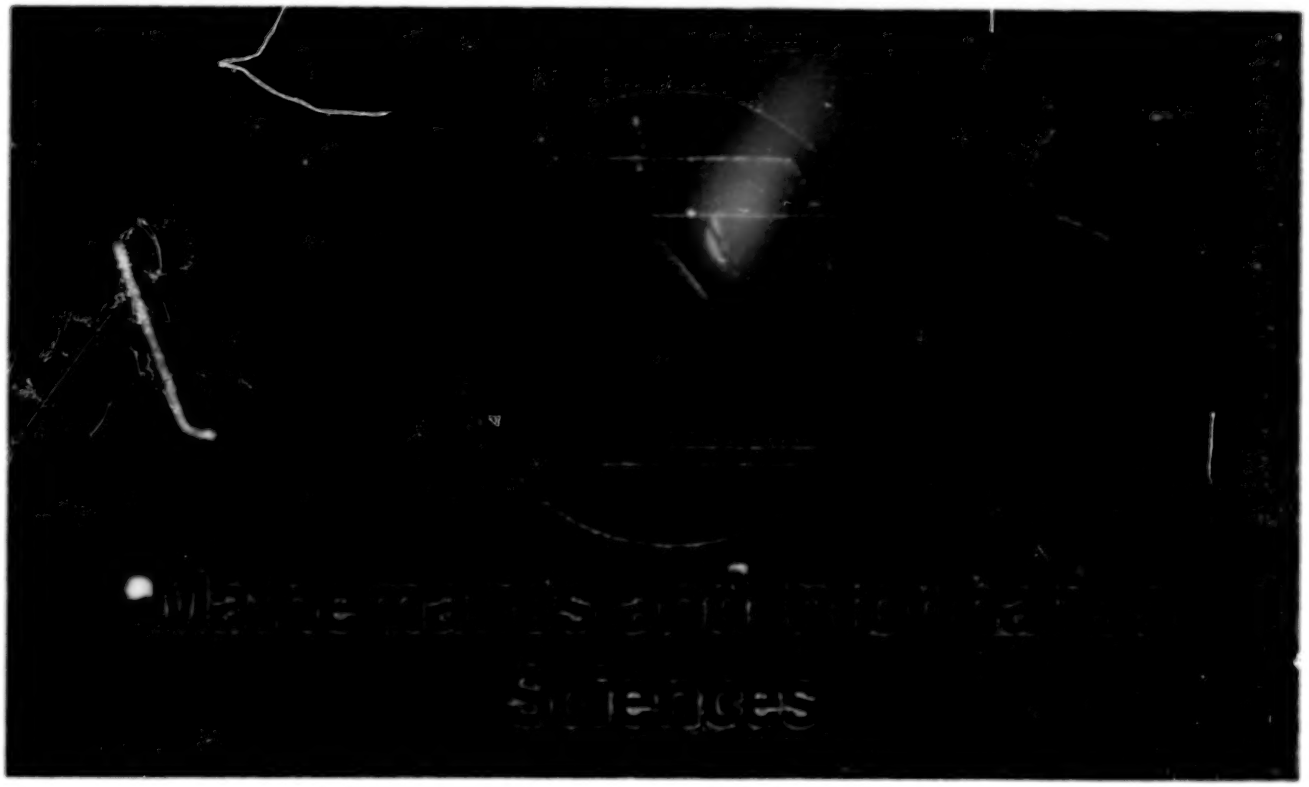

Hardware, Techniques, and Processes

69 An Image Processing Algorithm Based on FMAT

69 Excursion-Set-Mediated Genetic Algorithm

BLANK PAGE

An Image Processing Algorithm Based on FMAT

Information is deleted in ways that minimize adverse effects on reconstructed images.

Lyndon B. Johnson Space Center, Houston, Texas

The problem of extracting medial axis transformation (MAT) and skeleton (or thinning) plays a key role in image processing, analysis, and recognition because of the simplicity of image (and hence object) representation they allow. There has been extensive research done in extracting the medial axis of a region and skeleton of elongated objects from a two-tone image.

The present work proposes a new gray-scale generalization of MAT, called FMAT (short for Fuzzy MAT). It is formulated by making a natural extension to fuzzy-set theory of all the definitions and conditions (e.g., characteristic function of a disk, subset condition of a disk, and redundancy checking) used in defining a MAT of a crisp set. As a result, it does not need the image to have any kind of *a priori* segmentation, and it allows the medial axis (and skeleton) to be a fuzzy subset of the input image. The resulting FMAT (consisting of maximal fuzzy disks) is capable of reconstructing exactly the original image.

An attempt of obtaining an optimum FMAT for making the image MAT representation more economical is also made by maximizing compactness of the FMAT output with its various α-cuts. Such an optimum version keeps only those medial-axis pixels that are responsible for object regions of interest while ignoring the rest. This can also be regarded as an optimum (in the sense of minimizing spatial ambiguity) fuzzy skeleton of an image.

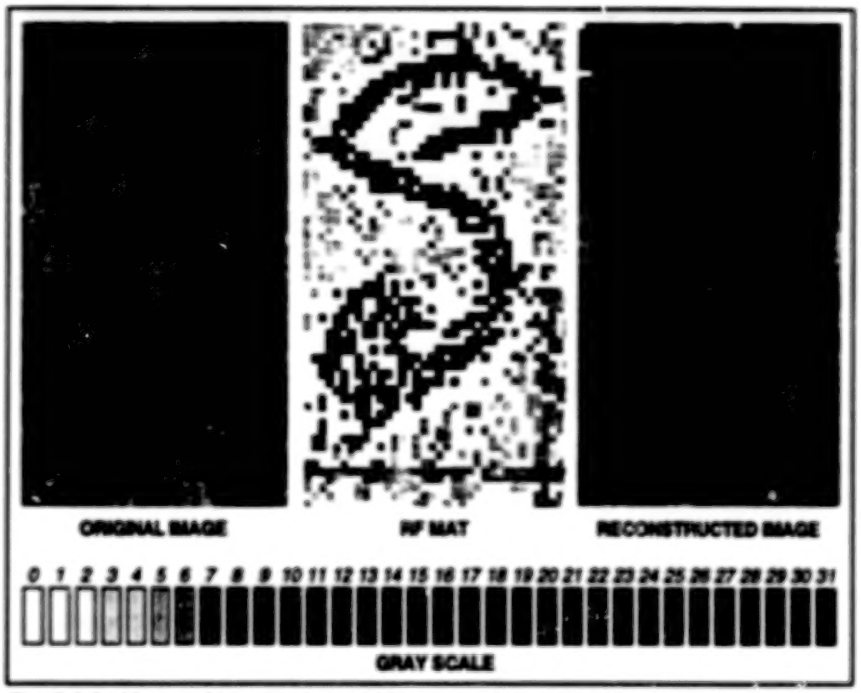

The Original Image of 60 × 36 pixels and 32 gray levels is converted to a reduced-redundancy FMAT (RFMAT), then reconstructed from the RFMAT.

This work was done by Lui Wang of **Johnson Space Center** *and Sankar K. Pal of the National Academy of Sciences. Further information is contained in a TSP [see page 1].*

This invention is owned by NASA, and a patent application has been filed. Inquiries concerning nonexclusive or exclusive license for its commercial development should be addressed to the Patent Counsel, Johnson Space Center [see page 1]. Refer to MSC-21997.

Excursion-Set-Mediated Genetic Algorithm

In comparison with other genetic algorithms, this one achieves a stronger condition for implicit parallelism.

Marshall Space Flight Center, Alabama

The excursion-set-mediated genetic algorithm (ESMGA) is an embodiment of a method of searching for and optimizing computerized mathematical models. Like other genetic algorithms, it incorporates powerful search and optimization techniques based on concepts analogous to natural selection and the laws of genetics. Going beyond the prior art of optimization via genetic algorithms, excursion sets have been introduced into the ESMGA to parameterize the implicit parallelism of the genetic algorithm and its exponential elevation of subthreshold solutions toward optimum.

Excursion sets provide a natural basis to control the performance of an adaptive genetic algorithm in terms of objective functions. An excursion set, A_u, is defined at a given excursion-level parameter u for an objective function $f(x)$ as follows: $A_u = \{x; f(x) > u\}$. Excursion sets introduce a nontrivial hierarchy in search space that is represented in the evolving genetic-algorithm population. Excursion sets and local optima above u are closely related. For example, if only local optimal solutions of importance turn out to be those above u, then these solutions certainly lie within A_u.

From one perspective, a genetic algorithm can be represented in two dimensions: (1) the way objective functions defined by the user map to a fitness measure and (2) the way a fitness measure is used to assign mathematical offspring to mathematical parents. Along these two dimensions, almost all genetic algorithms exhibit some form of multiple sampling and implicit parallelism. By mediating selection through the excursion sets and random-field theory, the ESMGA achieves a stronger condition for implicit parallelism, along with better performance.

Because one can generate excursion sets equally well in either objective-function space or fitness-function space, excursion levels introduce a natural hierarchical structure on the hypercube of available genomes. As an excursion level increases, a population is forced to rise (in terms of fitness) above the excursion level, and simultaneously the evolved

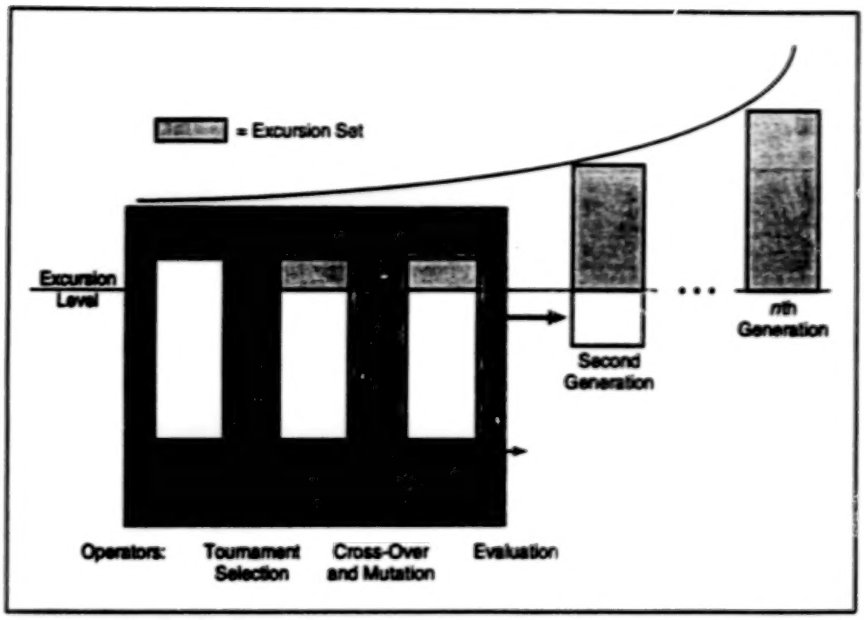

The Excursion-Set-Mediated Genetic Algorithm includes three stages of operations in each cycle, which is analogous to a biological generation.

population becomes distributed among the possible solutions in the excursion set. Thus, the introduction of excursion sets makes it possible to balance judiciously both internal and external representations and thus to provide a stronger condition for implicit parallelism.

The figure illustrates schematically what happens in the ESMGA. First, a random population of genomes is generated. For an arbitrarily chosen excursion level u, the possible genome space is partitioned into upper and lower portions. The upper set contains individuals characterized by fitness measures greater than or equal to the excursion threshold (equivalently, the excursion set at that level).

Next, during the selection stage, the upper (excursion-set) component of the population is retained and the lower portion is filled by tournament selection upon the entire population (the excursion set plus its complement). This stage introduces some bias against mating of similar individuals (analogous to prevention of incest).

The selection stage is followed by a modification stage, in which cross-over and mutation operators are applied only to the lower components. These operations produce a new population at generation 2. Finally, the new population is evaluated; individuals scoring above the excursion level are pushed up into the excursion set and preserved for future generations.

The three stages of selection, modification, and evaluation constitute one cycle of operations, which is analogous to one biological generation. The cycle is reiterated until all members of the population get pushed above the excursion level. Subsequent experiments repeat the internal genetic-algorithm dynamics for higher and higher excursion levels.

This work was done by David Noever of **Marshall Space Flight Center** *and Subbiah Baskaran of Science and Technology Corp. Further information is contained in a TSP [see page 1].*
MFS-26263

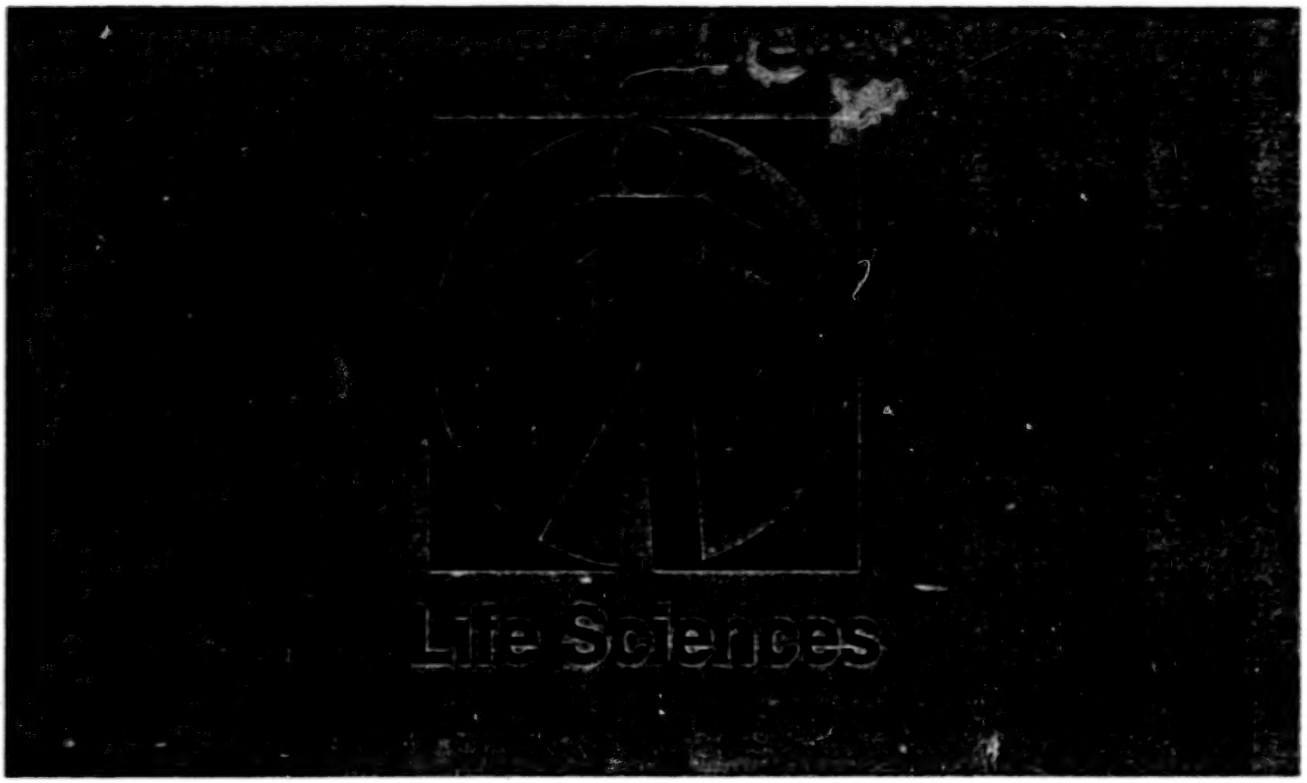

Hardware, Techniques, and Processes

73 Device Would Monitor Body Parameters Continuously
73 Slow-Release Fertilizers for Plants
74 Growing Three-Dimensional Cocultures of Cells

BLANK PAGE

Device Would Monitor Body Parameters Continuously

An electronic thermometer would record, process, and display temperature readings.

Lyndon B. Johnson Space Center, Houston, Texas

A proposed miniature electronic circuit would continuously measure the temperature of a human subject. Once mounted on the subject's skin with medical adhesive tape, this electronic thermometer would remain in thermal equilibrium with the subject's body; thereafter, there would be no need to wait until the thermometer reached body temperature before taking a reading, as is necessary when using a liquid-in-glass thermometer or a conventional thermocouple- or resistance-based temperature-measuring device connected to external circuitry.

The proposed electronic thermometer would include a small battery like that in a wristwatch, a temperature-sensing circuit element, a signal conditioner, a computer, and a display unit, all contained in a disk less than 1 in. (25 mm) in diameter and less than 1/4 in. (6 mm) thick (see figure). The circuit would record and display temperature readings at specified intervals of time. It would also compute maximum, average, and minimum temperatures and the rate of change of temperature from temperature readings taken during a specified observation interval.

The electronic thermometer would typically be positioned near the armpit because the thermal environment there is conducive to obtaining readings of internal body temperature. The device would be attached to the skin by use of an adhesive disk with an open center that would expose the display unit and small switches on the outer (upper in the figure) side of the disk.

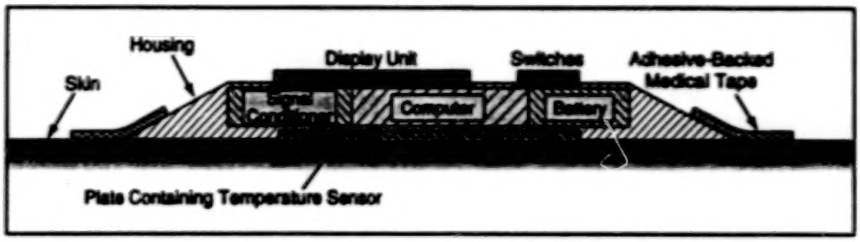

The Electronic Thermometer would be housed in a small disk that would be placed on the skin. The temperature sensor on the bottom would be in direct contact with the skin. This view is schematic only; it is not to scale.

All of the electronic components of the proposed electronic thermometer are readily available from commercial sources. The temperature-sensing element could be, for example, a thermocouple or resistance device mounted in a plate of metal or other highly thermally conductive material in contact with the skin. The temperature-sensing circuit element would produce a voltage that would vary as a function of temperature. This voltage would be fed to the signal conditioner, which would provide amplification, bridge balancing, and/or linearization as needed.

The conditioned signal would be digitized and the digitized value would be sent to the computer, which would compute the temperature from the voltage. The computer would include a microprocessor, a clock, and a memory circuit. The computer would send output data to the display unit, which could be a light-emitting-diode or liquid-crystal display device.

One of the small switches on the outer face would be used to turn the thermometer on and off. Other switches would be used to select the desired data output display. The design could provide for one or more of the switches to be used to set an alarm that would alert medical attendants if the subject's temperature exceeded a critical level. For use on a very young child, the electronic thermometer could be sewed into a shirt or other suitable garment; the device would thus be held in contact with the skin, and the child could not swallow it.

Replacement of the sensor and computing algorithm can change this continuous temperature monitor to a cardiorespiratory monitor. The replacements involve using a stethoscopic microphone in place of the temperature sensor and using a power spectrum algorithm to analyze and monitor the breathing and heart rates. Alarms would be triggered at preset levels and changes to normal levels.

This work was done by Joseph S. Cook, Jr., of **Johnson Space Center.** *Further information is contained in a TSP [see page 1].*
MSC-22341

Slow-Release Fertilizers for Plants

Pellets provide all of the micronutrients needed by plants of a given species.

Lyndon B. Johnson Space Center, Houston, Texas

A synthetic mineral provides growing plants with nutrients, including micronutrients (those consumed in trace quantities). The mineral dissolves slowly in moist soil or in a hydroponic solution, releasing its constituents.

The mineral is a synthetic apatite (which normally includes calcium phosphate and related compounds) into which the nutrients calcium, phosphorous, iron, manganese, copper, zinc, molybdenum, chlorine, boron, and sulfur are incorporated in the form of various salts. The table lists the starting materials used to synthesize the mineral.

The synthesis begins with the preparation of three stock solutions:

- **Solution A** – Compound 1 (see table) is dissolved in 0.5 L of 20 percent NH_3 in water.
- **Solution B** – Compounds 2 through 7 are dissolved in 0.46 L of deionized water, then 0.04 L of 20 percent NH_3 water is added.
- **Solution C** – Compounds 8 through 11 are dissolved in 20 mL of deionized water.

Solution B is stirred vigorously into solution A, then solution C is added and the mixture is stirred for another 5 min. The mixture is allowed to stand for 18 h, during which time the precipitate settles to the bottom. The supernatant liquid is then decanted and the precipitate is washed several times in deionized water. The washed precipitate is baked for 2 h at a temperature of 200 °C, then 2 h at 400 °C. The dry precipitate cake is crushed and pressed into pellets with 2.5 percent by weight lignosulfonate as a binder.

Each pellet has a homogeneous inorganic composition. The composition can readily be adjusted to meet the precise needs of a plant.

	Chemical	Number of Moles in Solution
1	$Ca(NO_3)_2 \cdot 4H_2O$	0.7272
2	$(NH_4)_2HPO_4$	0.328
3	Na_2CO_3	0.2
4	NH_4Cl	0.2
5	$Na_2B_4O_7$	0.003
6	$(NH_4)_6Mo_7O_{24} \cdot 4H_2O$	9×10^{-7}
7	$(NH_4)_2SO_4$	0.02
8	$Fe(NO_3)_2 \cdot 6H_2O$	0.01
9	$MnCl_2$	0.006
10	$Zn(NO_3)_2$	0.002
11	$Cu(NO_3)_2$	6.3×10^{-6}

Synthetic Apatite Is Prepared from solutions of a variety of chemicals. The concentrations reflect the needs of a plant for various nutrients.

This work was done by Douglas W. Ming of **Johnson Space Center** *and D. C. Golden of the National Research Council. Further information is contained in a TSP [see page 1].*

This invention is owned by NASA, and a patent application has been filed. Inquiries concerning nonexclusive or exclusive license for its commercial development should be addressed to the Patent Counsel, Johnson Space Center [see page 1]. Refer to MSC-21953.

Growing Three-Dimensional Cocultures of Cells

Tissuelike assemblies of mammalian cells grow when the right conditions are provided.

Lyndon B. Johnson Space Center, Houston, Texas

A laboratory process provides environmental conditions that favor the simultaneous growth of cocultures of mammalian cells of more than one type. The cultures become three-dimensional tissuelike assemblies that can serve as organoid models of the differentiation of cells. The process can be used, for example, to study the growth of human colon cancers, starting from mixtures of normal colonic fibroblasts and partially differentiated colon adenocarcinoma cells.

The cells are grown, possibly on microcarrier beads, suspended in a growth medium (nutrient fluid) in a bioreactor vessel described in a previous issue of *NASA Tech Briefs*. The vessel is rotated slowly about a horizontal axis to reduce the rate of the gravitational sedimentation of the cells and beads. The combination of slow rotation and gentle circulation allows neighboring beads and cells to remain in proximity to each other long enough to interact and assemble themselves into three-dimensional structures. The gentle circulation also minimizes shear stress, which can damage mammalian cells. The exchange of respiratory gases, the supply of nutrients, and the removal of metabolic waste products can be accomplished by perfusion of the growth medium through external equipment, direct injection into the culture medium, and/or diffusion of molecules across a membrane.

As an example, the version of the process in the case of the human colon cells includes the following steps (some steps have been omitted and combined for clarity and brevity):

1. The vessel is washed, sterilized, and stood with its axis vertical (not in the operating orientation).
2. Sterilized microcarrier beads of 175-μm diameter are suspended in the growth medium at a concentration of 5 g/L.
3. The vessel is filled with the bead-and-medium mixture to 90 percent of its volume.
4. The vessel is sealed and placed for 2 h in an incubator filled with a humidified mixture of 95 percent air and 5 percent carbon dioxide at the normal human body temperature of 37 °C.
5. The normal fibroblasts and the cancer cells are mixed together in the ratio of 9 to 1, trypsinized and washed on ice, suspended in the growth medium, and held on ice until inoculation.
6. The vessel is inoculated with enough of the cell mixture to obtain an average initial distribution of 10 cells per bead.
7. The small remaining empty volume in the vessel is filled with growth medium; then the vessel is sealed and placed with its axis oriented horizontally in the incubator.
8. The vessel is initially set into rotation at 10 to 15 r/min to suspend the single beads and cells and initiate growth.
9. After 24 h, the culture is inspected and the speed of rotation is adjusted, if necessary, in accordance with the progress of culture.
10. After another 24 h, the growth medium may have to be changed, depending on the metabolism and the types of cells. The determination is made on the basis of the numbers of cells, the pH, and the O_2 and CO_2 contents.
11. After yet another 24 h, the rate of rotation is adjusted daily, depending on the sizes of the three-dimensional aggregates of cells that begin to form at this stage.
12. The experiment is terminated when the desired three-dimensional aggregates have been formed, the rotation is no longer able to keep the aggregates suspended (or else the centrifugal force of increased rotational speed smashes the aggregates against the outer wall of the vessel), and/or when the metabolism of the cells begins to demand monitoring and service more often than only daily.

This work was done by David A. Wolf of **Johnson Space Center** *and Thomas J. Goodwin of Krug International. Further information is contained in a TSP [see page 1].*

This invention is owned by NASA, and a patent application has been filed. Inquiries concerning nonexclusive or exclusive license for its commercial development should be addressed to the Patent Counsel, Johnson Space Center [see page 1]. Refer to MSC-21560.

National Aeronautics and
Space Administration

75

END

DATE FILMED

01/25/96